Answers Research Journal 18 (2025): 377–419.
https://assets.answersresearchjournal.org/doc/v18/radiohalos_precambrian_grand_canyon_part_2.pdf

ARJ

Radiohalos in the Grand Canyon Precambrian Crystalline Basement Rocks. Part 2. The Schists

Andrew A. Snelling, Answers in Genesis, PO Box 510, Hebron, Kentucky 41048

Abstract

Schists within Grand Canyon's Precambrian crystalline basement were possibly created supernaturally on Creation Days 1–2. They were then uplifted by the upheaval on Creation Day 3. At the onset of the Flood they were beveled before Flood sediment layers were deposited unconformably over them. Fifty samples were collected from two schist units. Radiohalos in these samples were identified and counted. Thirty-six of the 37 Vishnu Schist samples contain ^{210}Po radiohalos, 33 also contain ^{238}U radiohalos and four contain ^{218}Po and ^{214}Po radiohalos. The thirteen Ramu Schist samples contain fewer ^{210}Po and ^{238}U radiohalos. The different apparent metamorphic conditions in the lithotectonic blocks were irrelevant. The two factors that control radiohalos numbers are the abundance of biotite flakes available to host radiohalos and the abundance of tiny zircon inclusions in them. Two models proposed previously to resolve the Po radiohalos enigma are creation by fiat of the host schists with the Po radiohalos during Creation Days 1–2, or rapid transport of the Po atoms by hydrothermal fluids while grossly accelerated radioactive decay was occurring during the Flood. Any radiohalos in these supernaturally created schists likely were annealed by the Creation Day 3 upheaval and the onset of the Flood. Thus, the origin of these radiohalos is consistent only with the hydrothermal fluid transport model for their formation during the Flood. Water trapped in the Flood-deposited sediment layers was heated by their burial and the residual heat generated by grossly accelerated radioactive decay. The favored model is that these hydrothermal fluids circulated into the underlying basement schists via fractures, schistosity, and cleavages where they transported Po atoms generated by grossly accelerated decay of ^{238}U within zircon crystals inside the schists' biotite flakes. Some of these Po atoms were scavenged from solution at defect sites along cleavage planes within the biotite flakes and produced Po radiohalos, many without adjacent ^{238}U radiohalos. Compared with a similar process that occurred in granite magmas that crystallized and cooled also during the Flood, this was a slower, less effective process that likely lasted for months. The ^{210}Po atoms being longer-lived than ^{218}Po and ^{214}Po atoms were transported further by these hydrothermal fluids of lesser volume and less vigorous circulation than those generated from granite magmas that were generated and crystallized during the Flood, as well as those hydrothermal fluids expelled by regional metamorphism of other Flood-deposited sediment layers during the Flood.

Keywords: Grand Canyon, inner Granite Gorges, Precambrian, Vishnu Schist, Rama Schist, ^{238}U radiohalos, ^{210}Po radiohalos, zircons, fiat creation, hydrothermal fluids, the Flood

Introduction

Grand Canyon is a classic region for the study of geology from an evolutionary perspective, because its rocks span much of the earth's claimed long history. From the granites and schists of the crystalline Precambrian basement in the inner Granite Gorges one can traverse upward through the tilted overlying Precambrian Grand Canyon Supergroup sedimentary strata sequence within the inner Granite Gorges, across the Great Unconformity marking the Precambrian-Phanerozoic boundary, then up through the flat-lying Paleozoic fossil-bearing sedimentary strata in the walls of the outer Canyon. To the north one can then climb the Grand Staircase through Mesozoic and Cenozoic sedimentary strata of the Colorado Plateau. Thus, the Grand Canyon region is an amazing place to study the sequence of strata produced during the earth's history, making it a showcase for the uniformitarian slow-and-gradual billions-of-years (deep time) interpretative framework.

Therefore, the same Grand Canyon-Grand Staircase region provides a unique opportunity and challenge for creation-Flood geologists to investigate the same strata sequence within a catastrophic creation-Flood interpretative framework, demonstrating that it confirms the biblical account of earth's history. Many research studies have already been undertaken and published. For example, it has been shown that many of the flat-lying Paleozoic sedimentary layers contain evidence of their rapid deposition, and that they can be traced beyond the Colorado Plateau as a stacked sequence of comparatively thin "pancake" layers that spread right across the North American continent, as would be expected from deposition in the global Flood cataclysm (Austin 1994; Clarey 2020; Clarey and Werner 2023; Snelling 2009, 2021a, b, 2022a, b; Whitmore et al. 2014; Whitmore and Garner 2018). But the scope of the Canyon's geology means that this task is ongoing.

Perhaps the biggest challenge is dealing with the granites and schists of the Precambrian crystalline basement within the young-earth time framework of the biblical account of only 6,000–7,000 years total for the earth's history. That history included two unique periods when today's rates for geological processes did not apply—the Creation Week when God created by fiat a fully-formed, fully-functioning universe within six literal 24-hour days, and the year-long global Flood cataclysm when geological process rates were hugely accelerated.

The granites and schists of the Precambrian crystalline basement by virtue of being foundational to the overlying sedimentary strata sequences have thus been interpreted as Creation Week rocks, formed by God supernaturally during Creation Days 1–2 (Austin 1994; Snelling 2009, 2022b). The fact that those rocks appear to have formed via processes such as melting and metamorphism of preexisting rocks respectively would seem irrelevant because God could have created them supernaturally. Jesus the Creator (John 1:1–3; Colossians 1:15–17; Hebrews 1:1–2) miraculously created more bread and fish from five loaves and two fish to feed 5,000 men plus women and children (John 6:1–13) without having to use accelerated natural processes of harvesting grown wheat, crushing it, then baking it, etc. Yet, those loaves and fish created by fiat probably looked the same as the ones in the boy's lunch. Thus we would expect granites and schists created supernaturally to look like those formed, for example, during the Flood cataclysm.

So how would an investigator today know whether granites and schists were created supernaturally by God or were produced by crystallization from magmas and metamorphism of preexisting rocks respectively? It was for this reason that when polonium (Po) radiohalos were identified in granites, they were called God's "fingerprints of creation" because the parent Po isotopes only have fleeting existences and thus the granites containing them must have been created by fiat (Gentry 1988). However, when Wise (1989) and Snelling (2000) highlighted that the Po radiohalos (microscopic halos due to crystal damage by radioactive decay) were also found in granites that intruded into Flood-deposited, fossil-bearing sedimentary layers, such granites had to form relatively rapidly during the Flood and thus could not have been created by fiat during the Creation Week. Therefore, Snelling and Armitage (2003) and Snelling (2005) proposed a hydrothermal fluid transport model for the formation of Po radiohalos, a model that has subsequently been successfully tested (Snelling 2008b, c, d, 2014a, 2018; Snelling and Gates 2009).

Nevertheless, Po radiohalos are also found in Precambrian crystalline basement granites that are regarded by some as the foundation rocks from and on which today's continents were formed (Wise 1989; Snelling 2000, 2023b). Thus, to understand these radiohalos better a careful systematic study was undertaken of radiohalos present in the granites of Grand Canyon's Precambrian crystalline basement (Snelling 2025), and in this follow-on study of radiohalos present in the schists that host those granites, particularly to assess the significance of the Po radiohalos within the earth's history, especially within the biblical framework.

The Grand Canyon Precambrian Schists—The Conventional Interpretation

The east-west trending Grand Canyon presents spectacular exposures for 200 km of the Lower Proterozoic (Paleoproterozoic) rocks of the crystalline basement beneath the Colorado Plateau (Karlstrom et al. 2003). In the Upper Granite Gorge, these rocks are continuously exposed from river mile 78 to 120 (as measured downstream from Lees Ferry), while there are discontinuous exposures in the Middle Granite Gorge from mile 127 to mile 137 (fig. 1) (Ilg et al. 1996; Karlstrom et al. 2003). The Lower Granite Gorge contains near-continuous outcrops from mile 207 to mile 261.

Powell (1876) was the first to identify the Precambrian "granite" and "Grand Canyon schists." Walcott (1889) identified the Vishnu "terrane" as a complex of schist and gneiss. Since then, the subdivisions of the Precambrian rocks have continued to be refined by numerous workers beginning with Noble and Hunter (1916). They identified domains of contrasting rock packages and recognized that differences reflected the presence of both metasedimentary and intrusive igneous rocks, and that some gneisses possibly were a basement on which the metasedimentary units were deposited. Subsequently, Campbell and Maxson (1938) identified different mappable units of the Vishnu and Brahma "Series" but underestimated the structural complexities and probably overestimated the stratigraphic thickness. Brown et al. (1979) also emphasized the complex deformational features and lumped all the metasedimentary and metavolcanic rocks under the name "Vishnu Complex," while Babcock et al. (1979) described some of the granite plutons that intruded those metamorphic rocks. Finally, Babcock (1990) summarized the complex geology of the Precambrian rocks in the granite gorges as then mapped and understood.

As a result of renewed detailed field mapping and photogeologic interpretation of high-resolution aerial photographs of the river corridor, Ilg et al. (1996) presented an updated description of the Precambrian granites and schists and provided a new map of

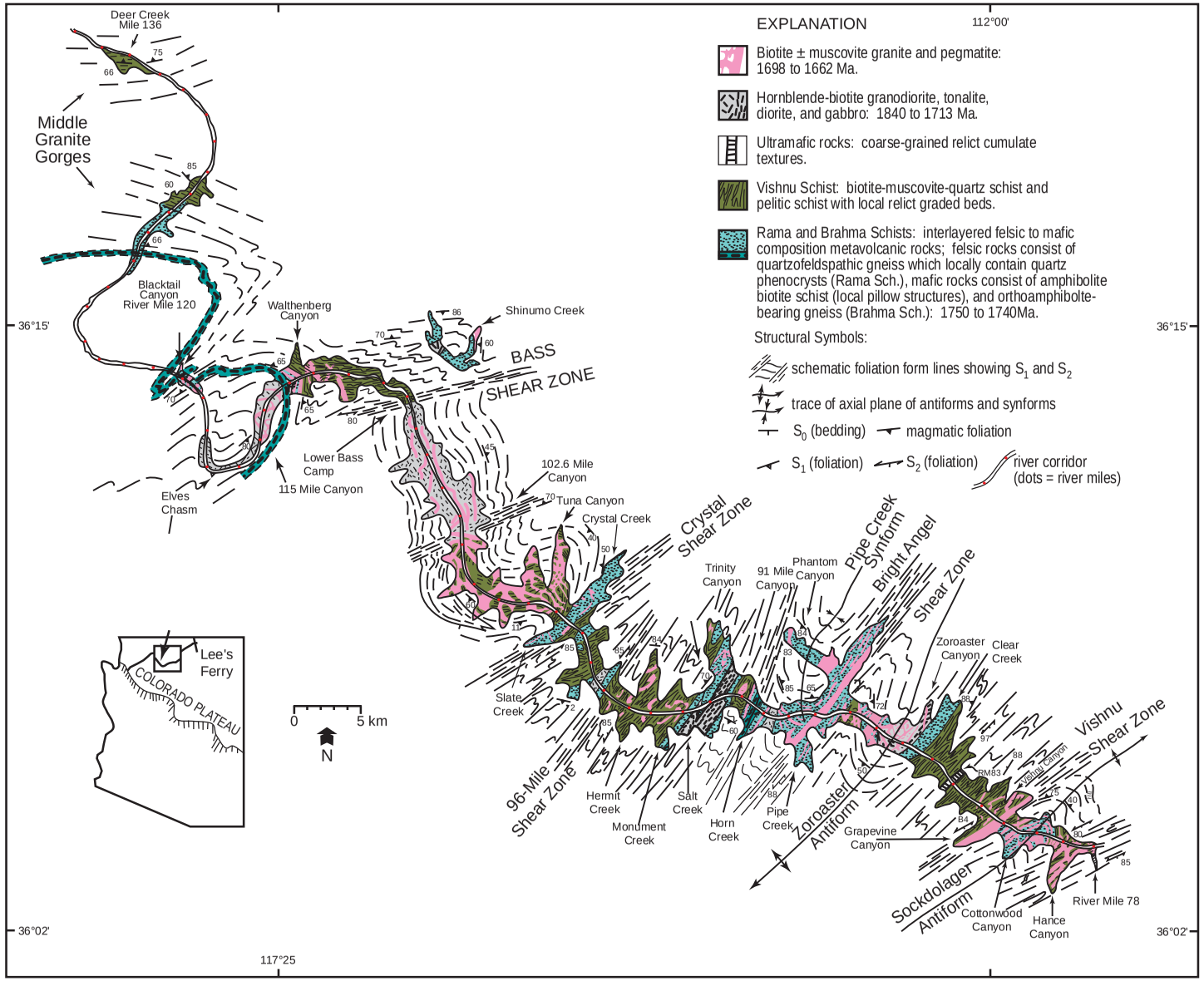

Fig. 1. Simplified geologic map of Paleoproterozoic (Lower Proterozoic) rocks in the Upper and Middle Granite Gorges, Grand Canyon, northern Arizona (after Ilg et al. 1996; Karlstrom et al. 2003). Form lines outside the Paleoproterozoic exposures show their interpretation of the trace of the regional foliation on the map surface. The transect is divided into metamorphic domains that are generally separated by shear zones.

the geology of the inner gorges that incorporated previous work. Ilg et al. (1996) provided new insights regarding the lithostratigraphy and the nature of the protoliths.

In updating the work of Ilg et al. (1996), Karlstrom et al. (2003) followed their strategy in recognizing the need simultaneously to pursue both tectonic and stratigraphic subdivisions of the Proterozoic crystalline basement rocks. The tectonic perspective is that the complex deformation and metamorphism of these rocks make it impossible to measure thickness and to confidently reconstruct regional stratigraphy. There are also important shear zones that are boundaries of unknown displacement, some possibly representing suturing of separate tectonic blocks that may once have been hundreds to even thousands of kilometers apart (Karlstrom et al. 2003). Thus, it is not certain that all the metasedimentary schists are strictly correlative—same age, same basin, same depositional sequence. However, the work of Hawkins et al. (1996), Ilg et al. (1996), and Karlstrom et al. (2003) permits a stratigraphic interpretation in which the metasedimentary rocks within the Canyon's inner gorges are broadly of similar rock type and age (1.73–1.75 Ga). Thus, the entire metasedimentary-metavolcanic package could have been deposited in a single basin, or in similar but tectonically separate basins. For these reasons those metasedimentary and metavolcanic units have been grouped together as the Granite Gorge Metamorphic Suite.

Early studies in the Grand Canyon suggested that the quartzofeldspathic Elves Chasm Gneiss and Trinity Gneiss were basement to the schists (Noble and Hunter 1916). Subsequent workers recognized that the gneisses were deformed intrusive rocks (Babcock 1990; Brown et al. 1979; Campbell and Maxson 1938), but there was still debate on whether the Elves Chasm and Trinity gneisses are possible basement for the Vishnu Schist. However, the mapping by Ilg et al. (1996) and geochronology studies by Hawkins et al. (1996) indicate that the gneisses have different ages in different areas. Thus, the Trinity Gneiss (Babcock et al. 1979) is interpreted as a deformed and metamorphosed granodiorite that intruded into the Granite Gorge Metamorphic Suite with a U-Pb zircon age of 1.73 Ga

In contrast, the Elves Chasm pluton is 1.84 Ga (Hawkins et al. 1996), apparently the oldest rock in the southwestern United States and likely the basement for the turbidites that are now the Vishnu Schist. It is dominantly hornblende-biotite tonalite to quartz diorite and is distinguished geochemically from other plutons in Grand Canyon (Karlstrom et al. 2003). The contact zone between the Elves Chasm pluton and the overlying Granite Gorge Metamorphic Suite is exposed in several places and is gradational over several meters. The composition of the contact zone is unusual, which suggested to Babcock (1990) that alteration took place during weathering before the overlying sediments were deposited that are now the Vishnu Schist.

Intrusive rocks, primarily granites, make up half the Precambrian crystalline rocks of Grand Canyon's inner gorges. Campbell and Maxson (1938) thought there was a single major period of granite intrusive activity and this led to lumping all the granites under the single name Zoroaster Granite (Babcock et al. 1979). However, the new mapping (fig. 1) (Ilg et al. 1996) and geochronology (Hawkins et al. 1996) show that the granitic rocks record an apparent long and complex development of the crust at numerous times between 1.84 and 1.37 Ga, with a wide variation in the types of granites based on their different petrology and geochemistry (Karlstrom et al. 2003). However, partial crystallization and differentiation as the magmas cooled would have produced granites of different compositions. Thus, a single rock name may be misleading, so the names of individual plutons or dike swarms are used. The mapped granite plutons and pegmatite complexes are depicted in cross-section, along with the metamorphic schists in the various tectonic blocks in fig. 2 (Dumond et al. 2007).

Metasedimentary and metavolcanic rocks of the Granite Gorge Metamorphic Suite make up the other half of the exposed rocks in the Precambrian crystalline basement of Grand Canyon (Ilg et al. 1996; Karlstrom et al. 2003). Overall, the Granite Gorge Metamorphic Suite consists of a variety of schists containing quartz, K-feldspar, plagioclase, biotite, muscovite and other metamorphic minerals in various assemblages such as garnet, staurolite, sillimanite, chloritoid, kyanite and cordierite. Based on the mappable rock types in the Upper Granite Gorge, Ilg et al. (1996) and Karlstrom et al. (2003) subdivided the schists and assigned names: Brahma Schist for mafic metavolcanic rocks, after the Brahma "series" of Campbell and Maxson (1938), and Rama Schist for felsic metavolcanic rocks. The term Vishnu Schist they assigned to the metamorphosed sedimentary rocks, as probably was intended by Walcott (1894), recommended by Noble and Hunter (1916) (their Vishnu schist), and proposed by Campbell and Maxson (1938) (their Vishnu "Series"). Rocks in the Lower Granite Gorge also fall into these three basic lithologic groups.

The Ramu and Brahma metavolcanic schists can be complexly interlayered, although at outcrop scale they are generally separable. Hawkins et al. (1996) reported that none of these mafic rocks have been directly dated, but they are intruded by or interlayered with felsite beds within amphibolite of

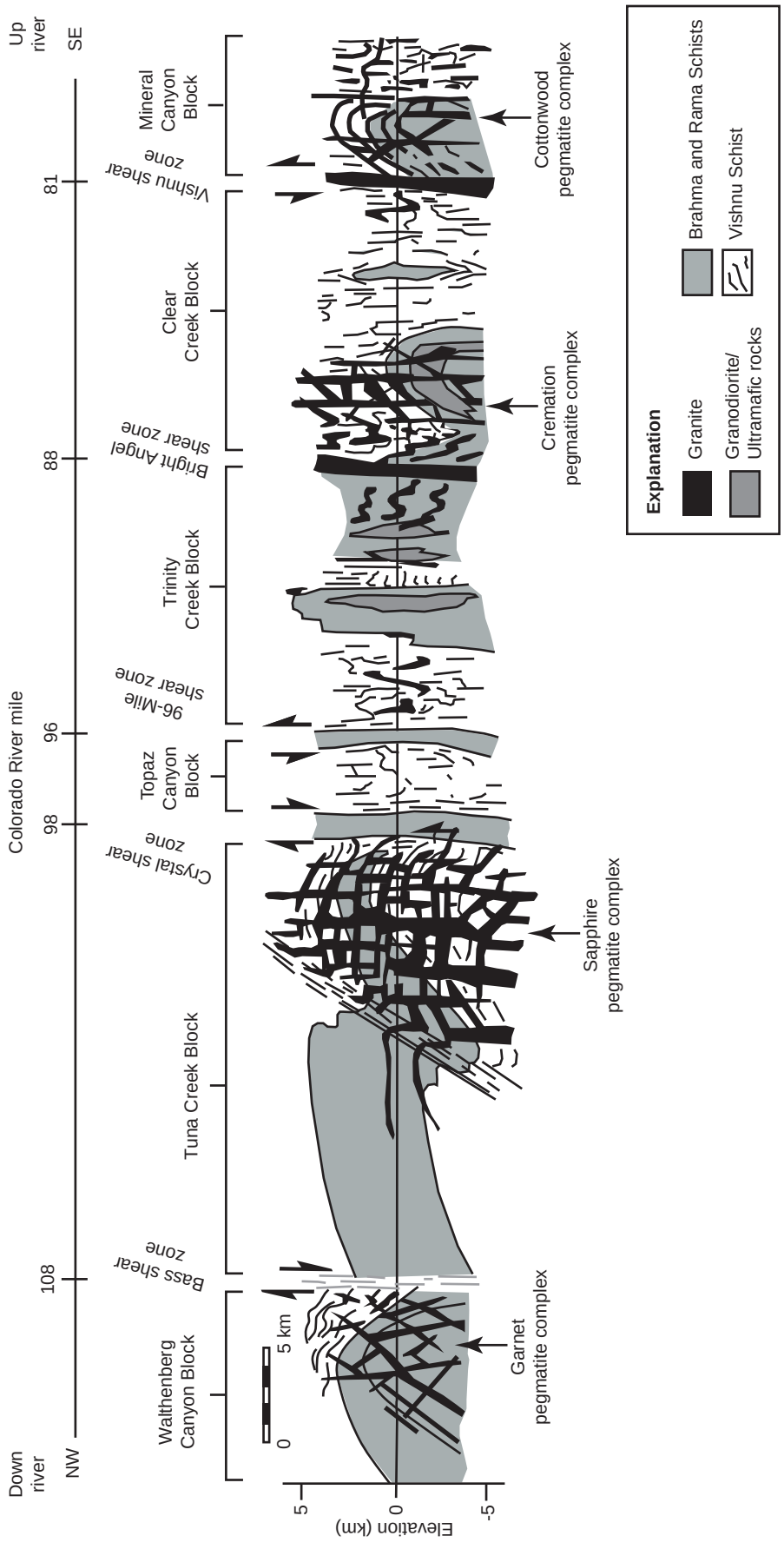

Fig. 2. Geologic cross-section of the Upper Granite Gorge, Grand Canyon (as shown in fig. 1) (after Dumond et al. 2007; Ilg et al. 1996). This cross-section was constructed by projecting folds up and down plunge into the section line. It shows their interpretation of the macroscopic geometry of Paleoproterozoic rocks in Grand Canyon before uplift and erosion. The section shows ~10 km of vertical structural relief and large F2 folds that repeat lithologies across the transect. The lithotectonic blocks-metamorphic domains are depicted. The high-strain zone boundaries or shear zones are typically developed on the limbs of large folds or adjacent to heterogeneities such as granite plutons or pegmatite dike complexes.

the Brahma Schist at Clear Creek (river mile 84.7) which yielded at zircon U-Pb date of 1.75 Ga. The Brahma Schist is also intruded by a 1.73 Ga dacite dike in Pillow Basalt Canyon (river mile 229.5), while a felsic gneiss within the Rama Schist in the Sockdolager antiform (river mile 79.6) yielded a zircon U-Pb date of 1.742 Ga (Hawkins et al. 1996). Contact relationships support variable relative ages between the mafic and intermediate metavolcanic rocks. In the Upper Granite Gorge, Rama Schist is underneath and older than the Brahma Schist in the Sockdolager antiform (river mile 79.6) and Shinumo Creek area (river mile 109.3). In the Diamond Creek and Travertine areas of the Lower Granite Gorge (river miles 226 and 229.2 respectively), Rama intermediate metavolcanic rocks and dikes appear younger than the Brahma amphibolites based on younging of metabasalt pillows and intrusion of the 1.73 Ga dacite dike into the amphibolites. However, Snelling (2008e) reported highly discordant whole-rock K-Ar model and Rb-Sr, Sm-Nd and Pb-Pb isochron ages for the Brahma Schist's massive amphibolites.

The Rama Schist consists of quartzofeldspathic schist and gneiss. It is dominated by massive fine-grained quartzofeldspathic rocks that locally preserve euhedral plagioclase laths. The unit also contains meta-rhyolites with well-preserved quartz phenocrysts and interlayered micaceous quartzofeldspathic schists and gneisses. The Rama Schist is commonly complexly injected with pegmatite and contains leucocratic layers that may in part reflect preferential partial melting of these rocks. The presence of euhedral plagioclase laths in a fine grained quartzofeldspathic matrix suggests that the protoliths of these rocks are metamorphosed felsic lapilli-crystal tuffs.

The Brahma Schist consists of amphibolite, hornblende-biotite-plagioclase schist, biotite-plagioclase schist, orthoamphibole-bearing schist and gneiss, and metamorphosed sulfide deposits. The petrology and geochemistry of Brahma Schist amphibolites were studied by Clark (1976), who divided the amphibolites and mafic schists into two main groups based on field occurrence and mineral assemblage: (1) anthophyllite-bearing and cordierite-anthophyllite–bearing rocks (orthoamphibole schists), and (2) "early amphibolites." It is conventionally accepted that the orthoamphibole-bearing (group 1) rocks are metamorphosed, hydrothermally altered, mafic marine volcanic rocks and that the "early amphibolites" (group 2) are metamorphosed basalts and basaltic tuffs.

Massive amphibolite (group 2) makes up 30%–40% of the Brahma Schist. This unit does not typically preserve primary igneous features. However, relict pillow structures are present in numerous locations (Ilg et al. 1996). The massive amphibolites have a tholeiitic character and trace element compositions consistent with an island-arc environment (Clark 1976, 1979). Biotite+plagioclase schist and hornblende+biotite+plagioclase schist (the remainder of group 2) make up >50% of the Brahma Schist in the Upper Granite Gorge. Strong tectonic layering has obscured primary igneous textures in most locations. However, original textures are preserved in several locations (for example, along the river trail between the Kaibab and Bright Angel bridges), where subangular quartz+plagioclase+biotite fragments are entrained in an amphibolitic matrix, suggesting that some of these rocks may have been volcaniclastic breccias. Interlayered with the biotite schist are discontinuous meter-scale lenses of garnet+diopside+epidote+calcite rocks. The protoliths of these lenses are possibly relatively thin layers of a calcareous shale (Campbell and Maxson 1938) or algal mats interbedded with submarine sediments (Babcock 1990).

The Brahma Schist also contains exposures of orthoamphibole-bearing rocks (group 1). Examples are exposed just below Waltenberg Canyon (river mile 115) and near Blacktail Canyon (around river mile 120). These rocks are characterized by gedrite + anthophyllite + cordierite + cummingtonite + biotite+garnet assemblages. They are interpreted to be hydrothermally altered, mafic marine volcanic rocks (Vallance 1967). The presence of relict pillow basalt, orthoamphibolite rocks, and associated sulfide mineralization indicates that the Brahma Schist was the product of dominantly mafic submarine volcanism. Large-scale interlayering of mafic to intermediate composition (Brahma) and felsic (Rama) volcanic rocks is similar to that found in the Yavapai Supergroup of central Arizona (Condie 1986), while the approximate ages for the mafic-felsic Rama-Brahma package is nearly identical in age to the 1.75–1.74 Ga Yavapai Supergroup of central Arizona (Karlstrom and Bowring 1993).

The Vishnu Schist consists of pelitic schist and quartz+biotite+muscovite schists interpreted as metamorphosed lithic-arenites, graywackes, and mudstones with calc-silicate lenses and pods that have been interpreted as deposited under submarine conditions on the flanks of eroding oceanic islands (Karlstrom et al. 2003). The metamorphosed lithic-arenite and graywacke sequences show thick sections (kilometer-scale) of rhythmically banded (centimeter- to meter-scale) coarser and finer layers, with locally well-preserved bedding and graded bedding (Clark 1976; Walcott 1894) suggesting deposition as submarine turbidites. Locally, the Vishnu Schist contains pelitic and semi-pelitic schists that variably

contain andalusite, sillimanite, staurolite, chloritoid, cordierite, and garnet. The original grain size in the Vishnu Schist metasedimentary rocks probably ranged from medium-grained sand to silt and clay.

Conglomerates are conspicuously absent in the Vishnu metasedimentary rocks (Campbell and Maxson 1938). Relict graded bedding associated with metavolcanic rocks containing pillow structures, the lack of coarse sediments, and geochemical data (Babcock 1990) indicate that the metasedimentary units may have accumulated in an oceanic island-arc environment, as suggested for the Yavapai Supergroup rocks of central Arizona (Anderson and Silver 1976; Bowring and Karlstrom 1990). The calc-silicate pods are numerous and are interpreted to have been concretions. The contact between the Vishnu Schist and the Brahma Schist is generally concordant, and the rocks are interlayered as in Clear Creek (river mile 84.6). However, the preserved graded bedding indicates that the Vishnu Schist was deposited stratigraphically above the Brahma Schist in the Waltenberg area (river mile 112–113).

Shufeldt et al. (2010) U-Pb dated 1035 detrital zircons from twelve spatially distributed samples of the Vishnu Schist and reported a bimodal $^{207}Pb/^{206}Pb$ age probability distribution with peaks at 1.8 Ga and 2.5 Ga. Of the youngest grains, 79 (7.5% of the 1035 grains) yielded a maximum depositional age of 1749±19.5 Ma for the Vishnu Schist, while only 13% of the detrital zircon ages overlapped with the published depositional age range of 1741–1750 Ma (Hawkins et al 1996). Ironically, Shufeldt et al. (2010) did not explain how the detrital zircon grains younger than that depositional age, as young as 1660 Ma, could have been deposited in the precursor sediments of the Vishnu Schist. Nevertheless, almost 81% of the detrital zircon grains are older than 1.75 Ga, suggesting that the predominance of the detritus in the Vishnu Schist came from older pre-1.75 Ga crust. Thus, they noted that 15% of the detrital zircon grains overlap with the 1.84 Ga age of the Elves Chasm pluton in central Grand Canyon, which supports field evidence that the precursor sediments of the Vishnu Schist were deposited on that 1.84 Ga crystalline basement. Otherwise, Archean grains aged 2.5–3.8 Ga compose 30% of the detrital zircon grains, with an additional 140 grains (13.5%) of earliest Paleoproterozoic age (2.45–2.5 Ga) thus contributing to the 2.48 Ga peak. Comparison with compilations of zircon ages from other cratons does not support provenances in the Wyoming, South China or Siberian cratons, so they concluded that unexposed proximal basement sources are likely, suggesting that the Vishnu sediments were derived from the nearby Mohave province Archean crust now in the subsurface that was unroofed during Vishnu deposition.

Finally, Dumond et al. (2007), Ilg et al. (1996), and Karlstrom et al. (2003, 2012) discuss the metamorphism and deformation of the precursor sediments and volcanics. The pelitic layers of the Vishnu Schist contain various assemblages of the metamorphic minerals garnet, sillimanite, staurolite, chloritoid, cordierite, kyanite, and andalusite (rare) that can be used to estimate the pressure (P) and temperature (T) history of the rocks. For example, the sillimanite-K-feldspar assemblage in the schists at Mineral Canyon (river mile 78) indicate a temperature of 750°C, the staurolite-garnet assemblage at Monument Creek (river mile 94) indicate lower temperatures of 550–600°C, and the andalusite crystals at Clear Creek (river mile 84.6) indicate temperatures of <550°C (Dumond et al. 2007; Karlstrom et al. 2012). In addition to recording P-T data, many metamorphic minerals, such as garnet, have textures that can be used to document the interaction and relative timing of deformation and metamorphic processes deep in the crust.

Thus, metamorphic assemblages vary across the Upper Granite Gorge, reflecting differences in bulk composition and peak-metamorphic conditions (Babcock 1990; Dumond et al. 2007; Ilg et al. 1996; Karlstrom et al. 2003, 2012). In general, domains with upper greenschist- to lower amphibolite-facies assemblages alternate with domains containing upper amphibolite- or granulite-facies rocks. On the basis of mineral assemblages and the calculated P-T estimates, the Upper Granite Gorge can be divided into six metamorphic domains (or tectonic blocks) (figs. 2 and 3). The lower-grade domains (for example, the Topaz Canyon block between river miles 96–98) are interpreted to record near-ambient peak-metamorphic conditions of >500°C at 6 kbar, while the three higher-grade domains, the Tuna Creek, Trinity Creek, and Mineral Canyon blocks, record peak-metamorphic conditions of >650–725 °C at 6 kbar and are generally associated with regions intruded by granite plutons and pegmatite dikes (figs. 2 and 3).

Although temperatures vary significantly from amphibolite- to granulite-facies domains, pressures are 6–8 kbar (0.6–0.8 GPa) along the entire canyon transect, equivalent to depths of 20–25 km (12–15 mi) (Dumond et al. 2007; Karlstrom et al. 2012). Because peak pressures were relatively uniform throughout the transect, tectonic juxtaposition of different crustal levels cannot account for the temperature differences recorded across the transect. Instead, a major component of the temperature difference apparently resulted from advective heat transfer that elevated ambient temperatures of >500°C by as much as 200°C correlate with regions of high pegmatite density, so

that the relatively local variation in metamorphic grade is attributed to regional metamorphism enhanced by heat provided by high metamorphic fluid flux and high pegmatite and/or granite dike densities in narrow (1–10 km [0.6-6 mi] wide) domains. This is best illustrated between river mile 77 and the Vishnu shear zone (river mile 81.5) (figs. 2 and 3) where calculated peak temperatures are between 650 and 725°C and pegmatite dike densities are quite high. Yet, immediately west of the Vishnu shear zone, peak temperatures are >500°C, and pegmatite dike densities drop to zero within 300 m of the shear zone in the Clear Creek block. However, it is also likely that deformation associated with shear zones telescoped or truncated some of the pluton- or dike-related thermal gradients.

At these high pressures and elevated temperatures at those depths in the crust the rocks were deformed plastically, so that layers in the Vishnu Schist were first thrust over themselves, then folded and refolded during such flow. The early F_1 (first generation) folds are cross-cut and hence older than the pegmatite dikes. The F_2 (second generation) folds not only fold the original sedimentary bedding and the bedding-parallel mineral alignment but also the pegmatite dikes. Those F_2 folds are commonly oriented vertically and have axes that are aligned northeast-southwest, indicating that the flow occurred as the rocks were deformed by NW-SE subhorizontal compression. During this F_2 compression, which forms the main fabric of these basement rocks, pre-existing bedding and all platy minerals such as micas were folded and rotated to be aligned perpendicular to the NW-SE horizontal compressive stress to form the penetrative schistosity. Thus the tectonic fabrics in the basement rocks of the Upper Granite Gorge are aligned in a northeasterly direction and the lineation is subvertical. However, not all the deformation involved compression and crustal thickening. In some areas stiffer blocks slide past each other across weaker shear zones of intense deformation.

History and Significance of U and Po Radiohalos

Radiohalos are minute circular zones of darkening (39–70 µm in diameter) surrounding tiny central mineral inclusions or crystals within some minerals. Often concentric darkened rings are distinguishable within the darkened circular areas. While radiohalos appear in fluorite, cordierite, quartz, and to a lesser extent K-feldspars, they are best observed in thin microscope sections of the black mica, biotite, where the tiny inclusions (or radiocenters) are usually zircon crystals. The significance of radiohalos is due to them being a physical, integral historical record of the decay of radioisotopes in the radiocenters over a period of time.

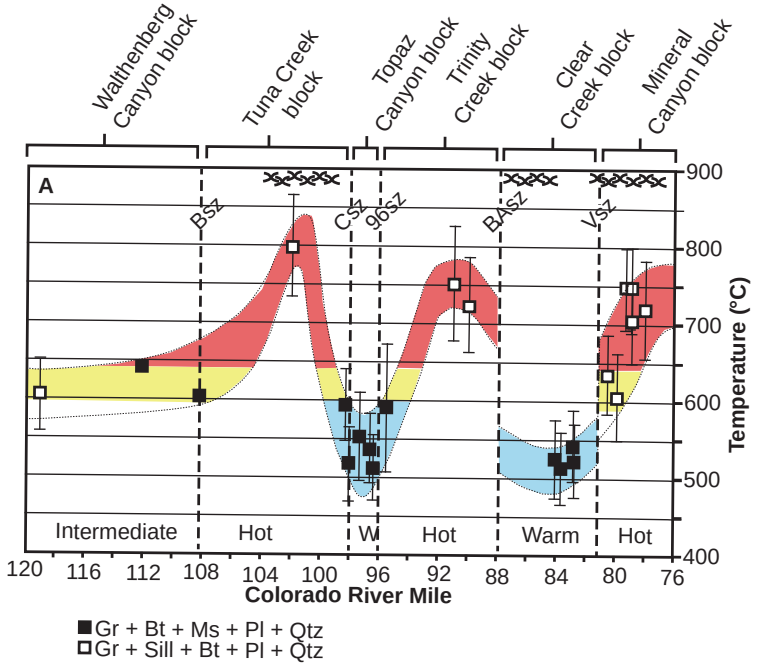

Fig. 3. Temperature (T) of metamorphism as measured mineral compositions, after Dumond et al. (2007) and Karlstrom et al. (2012). The crystalline basement rocks show different temperature regimes in different lithotectonic blocks-metamorphic domains. The highest temperatures were reached ~700–800°C in the Mineral Canyon, Trinity Creek, and Tuna Creek blocks in areas associated with granite and pegmatite dike swarms (cross-hatched pattern). The coolest temperatures of 500–550°C were found in the Clear Creek and Topaz Canyon blocks. Bsz=Bass shear zone, Csz=Crystal shear zone, 96sz=96-Mile shear zone, BAsz=Bright Angel shear zone, and Vsz=Vishnu shear zone.

First reported between 1880 and 1890, their origin was a mystery until the discovery of radioactivity. Then Joly (1907) and Mügge (1907) independently suggested that the darkening of the minerals around the central inclusions is due to the alpha (α) particles produced by α-decays in the radiocenters. These α-particles are "fired" in all directions like "bullets" and thus damage the crystal structure of the surrounding minerals. It is known as a Frenkel defect (a type of point defect) accumulation in which smaller atoms (the α-particles are essentially helium nuclei) dislodge larger atoms from their places in the crystal lattice creating vacancies in which the smaller atoms accumulate interstitially. This process produces concentric shells of darkening or discoloration (fig. 4). When observed in thin sections these shells are concentric circles with radii between 39 and 70 µm, simply representing planar sections through the concentric spheres centered around the inclusions (Gentry 1973).

Many years of subsequent investigations have established that the radii of the concentric circles of the radiohalos as observed in thin sections are related to the α-decay energies. This enables the radioisotopes responsible for the α-decays to be identified (Gentry 1974, 1984, 1986, 1988; Snelling 2000). Most importantly, when the central inclusions, or radiocenters, are very small (about 1 µm) the radiocenters around them have been unequivocally demonstrated to be products of the α-emitting members of the ^{238}U decay series to stable ^{206}Pb, and occasionally the ^{232}Th decay series to stable ^{208}Pb. It has been demonstrated that the radii of these rings correspond to the energies of specific α-particles in the ^{238}U decay series and their travel ranges (Gentry 1984). Thus, a fully-developed ^{238}U radiohalo should have eight visible concentric rings which correspond to the eight α-decay steps in the ^{238}U decay series. It has also been determined that such a halo requires between 500 million and 1 billion α-decays to be fully-developed and darkened (fig. 4) (Gentry 1988). The radii of the concentric multiple spheres, or rings in thin sections, correspond to the ranges in the host minerals of the α-particles from the α-emitting radioisotopes in the ^{238}U and ^{232}Th decay series (Gentry 1973, 1974, 1984) (fig. 5). Uranium-235 radiohalos have not been observed. This is readily accounted for by the scarcity of ^{235}U (only 0.7% of the naturally-occurring U), since large concentrations of the parent radionuclides are needed to produce the concentric ring structures of the radiohalos.

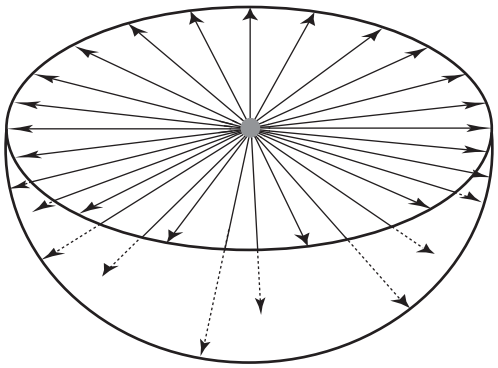

Fig. 4. Sunburst effect of α-damage trails. The sunburst pattern of α-damage trails produces a spherically colored shell around the halo radiocenter. Each arrow represents approximately 5 million α-particles emitted from the radiocenter. Radiohalo coloration initially develops after about 100 million α-decays, becomes darker after about 500 million, and very dark after about 1 billion (after Gentry 1988).

Ordinary radiohalos can be defined, therefore, as those that are initiated by ^{238}U or ^{232}Th α-decay, irrespective of whether the actual halo sizes closely match the respective idealized patterns (fig. 5). In many instances the match is very good, the observed sizes agreeing very well with the ^{4}He ion penetration ranges produced in biotite, fluorite, and cordierite

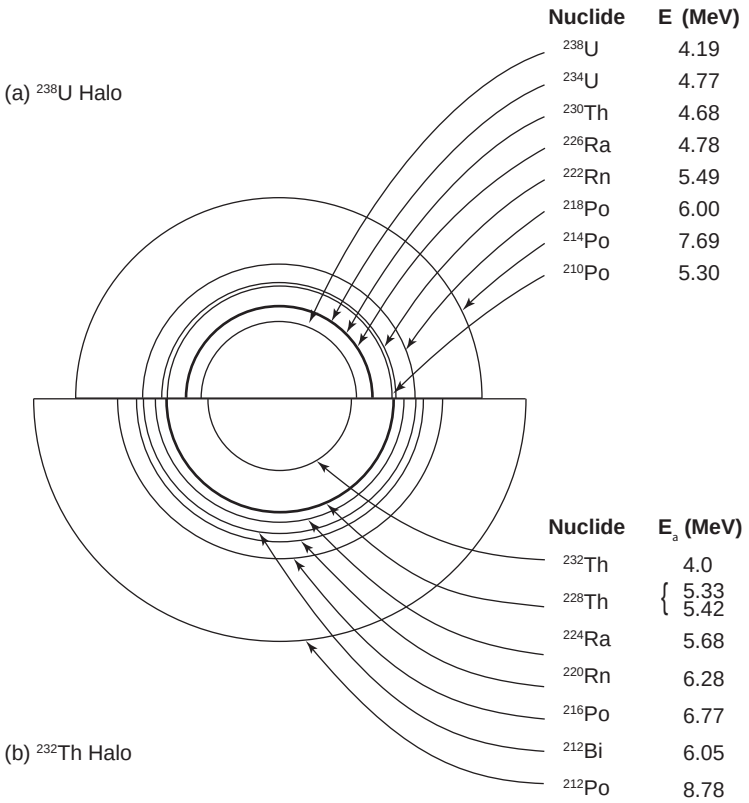

Fig. 5. Schematic drawing of (a) a ^{238}U radiohalo, and (b) a ^{232}Th radiohalo, with radii proportional to the ranges of α-particles in air. The nuclides responsible for the α-particles and their energies are listed for the different halo rings (after Gentry 1973).

(Gentry 1973, 1974). While U and Th radiohalos have been found in over 40 minerals, their distribution within these minerals is very erratic (Ramdohr 1933, 1957, 1960; Stark 1936). Thus far there have been no hypotheses proposed to explain the cause(s) of this erratic distribution. Radiohalos have even been found in diamonds (Armitage and Snelling 2008; Gentry 1998; Schulze and Nasdala 2018).

U and Th radiohalos usually are found in igneous rocks, most commonly in granitic rocks and in granitic pegmatites in which biotite is a major mineral. However, more recently radiohalos have also been reported as common in biotite in some metamorphic rocks (Snelling 2005, 2008b, c, 2023b). Thus biotite is quite clearly the major mineral in which U and Th radiohalos occur (Bower et al. 2016a, b). Wherever found in ubiquitous large (1–5 mm in diameter) biotite flakes the radiohalos are prolific and are associated with tiny (1–5 μm in diameter) U-bearing zircon grains or Th-bearing monazite grains as the radiocenters. The ease of thin section preparation, and the clarity of the radiohalos in these sections, have made biotite an ideal choice for numerous radiohalo investigations, namely, those of Joly (1917a, b, 1923, 1924), Lingen (1926), Iimori and Yoshimura (1926), Kerr-Lawson (1927, 1928), Wiman (1930), Henderson and Bateson (1934), Henderson and Turnbull (1934), Henderson, Mushkat, and Crawford (1934), Henderson and Sparks (1939), Gentry (1968, 1970, 1971), Snelling and Armitage (2003), and Snelling (2005). U, Th, and other specific halo types in most of these studies have been observed mainly in Precambrian rocks, so much remains to be learned about their occurrence in rocks from the other geological systems of the rock record. However, some studies have shown that they do exist in rocks stretching from the Precambrian to the Tertiary (Paleogene and Neogene) (Holmes 1931; Stark 1936; Wise 1989; Snelling and Armitage 2003; Snelling 2000, 2005, 2023b). Unfortunately, in some of those published studies the radiohalo types were not specifically identified.

Some unusual radiohalo types that appear to be distinct from those formed by ^{238}U and/or ^{232}Th α-decay have been observed (Gentry 1970, 1971, 1973, 1984, 1986; Gentry et al. 1973, 1976, 1978; Snelling 2000). Of these, only the Po (polonium) radiohalos can presently be identified with known α-radioactivity (Gentry 1967, 1968, 1973, 1974; Gentry et al. 1973, 1978). There are three Po isotopes in the ^{238}U-decay chain. In sequence they are ^{218}Po (half-life of 3.1 minutes), ^{214}Po (half-life of 164 microseconds), and ^{210}Po (half-life of 138 days). Po radiohalos contain only three rings, two rings or the one ring produced by these three Po α-emitters respectively (fig. 6). They are designated by the first (or only) Po α-emitter in the portion of the decay sequence that is represented. The presence in Po radiohalos of only the rings of the three Po α-emitters implies that the radiocenters which produced these Po radiohalos initially contained only either the respective Po radioisotopes that then parented the subsequent α-decays, or a non-α-emitting parent (Gentry 1971; Gentry et al. 1973). These three Po radiohalo types occur in biotite from granitic rocks (Gentry 1968, 1971, 1973, 1974, 1984, 1986, 1988; Gentry et al. 1973, 1978; Wise 1989; Snelling and Armitage 2003; Snelling 2005). Some typical radiohalos in biotite are shown in fig. 7.

Joly (1917b, 1924) was probably the first to investigate ^{210}Po radiohalos and was clearly baffled by them. Because Schilling (1926) saw Po radiohalos located only along cleavages and cracks in fluorite from Wölsendorf in Germany, he suggested that they originated from preferential deposition from secondary fluid transport of Po in U-bearing solutions. Henderson (1939) and Henderson and Sparks (1939) invoked a similar but more quantitative hypothesis to explain Po radiohalos along conduits in biotite. However, those Po radiohalos found occurring along much more restricted cleavage planes, similar to those found by Gentry (1973, 1974), have been more difficult to account for. Because the rings which should be produced by the Po precursors are

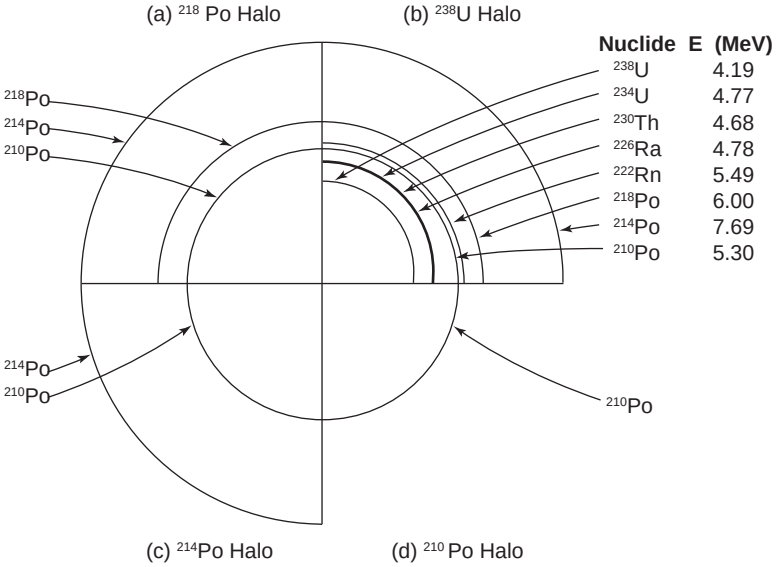

Fig. 6. Composite schematic drawing of (a) a ^{218}Po radiohalo, (b) a ^{238}U radiohalo, (c) a ^{214}Po radiohalo, and (d) a ^{210}Po radiohalo, with radii proportional to the ranges of α-particles in air. The nuclides responsible for the α-particles and their energies are listed for the different halo rings (after Gentry 1973).

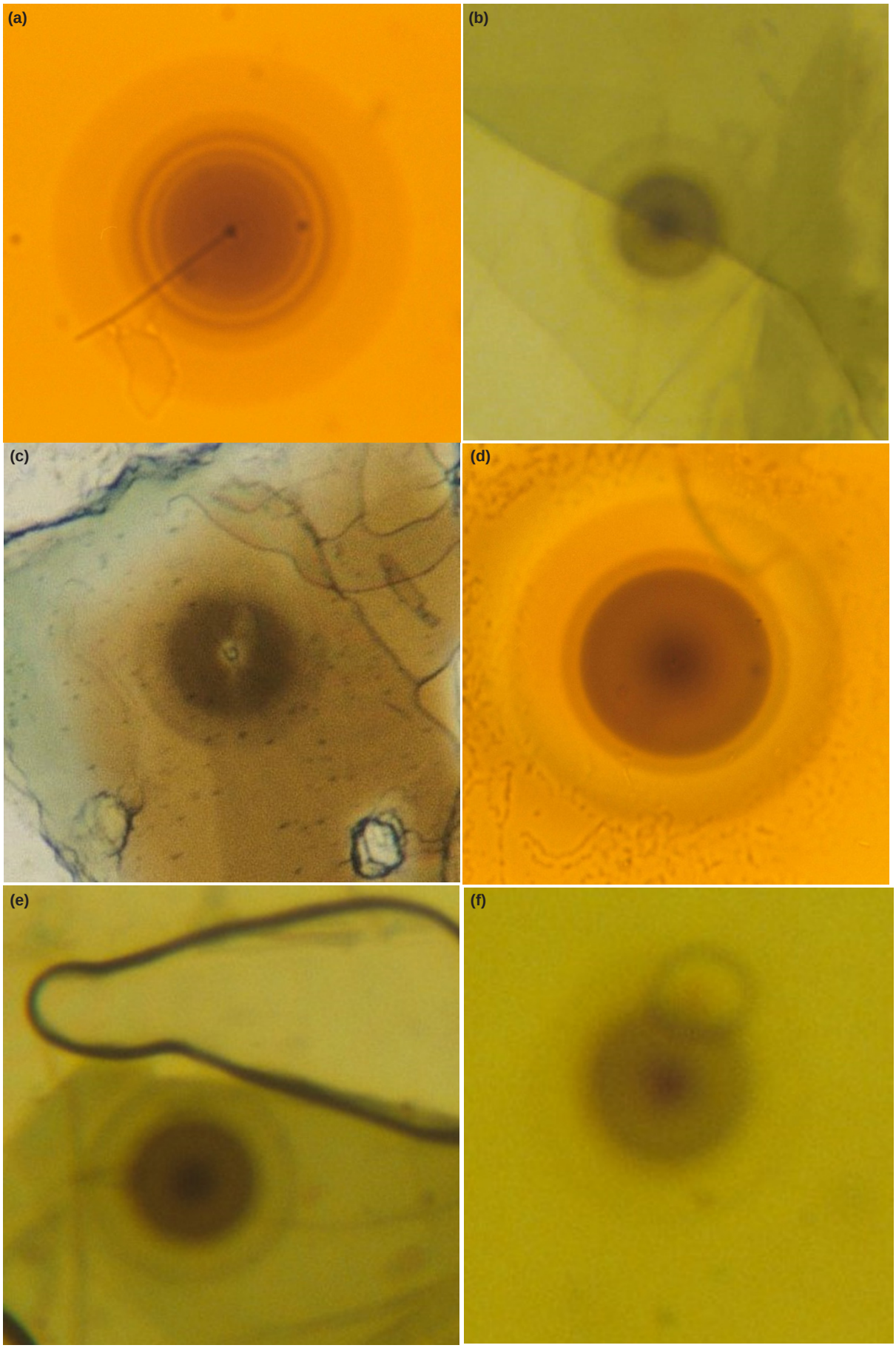
(a)
(b)
(c)
(d)
(e)
(f)

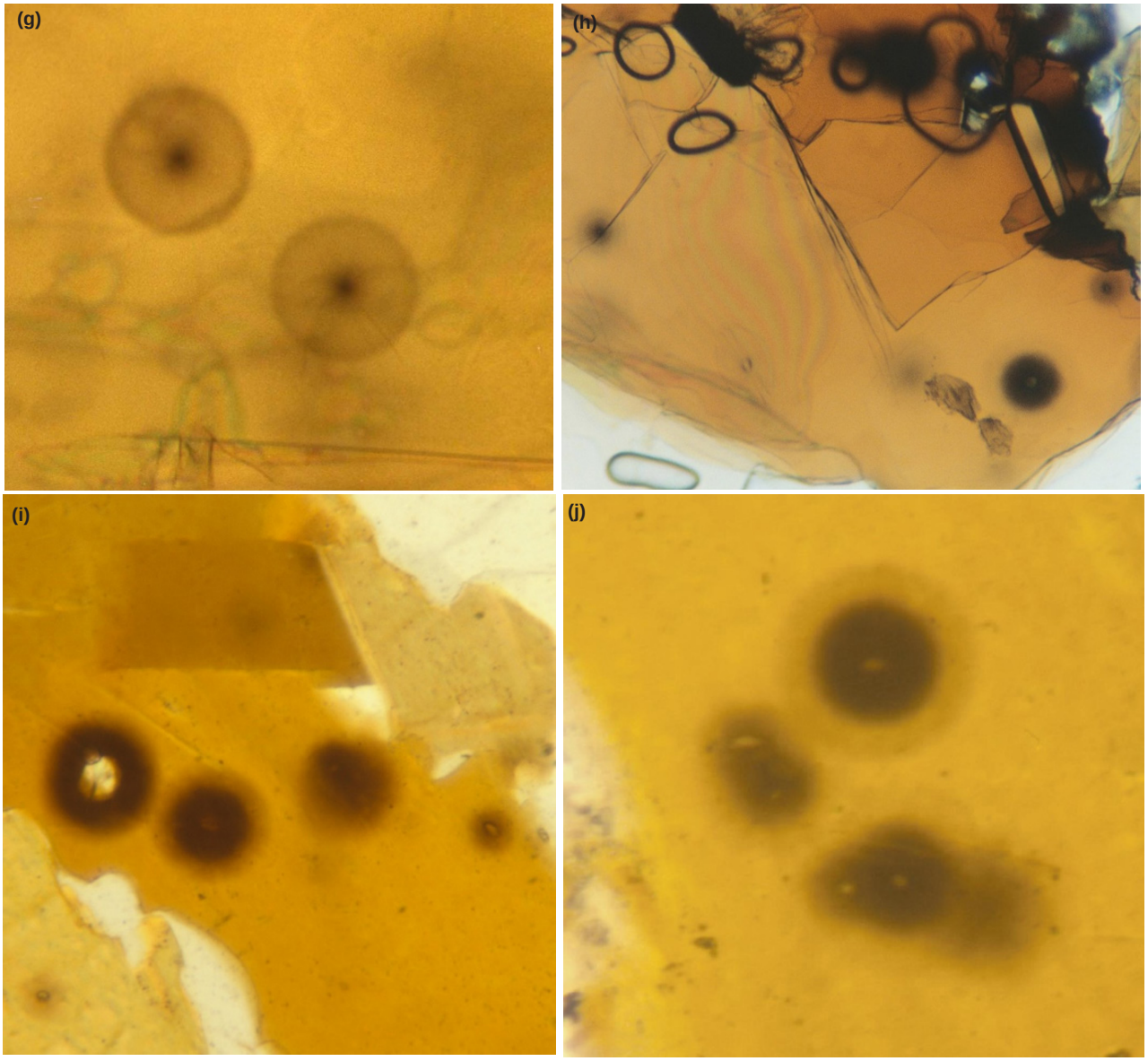

Fig. 7 (pages 387–388). Some typical examples of the different radiohalos found in granites and metamorphic rocks. All images are in focus, but where the radiohalos appear fuzzy it is due to faintness of the radiation damage or to the intense radiation damage broadening the outlines and the rings: (a) a ^{238}U radiohalo with well-defined rings; (b) a ^{238}U radiohalo; (c) an overexposed ^{238}U radiohalo; (d) a ^{218}Po radiohalo with well-defined rings; (e) a ^{218}Po radiohalo; (f) a ^{214}Po radiohalo; (g) two well-defined ^{210}Po radiohalos; (h) an overexposed ^{238}U radiohalo (bottom right), a ^{214}Po radiohalo (center left), and a ^{210}Po radiohalo (center right); (i) an extremely overexposed ^{238}U radiohalo due to a large zircon crystal as its radiocenter (left), another overexposed ^{238}U radiohalo (left of center), and a ^{214}Po radiohalo (right); and (j) two ^{238}U radiohalos with overexposed inner rings and three overexposed ^{210}Po radiohalos. Scales: ^{238}U radiohalo diameter ≈ 70 µm, ^{218}Po radiohalo diameter ≈ 70 µm, ^{214}Po radiohalo diameter ≈ 68 µm, and ^{210}Po radiohalo diameter ≈ 39 µm.

missing in many Po radiohalos (fig. 5) (Snelling, Baumgardner, and Vardiman 2003), the source of the Po for the radiohalos has been an area of contention (Snelling 2000). Was it primary, or did a secondary process transport it?

The reason given for these attempts to account for the origin and formation of the Po radiohalos by some secondary process is simple—the half-lives of the respective Po isotopes are far too short to be reconciled with the Po having been primary, that is, originally in the granitic magmas which are usually claimed to have slowly cooled to form the granitic rocks that now contain the Po-radiohalo-bearing biotite grains. The half-life of ^{218}Po, for example, is 3.1 minutes. However, this is not the only formidable obstacle for any secondary process that transported the Po into the biotite as, or after, the granitic rocks cooled. First, there is the need for the isotopic separation of the Po isotopes, or their α-decay precursors, from their parent ^{238}U having occurred naturally (Gentry

et al. 1973). Second, the radiocenters of very dark ^{218}Po radiohalos, for example, may need to have contained as much as 5×10^9 atoms (a concentration of greater than 50%) of ^{218}Po (Gentry 1974), yet the host minerals contain only ppm abundances of ^{238}U, which apparently means only a negligible supply of ^{218}Po daughter atoms is available for capture in a radiocenter at any given time. But these ^{218}Po atoms must also migrate or diffuse from their source at very low diffusion rates through surrounding mineral grains to be captured by the radiocenters before the ^{218}Po decays (Fremlin 1975; Gentry 1968, 1975).

Therefore, there are strict time limits for the formation of the Po radiohalos by primary or secondary processes in granites. Studies of some Po radiohalo centers in biotite (and fluorite) have shown little or no U in conjunction with anomalously high ^{206}Pb/^{207}Pb and/or Pb/U ratios, which would be expected from the decay of Po without the U precursor that normally occurs in U radiohalo centers (Gentry 1974; Gentry et al. 1973). Indeed, many ^{206}Pb/^{207}Pb ratios were greater than 21.8 reflecting a seemingly abnormal mixture of Pb isotopes derived from Po decay independent of the normal U-decay chains (Gentry 1971; Gentry et al. 1973). Thus, based on these data, Gentry advanced the hypothesis that the three different types of Po radiohalos in biotite represent the decay of primordial Po (that is, original Po not derived by ^{238}U-decay), and that the rocks hosting these radiohalos must be primordial rocks produced by fiat creation, given that the half-life of ^{214}Po is only 164 microseconds (Gentry 1979, 1980, 1982, 1983, 1984, 1986, 1988, 1989). He thus perceived that *all* granites must be Precambrian, and part of the earth's crust created during the Creation Week.

A Hydrothermal Explanation For Po Radiohalos

As a consequence of Gentry's creation hypothesis, the origin of the Po radiohalos has remained controversial and thus apparently unresolved. Of the 22 locations then known where the rocks contained Po radiohalos, Wise (1989) determined that six of the locations hosted Phanerozoic granitic rocks that intruded fossiliferous (and thus Flood-deposited) sedimentary strata, a large enough proportion to severely question Gentry's hypothesis of primordial Po in fiat created granitic rocks. Many of these Po radiohalo occurrences are also in proximity to higher than normal U concentrations in nearby rocks and/or minerals, suggesting ideal sources for fluid separation and transport of the Po. Subsequently, Snelling (2000) reviewed the literature on radiohalos. He thoroughly discussed the many arguments and evidences used in the debate that had ensued over the previous two decades and concluded that there were insufficient data on the geological occurrence and distribution of the Po radiohalos for the debate to be decisively resolved. He then recognized that the spatial association of Po radiohalos to ^{238}U radiohalos meant that the Po which parented the adjacent Po radiohalos may have been derived from the ^{238}U decay products in the radiocenters of the ^{238}U radiohalos. He also observed that many radiohalo-hosting biotite flakes had been hydrothermally altered. Furthermore, many of the host Phanerozoic granites had intruded into fossil-bearing sedimentary layers that therefore were deposited during the Flood. Thus, those and other granites intruded into fossil-bearing, Flood-deposited sedimentary layers had to form during the Flood subsequent to the deposition of those sedimentary layers and could not be creation rocks as postulated by Gentry (1988). Of course, this does not preclude many Precambrian granites having been created during the Creation Week.

Furthermore, Snelling (2000) found that there are now significant reports of ^{210}Po as a detectable species in volcanic gases, in volcanic/hydrothermal fluids associated with subaerial volcanoes and fumaroles and associated with mid-ocean ridge hydrothermal vents and chimney deposits (Hussain et al. 1995; LeCloarec et al. 1994; Rubin 1997), as well as in ground waters (Harada et al. 1989; LaRock et al. 1996). The distances involved in this fluid transport of the Po are several kilometers (and more), so there is increasing evidence of the potential viability of the secondary transport of Po by hydrothermal fluids during pluton emplacement, perhaps in the waning stages of the crystallization and cooling of granitic magmas (Snelling and Woodmorappe 1998; Snelling 2000, 2005, 2008a).

Consequently, Snelling and Armitage (2003) investigated the Po radiohalo occurrences in three Phanerozoic granitic plutons and logically argued for a model of Po radiohalo formation involving secondary transport of Po by hydrothermal fluids during crystallization and cooling of the granitic magmas. Their data and details of this hydrothermal fluid transport model were initially published by Snelling, Baumgardner, and Vardiman (2003), but full details encompassing these results were elaborated upon in Snelling (2005). He proposed that hydrothermal fluids infiltrating along the cleavage planes within biotite flakes dissolved ^{226}Ra, ^{222}Rn, and the Po isotopes emanating from ^{238}U decay within the zircon radiocenters of the ^{238}U radiohalos. At conducive sites downflow within the same biotite flakes, usually less than 1 mm distant to the tiny zircon sources, the Po isotopes were deposited and concentrated in what became the radiocenters for ^{218}Po, ^{214}Po, and ^{210}Po radiohalos as the Po isotopes decayed. Hydrothermal fluids are typically Cl-rich and are

known to be capable of dissolving ^{226}Ra, ^{222}Rn, and the Po isotopes, the latter particularly bonding with Cl (Bagnall 1957). Hydrothermal fluids also carry S, and because Po behaves geochemically the same as Pb it also bonds with S (Bagnall 1957). Furthermore, the mica sheets making up the biotite structure are weakly bonded by K, OH, and F ions, so S and Cl ions can occasionally substitute at point loci within the cleavage planes. It was thus postulated by Snelling (2005) that as the hydrothermal fluids carrying ^{222}Rn and the Po along the cleavage planes between the biotite sheets, Po atoms were attracted to those point loci where they decayed, only to be replaced by more Po atoms attracted to the same S or Cl point loci. The Po radiocenters were thus formed surrounded by Po radiohalos.

Whereas Po radiohalos would appear to indicate extremely rapid geological processes were responsible for their production (because of the extremely short half-lives of the Po isotopes responsible), ^{238}U and ^{232}Th radiohalos appear to be evidence of long periods of radioactive decay, assuming decay rates have been constant at today's rates throughout earth history. Indeed, it has been estimated that dark, fully-formed U and Th radiohalos require around 100 million years' worth of radioactive decay at today's rates to form (Gentry 1973, 1974; Humphreys 2000; Snelling 2000). Thus, the presence of mature U and Th radiohalos in granitic rocks globally throughout the geological record would indicate that at least 100 million years' worth of radioactive decay at today's rates had occurred. Therefore, the requirement of grossly accelerated ^{238}U decay is essential to this hydrothermal fluid model for the transport of the Po isotopes from the decay of ^{238}U in the radiocenters of ^{238}U radiohalos (Snelling 2005). Vardiman, Snelling, and Chaffin (2005) found that the greater the half-life and atomic weight of a radioisotope the greater the decay rate acceleration. Thus, whereas ^{238}U decay would have been grossly accelerated during some past geologically catastrophic event such as the Flood, the very short half-life Po radioisotopes would not have been appreciably affected. Several lines of evidence suggest that during the Flood when much of the fossil-bearing sedimentary rock record was accumulating, and when biotite-bearing granites were intruded into those sedimentary rocks, the decay rate of ^{238}U was grossly accelerated (Vardiman, Snelling, and Chaffin 2005). These include systematically-different radioisotope ages for the same rock units dated by multiple methods, helium diffusion in zircons, the quantities of fission tracks matching conventional Phanerozoic stratigraphic ages in tuff beds deposited during the Flood year, and radiocarbon in Phanerozoic coal beds and other organic materials, as elaborated in detail by Vardiman, Snelling, and Chaffin (2005). Thus, whereas today's very slow ^{238}U decay rate produces only a few Ra, Rn, and Po atoms very slowly, that grossly accelerated decay rate would have produced huge numbers of Ra, Rn, and Po atoms very rapidly, which were then easily transported the short distances within the host biotite flakes to precipitate in the adjacent Po radiocenters and produce the Po radiohalos.

Constrained by the biblical timescale, Humphreys (2000) and Vardiman, Snelling, and Chaffin (2005) proposed that these observable data require radioisotope decay to have been accelerated, but just by how much needs to be determined. If, for example, mature U and Th radiohalos were found in granitic rocks that were demonstrated to have formed during the Flood year, then that would imply at least 100 million years' worth of radioisotope decay at today's rates had occurred at an accelerated rate during the Flood year (Baumgardner 2000; Snelling 2000, 2005). Vardiman, Snelling, and Chaffin (2005) postulated the ^{238}U decay rate was accelerated by five orders of magnitude, so it could then be supposed the Po isotopes' decay rates were similarly accelerated, which could make their existence so fleeting there would not be sufficient time for hydrothermal transport to form radiocenters. However, as already noted, Vardiman, Snelling, and Chaffin (2005) found that the amount of acceleration was related to the present half-lives of the parent radioisotopes, the slower the present decay rate (or the longer the current half-life) resulting in the most acceleration. Thus, with such fast decay rates (short half-lives) today, the Po isotopes would scarcely have been accelerated at all. Furthermore, the accelerated decay rates would not have resulted in much larger radii for ^{238}U radiohalos, as ring radii are not affected by the decay rates but are related to the energies of the emitted α-particles (Gentry 1973, 1974).

In this hydrothermal model, the Po accumulated in the radiocenters by time integration as Po atoms were progressively deposited from the passing hydrothermal fluids (Snelling and Armitage 2003; Snelling 2005). So, instead of the Po radiohalos forming virtually instantaneously as proposed by Gentry (1988), the Po radiohalos formed over hours and days. However, whereas granitic magmas are intruded at 650–730°C, the radiohalos cannot form until the magma has crystallized and the temperature has dropped below 150°C, because above that temperature the α-tracks that produce the radiohalos are thermally annealed (Laney and Laughlin 1981). Yet, hydrothermal fluids probably began transporting Rn and the Po isotopes immediately after they were expelled from the crystallized granite at temperatures below 400°C. This has drastic time implications for

the formation of granites (Snelling 2008a). Whereas Gentry (1988) concluded that granites were created instantaneously by divine fiat, Snelling (2005, 2008a, 2014a) postulated that granite magmas crystallized and cooled within 6–10 days, which is still very radical compared to the uniformitarian timescale.

Snelling, Baumgardner, and Vardiman (2003) and Snelling (2005) have summarized this model for hydrothermal fluid transport of U-decay products (Rn, Po) in a six-step diagram. The final step concludes with the comment:

> With further passing of time and more α-decays both the ^{238}U and ^{210}Po radiohalos are fully formed, the granite cools completely and hydrothermal fluid flow ceases. Note that both radiohalos have to form concurrently below 150°C. The rate at which these processes occur must therefore be governed by the 138 day half-life of ^{210}Po. To get ^{218}Po and ^{214}Po radiohalos these processes would have to have occurred even faster (Snelling 2005).

Furthermore, if Po radiohalos are alongside U radiohalos in the same granitic rocks, then that would have implications as to the rate of formation and age of these granitic rocks formed during the Flood year within the biblical timescale. If the U and Po radiohalos both mostly formed during the 6–10 days while the granite plutons cooled during the Flood, then this implies 100 million years' worth of accelerated ^{238}U decay occurred in a timeframe of days to a few weeks. Thus the U-Pb isotopic systematics within the zircons in these granite plutons are definitely not providing absolute "ages" as conventionally interpreted.

Subsequently, case studies were undertaken to test this hydrothermal fluid transport model for the formation of Po radiohalos. Most remarkable was the fulfilled prediction of many more Po radiohalos at the staurolite isograd in regionally metamorphosed sandstones in the Great Smoky Mountains, Tennessee-North Carolina, where the metamorphic reaction would have released a lot of water (224 water molecules for every 54 units of muscovite reacting with chlorite; Snelling 2008b). Then, in the Cooma regional metamorphic complex of southeastern Australia the numbers of Po radiohalos increased where water was released in the high-grade zone and in the central granodiorite but decreased sharply in the zone of partial melting where water was dissolved into the melt, just as expected in the model (Snelling 2008c).

In granites, increased numbers of Po radiohalos were also found where they were predicted to be based on the release of hydrothermal fluids during granite crystallization and cooling (Snelling 2008a). In the Shap Granite of northern England, prolific Po radiohalos matched the higher volume of hydrothermal fluids associated with that granite's large K-feldspar phenocrysts (Glazner and Johnson 2013; Snelling 2008d). The nested plutons of the Tuolumne Intrusive Suite, Yosemite, California (Glazner et al. 2022) contain increasing numbers of Po radiohalos proportional to the increased volumes of active hydrothermal fluids within the sequentially emplaced intrusions (Snelling and Gates 2009). High numbers of Po radiohalos and active hydrothermal fluids coincide with the large K-feldspar phenocrysts in the second to last pluton and the connection to explosive volcanism of the last pluton (Bateman and Chappell 1979; Glazner and Johnson 2013; Glazner et al. 2022; Snelling and Gates 2009). The Bathurst Batholith west of Sydney, Australia, consists of an enormous pluton of 1600 km^2 (620 sq. mi) (the Bathurst Granite) intruded into fossiliferous sedimentary strata and numerous smaller related satellite plutons and dikes, which field and textural data have established were sequentially intruded while still hot (Snelling 2014a). The presence of Po radiohalos in all three sequentially-intruded granite phases is evidence that all this intrusive activity, and the cooling of all three granite phases, must have occurred within a week or two so that these Po radiohalos in them formed subsequently within days to weeks. And Snelling (2018) successfully tested the use of Po radiohalos as an exploration guide to locate hydrothermal ore deposits associated with granites, higher numbers of Po radiohalos being spatially associated with hydrothermal ore veins within granites in the New England region of northern New South Wales, Australia.

Finally, Snelling (2023b) tabulated the radiohalos data he had amassed from two decades of radiohalos research on samples of numerous granites and metamorphic rocks from locations around the globe of various geological ages, both Precambrian and Phanerozoic. His data clearly showed the peak occurrence of radiohalos was in Flood-related rocks when hydrothermal fluids would be prevalent during catastrophic geological processes. Yet Po radiohalos were still present, albeit in small numbers, within some Precambrian (pre-Flood) granites. Given the observation that radiohalos are annealed at 150°C (Laney and Laughlin 1981), Snelling (2023b) thus proposed that any earlier pre-Flood radiohalos in those rocks may well have been annealed in the deformation of continental rocks during Creation Day 3 when God caused the waters on the earth's surface to be gathered together into one place so that the dry land was formed (Genesis 1:9) and/or at the onset of and during the Flood. If that were the case, then the radiohalos observed in today's pre-Flood rocks were then generated subsequently during the Flood.

Therefore, since Snelling (2005, 2006, 2008b, c, 2023b) has demonstrated that U and Po radiohalos are also found in biotite flakes in metamorphic rocks, and Snelling (2025) had documented U and Po radiohalos in biotite flakes in Grand Canyon's Precambrian crystalline basement granites, it was logical and feasible to also explore for the occurrence of U and Po radiohalos in the biotite-bearing schists that host those granites in Grand Canyon's Precambrian crystalline basement. The Vishnu and Rama Schists were thus targeted for sampling because they contain abundant biotite flakes and their apparent precursor pelitic sediments and felsic volcanics would have included sufficient zircon grains. On the other hand, the Brahma Schist was ignored because as described above it rarely contains sufficient biotite flakes and its apparent precursor basalts are not known to contain zircon grains.

Field and Laboratory Methods

Field procedure

During several raft trips spaced over almost two decades 50 samples of the Vishnu (37) and Ramu (13) Schists in the inner gorges of Grand Canyon were systematically collected with research and collecting permits approved by the Grand Canyon National Park. Suitable outcrops were chosen along the Colorado River corridor and samples were collected from many exposures of the schists approximately every half to one mile. Samples were collected using a steel chisel and heavy-duty hammer. Some typical outcrops are shown in fig. 8. Location details for each sample were recorded with a hand-held Garmin GPS unit as well as being plotted on maps of the Colorado River corridor. Their locations are listed in table 1, measured in river miles downstream from Lees Ferry.

Laboratory procedure

Snelling and Armitage (2003) and Snelling (2005) devised a method of counting radiohalos for each sample investigated from a designated number of thin sections (usually 50) with approximately 20 biotite flakes per thin section. This allowed for statistical comparisons between samples and rock types. Thus, for this study it was necessary to follow that same procedure to tabulate the needed radiohalos data for these rock samples, which also enables the data to be compared with samples from other rock units from the larger geologic record.

A standard petrographic thin section was obtained for each sample. In the laboratory, a scalpel and tweezers were used to pry flakes of large, primary biotite loose from the sample surfaces, or where necessary portions of the samples were crushed to liberate the constituent mineral grains. Biotite flakes were then handpicked with tweezers from each crushed sample and placed on a piece of Scotch tape™ fixed to the flat surface of a laminated board on a laboratory table with its adhesive side up. Once numerous biotite flakes had been mounted on the adhesive side of this piece of tape, a fresh piece of Scotch tape™ was placed over them and firmly pressed along its length so as to ensure that the two pieces were stuck together with the biotite flakes firmly wedged between them. The upper piece of tape was then peeled back in order to pull apart the sheets composing the biotite flakes, and this piece of tape with thin biotite sheets adhering to it was then placed over a standard glass microscope slide, adhesive side down, so that the thin biotite flakes were held rigidly between the slide and the tape. This procedure was repeated with another piece of Scotch tape™ placed over the original tape and biotite flakes affixed to the board, the adhering biotite flakes being progressively pulled apart and transferred to microscope sides. As necessary, further handpicked biotite flakes were added to replace those fully pulled apart. In this way tens of microscope slides were prepared for each sample, each with many (at least 20 to 30) thin biotite flakes mounted on it. This is similar to the method pioneered by Gentry (1988). A minimum of 50 microscope slides was prepared for each sample (at least 1,000 biotite flakes) to ensure good representative sampling statistics.

Each thin section for each sample was then carefully examined under a petrological microscope in plane-polarized light, and all radiohalos present were identified, noting any relationships between the different radiohalo types (^{238}U, ^{232}Th, ^{218}Po, ^{214}Po, and ^{210}Po). The numbers of each type of radiohalo in each slide were counted by progressively moving the slide backwards and forwards across the field of view, and the numbers recorded for each slide were then tallied and tabulated for each sample. Because of the progressive peeling apart of many of the same biotite flakes during the preparation of the microscope slides due to biotite's perfect basal cleavage, many of the radiohalos appeared on more than one microscope slide. Only radiohalos whose radiocenters were clearly distinguishable were counted. This procedure ensured each radiohalo was only counted once.

Results

Fig. 9 provides images at bench scale (~25 mm wide by ~65 mm long) of the thin sections of some samples of the Vishnu and Rama Schists. These illustrate the variability in the mineralogy and textures of these schists.

For example, fig, 9a and b are two pieces from the same Vishnu Schist sample VS-1A and 1B, yet (a) consists of mostly quartz with some biotite flakes,

Fig. 8. Some typical Vishnu Schist outcrops from which samples were collected: (a) sample GCM-33 at river mile 93.2; (b) sample GCM-34 at river mile 93.4; (c) sample GCM-35 at river mile 97.3; (d) sample GCM-36 at river mile 98.6; (e) sample GCM-37 at river mile 99.0; (f) sample GCM-38 at river mile 99.4; (g) sample GCM-39 at river mile 100.1; and (h) sample GCM-40 at river mile 100.5. The cold chisel is approximately 25 cm (10 in.) long.

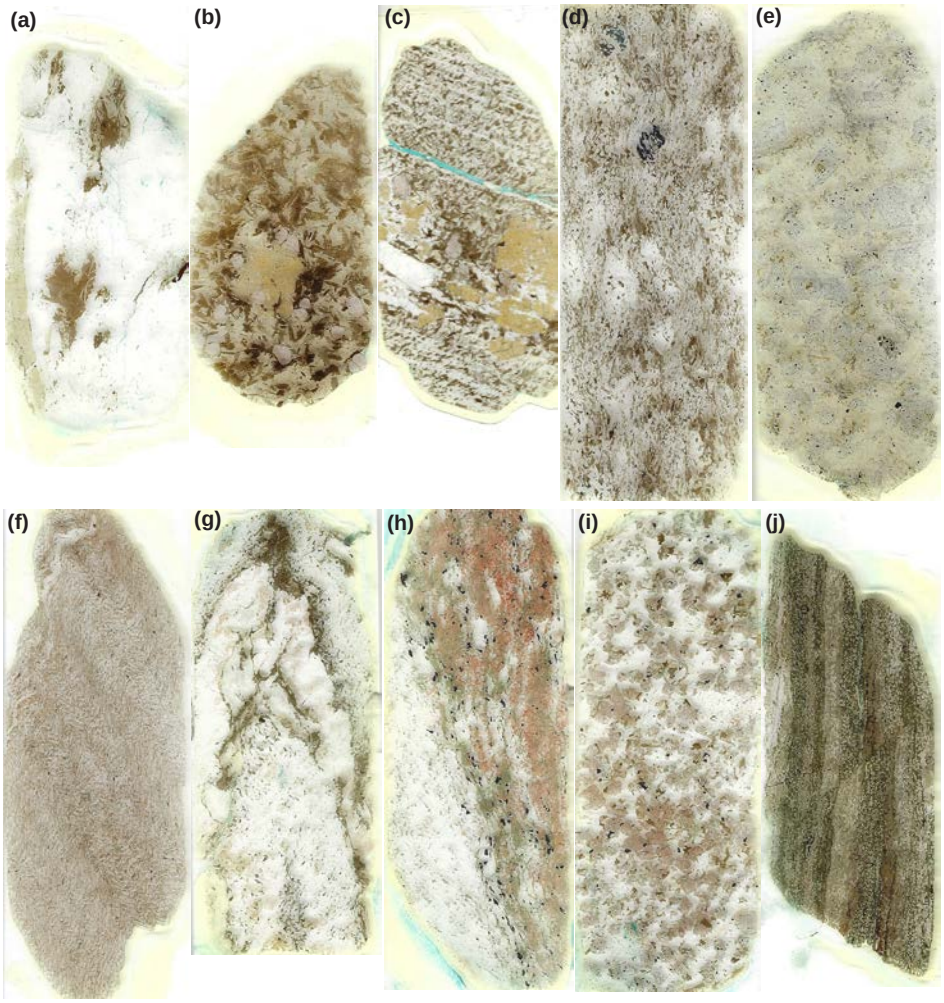

Fig. 9. Selected thin sections all at the same benchtop scale (~25 mm wide by ~65 mm long) for some of the samples of the schists, showing the variations in them, even within the same sample: (a) Vishnu Schist sample VS-1A, river mile (a) Vishnu Schist sample VS-1A, river mile 84.0; (b) Vishnu Schist sample VS-1B, river mile 84.0; (c) Vishnu Schist sample VS-2, river mile 84.0; (d) Vishnu Schist sample VS-3, river mile 91.2; (e) Vishnu Schist sample VS-4, river mile 91.2; (f) Vishnu Schist sample VS-5, river mile 108.6; (g) Vishnu Schist sample VS-6, river mile 78.4; (h) Vishnu Schist sample VS-7, river mile 78.4; (i) Ramu Schist sample ECG-08, river mile 118.8; and (j) Ramu Schist sample ECG-09, river mile 118.8.

whereas (b) consists of less quartz, a lot of biotite flakes and a garnet porphyroblast. Furthermore, fig. 9c, Vishnu Schist sample VS-2 is very similar to VS-1B (fig. 9b) with a very similar quartz-biotite-garnet assemblage. This is not surprising given that both samples are from the same general location, river mile 84.0 (table 1). However, sample VS-2 has been cut perpendicular to the schistosity so the schistosity is very clear, whereas in sample VS-1A and B the schistosity is not evident.

Vishnu Schist sample VS-3 (fig. 9d) is different again, with the sample consisting of mainly quartz and biotite, but with some small grains of bluish tourmaline. The thin section was not cut perpendicular to the schistosity, although some foliation is evident vertically in the image. Vishnu Schist sample VS-4 (fig. 9e) is from the same general location, river mile 91.2 (table 1), so it is not surprising that it is similar to sample VS-3. It also consists of quartz, with much less biotite and a lot more tourmaline crystals (a very pale gray-blue) and the thin section was cut perpendicular to the long axes of the tourmaline crystals and not perpendicular to the schistosity so no foliation is evident. On the other hand, Vishnu Schist sample VS-5 (fig. 9f) from river mile 108.6 (table 1) is a quartz-muscovite-biotite schist with faintly-visible crenulated schistosity due to the predominance particularly of muscovite, biotite being subordinate. Vishnu Schist samples VS-6 and VS-7 (fig. 9g and h respectively) are from river mile 78.4, the latter sample being from nearby up a side canyon. Yet the samples are very different in these thin sections, VS-6 being dominated by quartz with subordinate biotite and traces of garnet, while VS-7 contains abundant garnet (light red) with quartz and again subordinate biotite. The dominance of quartz and garnet crystals

Table 1. Radiohalos counted in each sample of the Precambrian Vishnu and Rama Schists with their locations in the Upper and Middle Granite Gorges, and summaries of radiohalos numbers for each schist in the various lithotectonic blocks-metamorphic domains, as per Dumond et al. (2007) and Karlstrom et al. (2012), as depicted in fig. 3.

Rock Unit	Location (River Mile)	Sample Number	Samples (slides)	Radiohalos					Number of Radiohalos per slide	Number of Po Radiohalos per slide	Ratios		
				^{210}Po	^{214}Po	^{218}Po	^{238}U	^{232}Th			^{210}Po:^{238}U	^{210}Po:^{214}Po	^{210}Po:^{218}Po
Vishnu Schist	**Upper Granite Gorge**												
	Mineral Canyon Block												
	77.4	GCM-01	50	54	0	0	18	0	1.44	1.08	3:1	—	—
	78.3	GCM-02	50	4	0	0	0	0	0.08	0.08	—	—	—
	78.4 (sc)	VS-6	50	1146	0	0	72	0	24.36	22.92	15.9:1	—	—
	78.4	VS-7	50	22	0	0	1	0	0.46	0.44	22.0:1	—	—
	78.4 (sc)	VS-15	50	169	0	0	10	0	3.58	3.38	16.9:1	—	—
	80.5	GCM-15	50	914	0	0	1283	0	43.94	18.28	0.71:1	—	—
	Total	**6 samples**	**300**	**2309**	**0**	**0**	**1384**	**0**	**12.31**	**7.70**	**1.67:1**	—	—
	Clear Creek Block												
	81.3	GCM-16	50	24	0	0	8	0	0.06	0.48	3:1	—	—
	82.3	GCM-17	50	227	0	0	70	0	5.94	4.54	3.24:1	—	—
	83.0	GCM-18	50	463	1	0	244	0	14.16	9.28	1.90:1	—	—
	84.0	VS-1	50	2270	0	0	1118	0	67.8	45.4	2.03:1	—	—
	84.0	VS-2	50	2331	5	2	834	0	63.44	46.8	2.79:1	466.2:1	1165.5:1
	84.0	GCM-04	50	683	0	0	1271	0	39.08	13.66	0.54:1	—	—
	84.05	GCM-05	50	313	1	0	135	0	8.98	6.28	2.32:1	313:1	—
	84.2	GCM-06	50	676	0	0	420	0	21.92	13.52	1.61:1	—	—
	Total	**8 samples**	**400**	**6987**	**7**	**2**	**4100**	**0**	**27.74**	**17.49**	**1.70:1**	**998.1:1**	**3493.5:1**
	Trinity Creek Block												
	91.2	VS-3	50	1041	7	2	200	0	25.0	21.0	5.21:1	148.71:1	520.5:1
	91.2	VS-4	50	0	0	0	0	0	0	0	—	—	—
	93.2	GCM-33	50	17	0	0	6	0	0.46	0.34	2.83:1	—	—
	93.4	GCM-34	50	626	0	0	1563	0	43.78	12.52	0.40:1	—	—
	93.8	GCM-23	50	284	0	0	298	0	11.64	5.68	0.95:1	—	—
	94.4	GCM-24A	50	10	0	0	4	0	0.28	0.24	2.5:1	—	—
	94.4	GCM-24B	50	196	0	0	534	0	14.6	3.92	0.37:1	—	—
	95.5	GCM-25	50	7	0	0	1	0	0.16	0.14	7:1	—	—
	Total	**7 samples**	**400**	**2181**	**7**	**2**	**2606**	**0**	**11.99**	**5.48**	**0.84:1**	**311.6:1**	**1090.5:1**

	Topaz Canyon Block												
	96.4	GCM-26	50	206	0	0	91	0	5.94	4.12	2.26:1	—	—
	96.8	GCM-27	50	268	0	0	127	0	7.90	5.36	2.11:1	—	—
	97.3	GCM-35	50	183	0	0	40	0	4.44	3.64	4.55:1	—	—
	98.0	GCM-28	50	303	0	0	81	0	7.72	6.06	3.74:1	—	—
	Total	**4 samples**	**200**	**960**	**0**	**0**	**339**	**0**	**6.50**	**4.80**	**2.83:1**	**—**	**—**
	Tuna Creek Block												
	98.6	GCM-36	50	892	0	0	219	0	22.22	17.84	4.07:1	—	—
	99.0	GCM-37	50	47	0	0	2	0	0.98	0.94	23.5:1	—	—
	99.4	GCM-38	50	29	0	0	0	0	0.58	0.58	—	—	—
	100.1	CGM-39	50	1519	0	0	815	0	46.68	30.38	1.86:1	—	—
	100.5	GCM-40	50	38	0	0	0	0	0.76	0.76	—	—	—
	Total	**5 samples**	**250**	**2525**	**0**	**0**	**1036**	**0**	**17.81**	**12.63**	**2.44:1**	**—**	**—**
	Waltenberg Canyon Block												
	108.5	GCM-10	50	824	0	0	591	0	28.30	16.48	1.39:1	—	—
	108.6	VS-5	50	925	0	0	141	0	21.32	18.5	6.56:1	—	—
	117.2	GCM-29	50	16	0	0	10	0	0.52	0.20	1.6:1	—	—
	119.4	GCM-30	50	131	0	0	10	0	2.82	2.62	13.1:1	—	—
	Total	**4 samples**	**200**	**1896**	**0**	**0**	**752**	**0**	**13.24**	**9.48**	**2.52:1**	**—**	**—**
	Middle Granite Gorge												
	135.6	GCM-31	50	1536	0	0	1025	0	51.22	30.72	1.5:1	—	—
	138.5	GCM-11	50	22	0	0	11	0	0.66	0.44	2:1	—	—
	138.5	GCM-32	50	110	0	0	55	0	3.30	2.20	2:1	—	—
	Total	**3 samples**	**150**	**1688**	**0**	**0**	**1091**	**0**	**18.53**	**11.25**	**1.55:1**	**—**	**—**
	Grand Total	**37 samples**	**1900**	**18,526**	**14**	**4**	**11,308**	**0**	**15.71**	**9.76**	**1.64:1**	**1323:1**	**4361:1**
Ramu Schist	**Upper Granite Gorge**												
	Mineral Canyon Block												
	79.2	GCM-12	50	90	0	0	26	0	2.32	1.80	3.46:1	—	—
	79.2	GCM-13	50	0	0	0	0	0	0	0	—	—	—
	79.4	GCM-03	50	416	0	0	311	0	14.54	8.32	1.34:1	—	—
	79.8	GCM-14	50	2	0	0	0	0	0.04	0.04	—	—	—
	Total	**4 samples**	**200**	**508**	**0**	**0**	**337**	**0**	**4.23**	**2.54**	**1.51:1**	**—**	**—**

Clear Creek Block												
84.3	GCM-07	50	131	0	0	36	0	3.34	2.62	3.64:1	—	—
84.4	GCM-08	50	792	0	0	628	0	28.4	15.84	1.26:1	—	—
84.4	GCM-20	50	0	0	0	0	0	0	0	—	—	—
84.5	GCM-09	50	265	0	0	222	0	9.74	5.3	1.19:1	—	—
84.5	GCM-19	50	77	0	0	12	0	1.78	1.54	6.42:1	—	—
Total	**5 samples**	**250**	**1265**	**0**	**0**	**898**	**0**	**8.65**	**5.06**	**1.41:1**	—	—
Trinity Creek Block												
92.1	GCM-21	50	49	0	0	3	0	1.04	0.98	16.33:1	—	—
92.5	GCM-22	50	5	0	0	0	0	0.10	0.10	—	—	—
Total	**2 samples**	**100**	**54**	**0**	**0**	**3**	**0**	**0.57**	**0.54**	**18.0:1**	—	—
Waltenberg Canyon Block												
118.8	ECG-8	50	571	0	0	54	0	12.50	11.42	10.6:1	—	—
118.8	ECG-9	50	0	0	0	0	0	0	0	—	—	—
Total	**2 samples**	**100**	**571**	**0**	**0**	**54**	**0**	**6.25**	**5.71**	**10.57:1**	—	—
Grand Total	**13 samples**	**650**	**2398**	**0**	**0**	**1292**	**0**	**5.68**	**3.69**	**1.86:1**	—	—

* sc—these samples were collected from a side canyon

in these samples and the subordinate biotite results in a coarser-grained texture and poorly-developed schistosity, even though the thin sections have been cut perpendicular to the metamorphic mineralogical layering.

Ramu Schist samples ECG-8 and ECG-9 (fig. 9i and j respectively) are from river mile 118.8 and even though collected in such close proximity they are very different from one another in these two thin sections. ECG-8 is coarse-grained and is dominated by quartz and garnet (light red) crystals with very minor biotite so no schistosity is evident. On the other hand, ECG-9 is fine-grained and is dominated by biotite and tiny quartz grains so there is very clear schistosity evident.

Fig. 10 shows what several samples of the Vishnu Schist look like under the petrographic microscope. In plane-polarized light (fig. 10a–e, g–i, and k, l) the biotite flakes that host the radiohalos are brown or olive brown, the various shades or intensities of brown being due to their orientation with respect to the polarizing filter and microscope stage angle. The biotite flakes are usually much larger than the tiny-small flakes of muscovite which are clear and often ubiquitous. The muscovite flakes typically control the schistosity. Quartz grains are usually the other main constituent.

Vishnu Schist sample VS-1B (fig. 10a, b) is dominated by relatively large brown biotite flakes with the black dots being radiohalos. However, in fig. 10b (upper left) is a large garnet crystal, easily identified due to its high relief and cross-cutting fractures. A similar former garnet crystal is also present in fig. 10a (bottom left) but it has been altered to chlorite (pale green), such alteration also being present in fig. 10b around the lower edge on the dominant garnet crystal. Otherwise, small patches of quartz are between the ubiquitous tiny-small edge-on muscovite flakes that are aligned in all directions scattered through the sample, even cross-cutting some biotite flakes.

Vishnu Schist sample VS-2 (fig. 10c–g) is also dominated by relatively large brown biotite flakes with the black dots being radiohalos. Similarly to VS-1, which was collected close by at river mile 84.0 (table 1), small patches of quartz are between the ubiquitous tiny-small edge-on muscovite flakes that are aligned in all directions scattered through the sample, even cross-cutting some biotite flakes. Garnet is also occasionally present (fig. 10d, bottom left), easily identified due to its high relief and cross-cutting fractures. The biotite flakes are not always aligned, so the thin section probably was not cut perpendicular to the schistosity. Although the cleavage planes within

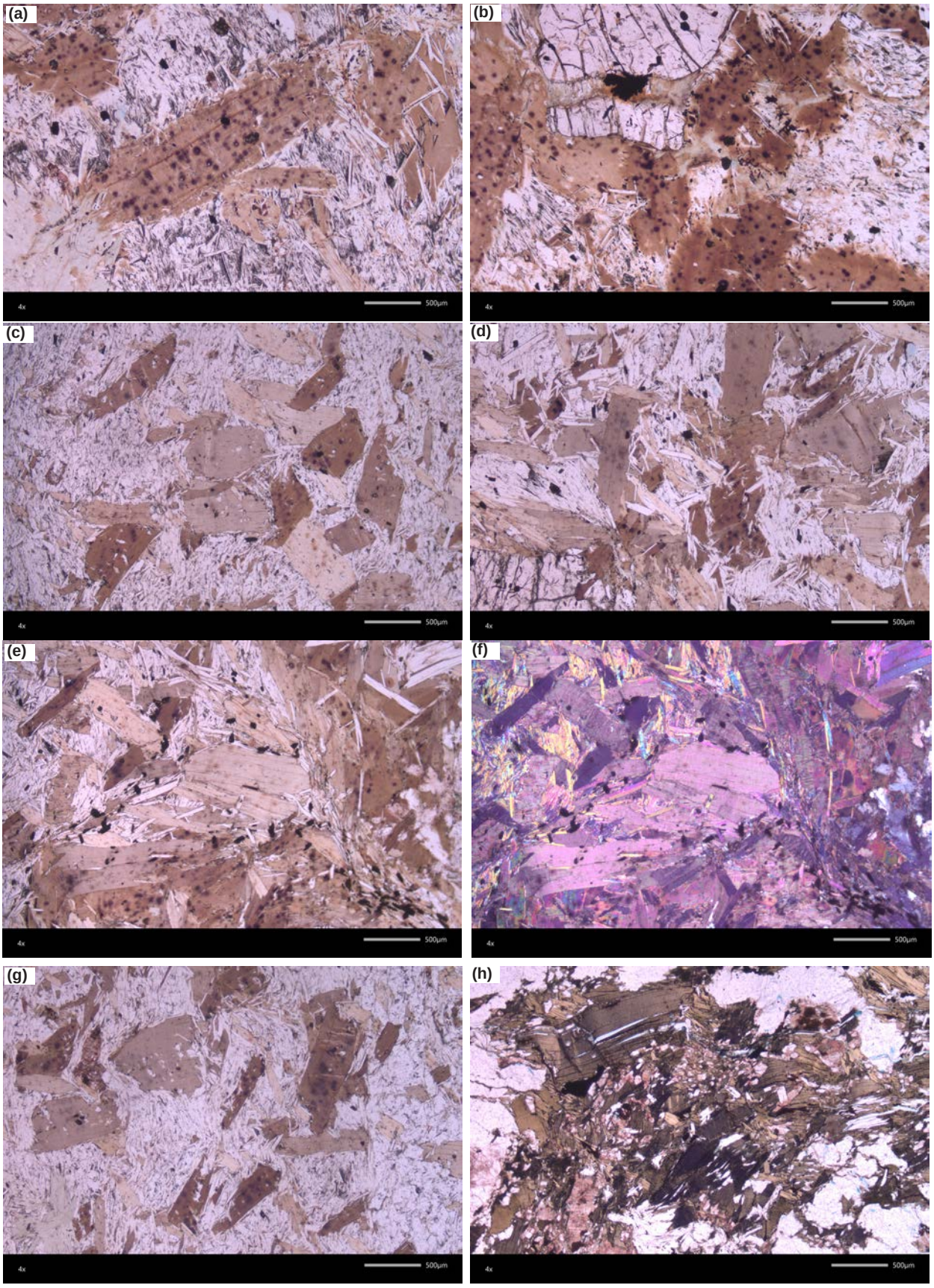
(a)
4x
500µm
(b)
4x
500µm
(c)
4x
500µm
(d)
4x
500µm
(e)
4x
500µm
(f)
4x
500µm
(g)
4x
500µm
(h)
4x
500µm

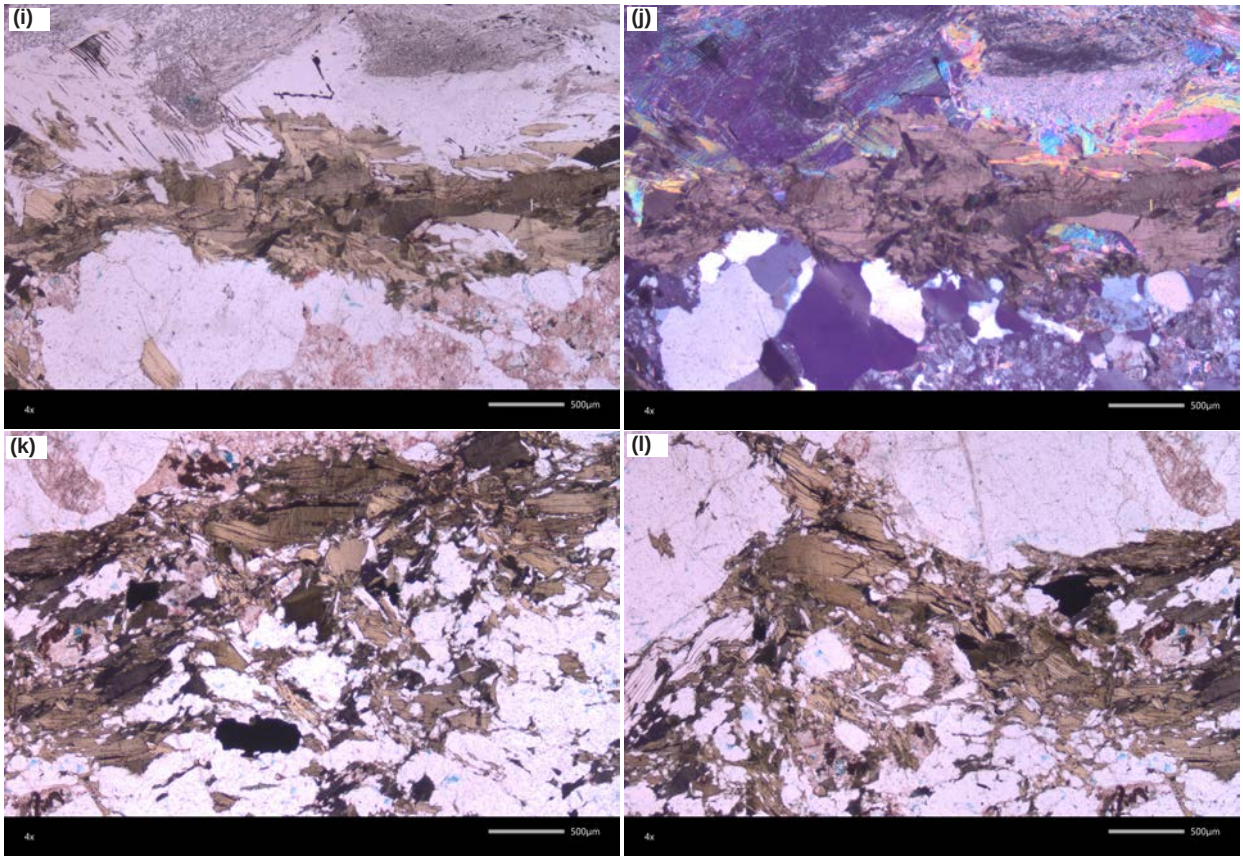

Fig. 10 (pages 398 and 399). Some typical samples of the schists viewed under the petrographic microscope in plane polarized light (a)–(e), (g)–(i), and (k)–(l) and under crossed polars (f), (j). The scale bars = 500 µm. (a), (b) Vishnu Schist sample VS-1B, river mile 84.0; (c)–(g) Vishnu Schist sample VS-2, river mile 84.0; and (h)–(l) Vishnu Schist sample VS-6, river mile 78.4.

the biotite flakes are evident, where it is not visible probably indicates some alteration of the biotite has occurred. Fig. 10f is the same field of view as in fig. 10e, except it is in cross-polarized light, displaying the brilliant interference colors particularly of the small muscovite flakes.

Vishnu Schist sample VS-6 (fig. 10 h–l) contains a lot more quartz and the grains/crystals are much larger than in samples VS-1 and VS-2. While those samples come from the same location (river mile 84.0), VS-6 was collected from river mile 78.4 in a side canyon (table 1). So, the difference in the precursor sediment at this location has resulted in the differences seen in this schist sample, such as some obvious evidence of localized brittle deformation because some biotite flakes have been somewhat shattered and bent (fig. 10h, k, and l). The biotite flakes are concentrated in bands between alternate bands consisting of quartz and garnet (pinkish grains), as seen in fig.10h–l. Whereas the more competent bands containing the harder quartz and garnet grains which were shattered by the brittle deformation, in the less competent bands with softer and more flexible (plastic) biotite flakes some of those flakes were bent by the deformation. Fig. 10j is the same field of view as in fig. 10i, except it is in cross-polarized light, displaying the brilliant interference colors particularly of the small muscovite flakes, while the sub-grains of quartz are demarked by displaying as white or various shades of gray due to slight differences in their crystallographic orientation relative to the orientation of the microscope stage.

Table 1 lists the results of all the radiohalos counted in each of the samples with their locations provided. It also summarizes the total radiohalos numbers in all samples of the Vishnu and Rama Schists, plus summaries of each block of samples pertaining to the named metamorphic and tectonic domains (figs. 2 and 3). Note that all the samples were collected from the Upper Granite Gorge (river miles 77.4–119.4), except for Vishnu Schist samples GCM-11, 31 and 32 which were collected from the Middle Granite Gorge (river miles 135.6–138.5). In the table the numbers of each type of radiohalo observed and counted are listed, the numbers of all radiohalos and Po radiohalos per slide (the total numbers counted divided by the number of microscope slides), and the relevant ratios (primarily the $^{210}Po/^{238}U$ ratio). The numbers of all radiohalos and Po radiohalos per slide and the $^{210}Po/^{238}U$ ratios

are extremely important for statistical comparisons between samples from the same rock unit and then also between rock units.

Fig. 11 provides photomicrographs of a few examples of the ubiquitous radiohalos observed in some samples from the Vishnu Schist. They are mostly overexposed ^{238}U and ^{210}Po radiohalos, there being many in some biotite flakes (VS-1, fig. 11a–e and VS-2, fig. 11f–i), hundreds of each in some samples (table 1), as well as uncounted incomplete radiohalos where the plane of observation has not passed through the radiocenters. There are a few ^{214}Po radiohalos (VS-2, fig. 11i) and ^{218}Po radiohalos (VS-3, fig. 11j), though these are two of only three samples in which they have been found (table 1). Where the biotite flakes have been deformed in VS-6 (fig. 11, and n) there are fewer ^{238}U and ^{210}Po radiohalos.

Discussion

Are these Creation Week schists?

Some creation geologists may argue these schists in the Precambrian crystalline basement of Grand Canyon were not created supernaturally during Creation Week, as proposed by other creation geologists (Austin 1994; Snelling 2009, 2022b), but perhaps were precursor sediments and volcanics that were metamorphosed into the schists during the Flood. However, a number of critical observations do not support that contention. So, before proceeding to interpret the radiohalos occurring in these schists it is necessary to settle exactly when these schists were formed, here argued as being created by God during Creation Days 1–2.

First, these Precambrian (Paleoproterozoic) schists and the granites they host were deformed then eroded before the Precambrian Grand Canyon Supergroup sediment layers were deposited unconformably on them, starting with the ~1254–1100 Ma Unkar Group (Timmons et al. 2005, 2012), which some creation geologists contend may have been deposited at the outset of the Flood. The best exposure of this unconformity is at river level from miles 74 to 78 downstream from Lees Ferry. At the base of the Bass Formation, the lowermost and first-deposited unit is the Hotauta Conglomerate Member which consists of >80% clasts of granite and quartzite (Timmons et al. 2012). Furthermore, detrital zircon grains recovered from several Unkar Group sedimentary layers include grains eroded from nearby Grand Canyon granites, as indicated by the geochemical "fingerprint" of their U-Pb "ages" (Timmons et al. 2005, 2012). Thus, even if some creation geologists interpret the Unkar Group sedimentary layers as deposited at the outset of the Flood, these underlying basement schists were already formed and hosting the granites prior to the outset of the Flood.

Some creation geologists may speculate that heating of the initial crust may have occurred at depth due to accelerated nuclear decay in the months preceding the outset of the Flood. The generated melts may then have worked their way upwards causing regional metamorphism across the entire continental crust. This process may have been started by God so that the "fountains of the great deep" would burst open breaking up that crust (Genesis 7:11) as a result of the magma generation and hydrothermal activity. However, magma generation is the result of regional metamorphism, not its cause – for example, the Cooma Metamorphic Complex, southeastern Australia (Snelling 2008c). According to conventional reasoning, the regional metamorphism that produced Grand Canyon's schists resulted from a severe tectonic upheaval, as evidenced by the severe deformation and folding. The heat and pressure involved would then have also generated via partial melting the granitic magmas that intruded the schists. These crystalline basement rocks were subsequently uplifted and eroded *before* the Unkar Group sediments of the Grand Canyon Supergroup with eroded detritus from the schists and granites were deposited on them.

Second, these Precambrian (Paleoproterozoic) schists and the granites they hosted were subsequently uplifted, and the Precambrian (Mesoproterozoic and Neoproterozoic) Grand Canyon Supergroup sediment layers overlying them unconformably were concurrently tilted and deformed. The schists, granites, and Grand Canyon Supergroup strata were then all eroded before the Phanerozoic sedimentary layers were then unconformably deposited on them (Karlstrom and Timmons 2012). If the Grand Canyon Supergroup sediment layers were deposited at the outset of the Flood, as some creation geologists propose, then there had to be two separate tectonic upheavals in quick succession. The first would have exposed and eroded the crystalline basement schists and granites so then the Grand Canyon Supergroup sediment layers were deposited on them. Once those sediment layers had hardened, then the second tectonic upheaval needed to occur to uplift, tilt and fault the Grand Canyon Supergroup. This second major tectonic upheaval occurred before the massive erosion that produced the Great Unconformity. This included faulting with huge displacements of thousands of meters to downthrust blocks of Grand Canyon Supergroup rocks so that they were preserved in place when the subsequent massive erosion completely beveled the crystalline basement and the surviving blocks of Grand Canyon Supergroup rocks (Karlstrom and Timmons 2012). Thus, in many places through the inner gorges of Grand Canyon the 3600-meter-thick

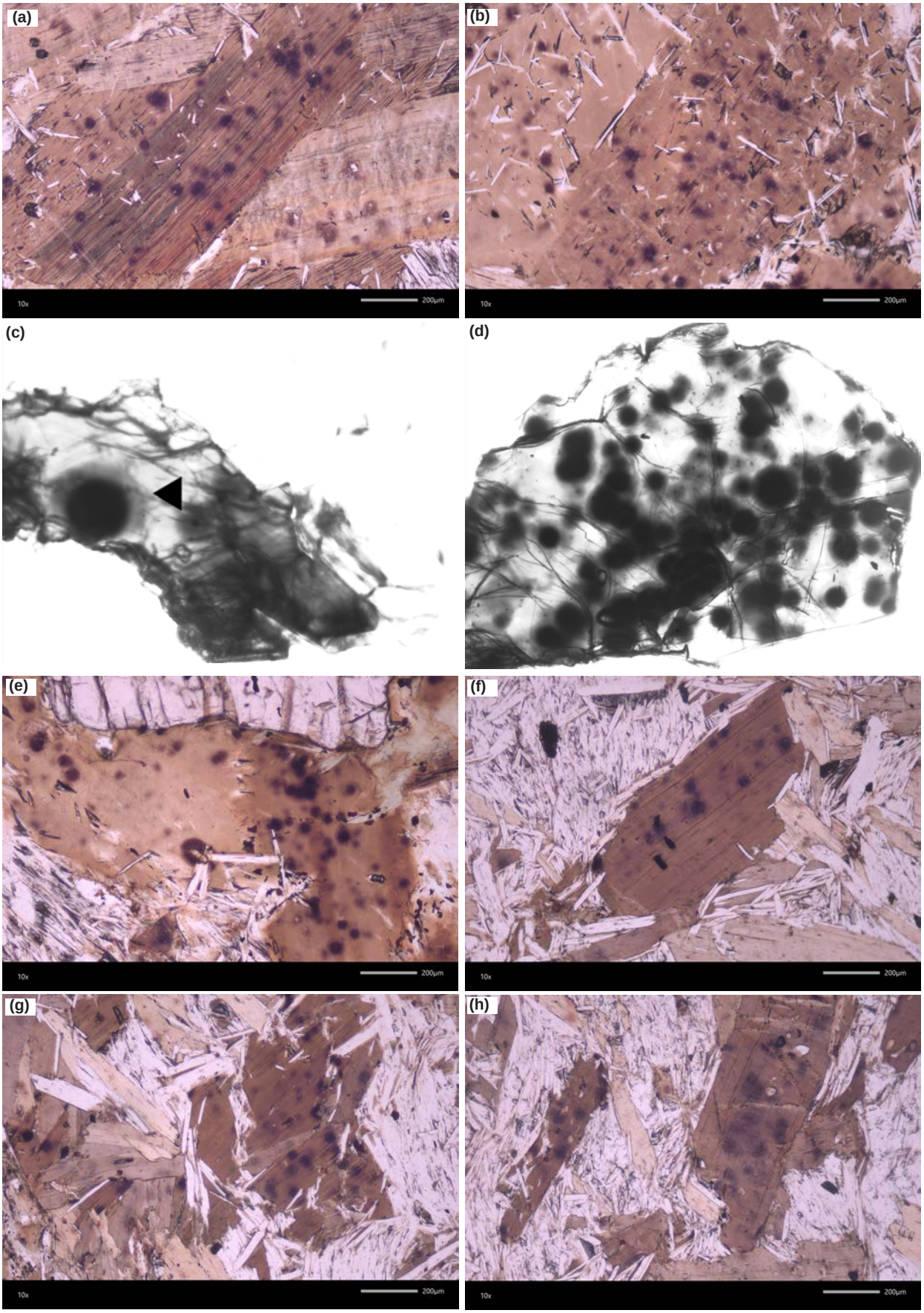
(a)
10x
200µm
(b)
10x
200µm
(c)
(d)
(e)
10x
200µm
(f)
10x
200µm
(g)
10x
200µm
(h)
10x
200µm

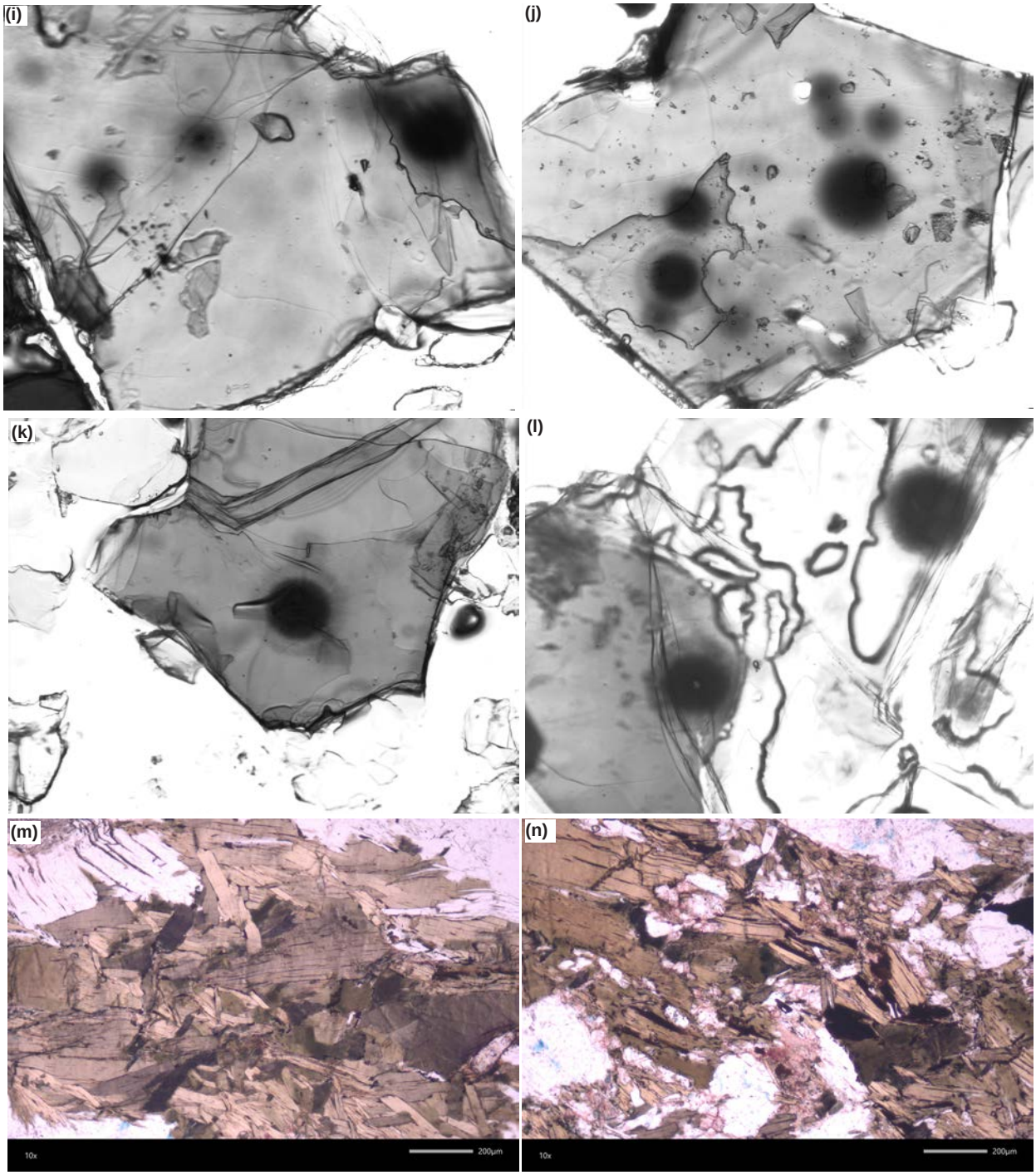
(i)
(j)
(k)
(l)
(m)
(n)
10x
200µm
10x
200µm

Fig. 11 (pages 401–402). Typical radiohalos in some samples of the schists: (a), (b) Vishnu Schist sample VS-1B, river mile 84.0, scale bars = 200 µm, the larger radiohalos are overexposed ^{238}U radiohalos and the ubiquitous smaller radiohalos are overexposed ^{210}Po radiohalos; (c) Vishnu Schist sample VS-1B, river mile 84.0, an overexposed ^{238}U radiohalo (arrowed), diameter ~70 µm; (d) Vishnu Schist sample VS-1B, river mile 84.0, the largest radiohalos are overexposed ^{238}U radiohalos, diameter ~70 µm, the smaller radiohalos are overexposed (darker) and regular (lighter with radiocenters visible) ^{210}Po radiohalos, diameter ~39 µm, and the in-between-sized and smaller faint radiohalos are without visible radiocenters because they are not in the plane of observation; (e) Vishnu Schist sample VS-1B, river mile 84.0, scale bar = 200 µm, the few larger radiohalos are overexposed ^{238}U radiohalos and the many smaller radiohalos are overexposed ^{210}Po radiohalos; (f)–(h) Vishnu Schist sample VS-2, river mile 84.0, scale bars = 200 µm, the few larger radiohalos are overexposed ^{238}U radiohalos and the smaller radiohalos are overexposed (darker) and regular (lighter with radiocenters visible) ^{210}Po radiohalos; (i) Vishnu Schist sample VS-2, river mile 84.0, a very overexposed ^{238}U radiohalo, diameter ~70 µm (right), a ^{214}Po radiohalo, diameter ~68 µm (middle), and an overexposed ^{210}Po radiohalo, diameter ~39 µm (left); (j) Vishnu Schist sample VS-3, river mile 91.2, a very overexposed ^{238}U radiohalo, diameter ~70 µm (right), an overexposed ^{218}Po radiohalo, diameter ~70 µm (lower left), a ^{214}Po radiohalo with a faint outer ring, diameter ~68 µm (center left), and seven scattered regular ^{210}Po radiohalos with radiocenters visible, diameter ~39 µm; (k) Vishnu Schist sample VS-5, river mile 108.6, an overexposed ^{238}U radiohalo with a faint outer ring, diameter ~70 µm; (l) Vishnu Schist sample VS-6, river mile 78.4, an overexposed ^{238}U radiohalo with a faint outer ring, diameter ~70 µm (left) and a very overexposed ^{238}U radiohalo, diameter ~70 µm (right); and (m), (n) Vishnu Schist sample VS-6, river mile 78.4, scale bars = 200 µm, many radiation stains representing partially preserved radiohalos, with a partial overexposed ^{238}U radiohalo (lower left) and an overexposed ^{210}Po radiohalo (center) in (m).

Grand Canyon Supergroup (Timmons et al. 2012) has been eroded away at the Great Unconformity, as well as an unknown thickness of the underlying schists and granites.

This scenario of these two major tectonic upheavals with a time gap between them all occurring at the outset of the Flood, while possible, complicates the outset of the Flood. However, whether the Grand Canyon Supergroup represents earliest Flood deposition is not entirely relevant to this study or this discussion, since it has been established above that the basement schists were probably Creation Week rocks. The observation that there is putative stromatolitic layering in the Bass Formation of the Grand Canyon Supergroup is not necessarily diagnostic of Flood deposition since the Genesis creation account does not specify when God created bacteria, which could have been created prior to the latter half of Creation Day 3 when the plants were created. After all, the soil God prepared for the plants earlier on Creation Day 3 would likely have contained bacteria as they are essential to the best soil. Furthermore, the organic matter derived from microorganisms in a few Proterozoic sedimentary strata elsewhere that subsequently generated "live" oil, for example, in the Mesoproterozoic Velkerri Formation of the McArthur Basin of northern Australia (Craig et al. 2013; Crick et al. 1988; Dutkiewicz et al. 2007; Jackson et al. 1986), may have also been due to the catastrophic sedimentation during the Creation Day 3 upheaval that is postulated here deposited at least the Unkar Group of the Grand Canyon Supergroup. Detailed discussion of these issues is beyond the scope of this study and is not relevant to the timing of formation of the basement schists.

Many creation geologists regard the Great Unconformity as marking the onset of the Flood (Austin 1994; Austin and Wise 1994; Wise and Snelling 2005; Snelling 2009, 2022b), not least because it is almost a global erosion surface (Peters and Gaines 2012). Though not always at the Precambrian-Cambrian boundary, it marks the onset of massive waves spreading across the edges and across the bulk of the continents as the Flood progressed. That the Great Unconformity sits directly on the Precambrian crystalline basement's granite plutons can be seen in many places above the river corridor within the inner gorges of Grand Canyon. Furthermore, the first of the Phanerozoic sediment layers deposited on the Great Unconformity in Grand Canyon by the floodwaters was the Tapeats Sandstone and it contains many K-feldspar and zircon grains, and some muscovite flakes, that are demonstrably derived from erosion of the nearby underlying granites and schists (Snelling 2021a). Indeed, the overlying Bright Angel and Muav Formations also contain similar grains and flakes that are demonstrably derived from erosion of the nearby underlying granites and schists (Snelling 2021b, 2022a).

And finally, there are the interrelationships between the schists and the granites they host. It has been interpreted that the 1.84 Ga Elves Chasm pluton (Hawkins et al. 1996) is likely the basement for the turbidites that are now the Vishnu Schist (Karlstrom et al. 2003). The contact zone between the Elves Chasm pluton and the overlying Granite Gorge Metamorphic Suite is exposed in several places and is gradational over several meters. The composition of the contact zone is unusual, which suggested to Babcock (1990) that alteration took place during weathering before the overlying sediments were deposited that are now the Vishnu Schist. Furthermore, the regional metamorphism that formed the schists was accompanied by deformation

and magmatism when the granite plutons were apparently intruded into the schists (Karlstrom et al. 2012). However, these intrusions generally did not bake and metamorphose the schists adjacent to them, although the pegmatite dike swarms intruded into some of the lithotectonic blocks (metamorphic domains separated by shear zones) appear to have created the hottest metamorphic rocks in the crystalline basement as determined by the mineral assemblages in the schists (Dumond et al. 2007; Karlstrom et al. 2012). Thus, the whole package of schists and granites combined to form the crystalline basement was generated almost simultaneously, albeit slowly within the uniformitarian timescale.

Combining all these observations and evidences it may be reasonable to interpret both the schists and the granites in Grand Canyon's crystalline basement as pre-Flood rocks, and that the granites were not generated and intruded during the Flood. On the contrary, these schists (or at least their precursors) and granites are likely Creation Week rocks created by God on Creation Days 1–2 as contended here and by many creation geologists.

Were these schists created by fiat?

A further contention that needs to be settled before proceeding to interpret the radiohalos occurring in these schists is to discuss how these schists were created, as it has implications for when and how the radiohalos formed. Specifically, were these schists formed by time progressive processes as precursor sedimentary and volcanic rocks underwent metamorphism, melting, and granite plutonism before the creation of plant life partway through Creation Day 3, or were these schists and granites created by fiat, that is, in a single step as fully-formed rocks?

Humphreys (2005) found 1.5 billion years' worth of radiogenic Pb and almost that much helium (α-particles in the form of retained radiogenic helium) in zircons within the Precambrian Fenton Hill granodiorite of New Mexico. While the year-long Flood event would account for about 600 million years' worth of accelerated radioisotope decay, it could be contended that it still leaves 900 million years' worth of accelerated nuclear decay which thus may have occurred before the creation of plant life on Creation Day 3 as the rocks of Creation Days 1–2 underwent metamorphism, melting, and plutonism. However, the 1,500 million years' worth of decay products in the Fenton Hill granodiorite is based on assuming those decay products all came from accelerated radioisotope decay. Could God have created by fiat the granites and schists with some Pb isotopes and helium already in them? After all, when He created the element Pb, why would He not create all the Pb isotopes? In other words, He would have created Pb isotopes that today we interpret as derived by radioisotope decay, when in fact no radioisotope decay had yet occurred. Would there not have been a starting isotopic composition of the first created rocks? And besides, the radiohalos in the Fenton Hill granodiorite only record physical evidence of 100 million years' worth or so of radioisotope decay as measured at today's decay rate.

Space precludes detailed discussion and development of this issue of the initial composition of Pb and other isotopes of the earth's first created crustal rocks. However, it could be argued that the reason the earth yields the same Pb-Pb "age" as most of the meteorites (for example, Snelling 2014b, c, d, 2015a, b) is that the parent asteroids were created on Creation Day 4 of the same initial materials God used to create the earth and its initial crustal rocks on Creation Days 1–2. Similarly, God made man's body from the same dust of the earth He used to create the animals. Many studies of the Pb isotopic compositions of ocean island basalts found they define a series of linear arrays corresponding to Pb-Pb isochrons with "ages" of between 1 Ga and 1.5 Ga for what are only recently-erupted lava flows (Sun 1980). The significance of these false Pb-Pb isochron data arrays remains elusive, because they have more radiogenic Pb in them than they should have if the earth's age is 4.57 Ga (Dickin 2005). This problem has been called the "lead paradox" and still remains unsolved. What is clear is that Pb-Pb dating of these recent basalts produces anomalous old ages that represent the inheritance of the Pb isotopic compositions of the magmas' mantle sources, perhaps ultimately derived from their primordial composition.

However, the particular Pb isotopes found in zircons are extremely specific. The most common Pb isotope in nature, ^{204}Pb, generally is undetectable in almost all zircons. There is a good reason for this, namely, because Pb ions, due to their size and charge, do not readily substitute for Zr ions in the zircon lattice. Hence, in the context of a cooling and crystallizing silicate melt, it is extremely rare for Pb ions to be included within a growing zircon crystal. By contrast, U and Th ions, because they have the same valance and are of similar size as Zr ions, readily substitute for Zr in the zircon lattice. It is therefore eminently understandable why the specific Pb isotopes so commonly found in measurable concentrations in zircons are ^{206}Pb and ^{208}Pb, which are the stable decay products of ^{238}U and ^{232}Th, the primary U and Th isotopes in zircons.

Moreover, measurement of the ^{238}U and ^{206}Pb concentrations in zircons has been applied widely, probably many tens of thousands of times, to obtain relative ages of Archean and Proterozoic (that is, Creation Days 1–3) rocks around the world for the past

several decades. The consistency of these relative dates seems exceptionally good. Thus, it would seem nigh to unimaginable to conceive that a genuine physical process of radioisotope decay in these rocks, as implied by these radioisotope determinations, is not real.

On the other hand, if accelerated nuclear decay occurred on Creation Days 1–3 prior to the creation of plant life, what does that imply about subsequent radioactive decay? Did it continue at a much slower rate (similar to today's rate) through the rest of the Creation Week and pre-Flood era until God accelerated nuclear decay again in the weeks or months leading up to the outset of the Flood? That would mean this postulated radioactive decay with its radiation harmful to life occurred in God's "very good" Creation prior to the Curse. Or did God completely turn off nuclear/radioactive decay after its acceleration early in Creation Week had served His purposes? We can only speculate.

Thus, it could instead be argued that it is not necessary to postulate grossly accelerated radioactive decay during Creation Days 1–3. That was a time frame in which the Creator's fiat supernatural activity occurred, before today's post-Creation-Week operational and thermodynamics rules were instigated to sustain the created order. It would seem somewhat presumptuous to suggest that God needed to use accelerated radioisotope decay to accompany His process of fiat creation of these rocks. When Jesus the Creator (John 1:1–3, Colossians 1:15–17) turned water into wine (John 2:1–11), His fiat supernatural activity did not necessarily follow today's thermodynamic rules. We do not explain Jesus' miracle of His creation of more bread and fish from the five loaves and two fish (Matthew 14: 15–21) by suggesting the bread came from accelerated growth of wheat whose grains were crushed and then baked as bread or fish that hatched and grew at an accelerated speed. So why would we suggest these created schists and granites came into being via accelerated metamorphism and magmatism of precursor rocks? We would then have to explain where those precursor sedimentary and volcanic rocks came from. Eventually at some point in the chain of reasoning we would have to admit God created the first rocks by fiat just as the rocks were, in whatever form He chose. So why not simply accept these schists and granites were created by fiat much as they are, though as seen today likely affected by subsequent events after they were created?

In doing what He did God did not deceive us, no more than Jesus deceived His onlookers. Indeed, God has told us what He did and when He did it, and God does not lie (Titus 1:2). Thus, God tells us when He used progressive processes, such as when He first made man's body from the dust of the ground and then breathed into his nostrils the breath of life (Genesis 2:7). And God certainly tells us He first formed the earth, the seas, and the heavens before filling them, which constituted a progressive process. Furthermore, 2 Peter 3:5 states that "the earth was formed out of water and by water" which suggests, at a minimum, that God possibly used process to transform water into the earth's first rocks, an inference that appears to be at least allowed by Genesis 1:2 which states that initially "the earth was formless (or without form) and void (empty)."

However, it is suggested here that we do not need to postulate grossly accelerated metamorphic and magmatic processes to transform precursor sediments and volcanics into schists and granites any more than postulating Jesus used grossly accelerated processes to produce more bread and fish. I contend that the resultant schists and granites are not testimony to illusionary metamorphism and magmatism, in spite of the claimed compelling evidence that pre-Flood rocks consistently record what may be regarded as a large amount of pre-Flood nuclear decay process. We need to remember that isotopic measurements are always subject to interpretation based on assumptions. On the other hand, God simply tells us He created the earth and its rocks and then on creation Day 3 He separated the waters to raise rocks to form the dry land. We are the ones who postulate those rocks were formed by metamorphic and magmatic processes based on our experience and observations today, when God is sustaining the earth and universe (Colossians 1:17), by projecting today's processes back into the Creation Week and suggesting they must have occurred at a grossly accelerated rate. Of course, on the other hand, nearly all creation geologists agree that God used accelerated geological processes during the Flood, though such acceleration was not likely instantaneous but progressive.

So were these schists created by fiat? Or did God use processes of grossly accelerated metamorphism? Ultimately we cannot be dogmatic either way as God's Word is silent, except that God does tell us when He used progressive processes. Jesus used a progressive process when He first put mud on the eyes of a blind man and then sent him to wash the mud off so his sight was healed (John 9:1–7), but for other blind men He simply restored their sight in one supernatural act. At least we can agree that God created supernaturally during the Creation Week by whatever means God chose, so ultimately these schists were created supernaturally.

The distribution of radiohalos

Now that we have discussed the above fundamental issues we can discuss the distribution

of radiohalos in these schists. From the grand totals for each schist unit summarized in table 1 it is obvious that there are more radiohalos, both ^{238}U and ^{210}Po radiohalos, in the Vishnu Schist than in the Rama Schist. Because there are more samples of the Vishnu Schist in which radiohalos were counted, the best measure of radiohalos frequency for comparison are the numbers of radiohalos and numbers of Po radiohalos per slide. By this measure the Vishnu Schist samples have 15.71 radiohalos per slide and 9.76 Po radiohalos per slide in 37 samples, whereas the Ramu Schist samples have only 5.68 radiohalos per slide and 3.69 Po radiohalos per slide in thirteen samples. Furthermore, whereas there were 18,526 ^{210}Po radiohalos counted in the 37 Vishnu Schist samples, there were four ^{218}Po and 14 ^{214}Po radiohalos counted. For comparison, in the thirteen Ramu Schist samples only 2,398 ^{210}Po radiohalos were counted and no ^{218}Po or ^{214}Po radiohalos.

Another interesting statistic which is potentially significant is the ratio of ^{210}Po radiohalos to ^{238}U radiohalos. For the 37 Vishnu Schist samples this ratio is 1.64:1, whereas for the 13 Ramu Schist samples it is slightly higher at 1.86:1. That means there are comparatively slightly more ^{210}Po radiohalos for every ^{238}U radiohalo in the Ramu Schist samples.

Table 1 also provides the radiohalo details for each of the 50 samples. Of the 37 Vishnu Schist samples only one (2.7%) has no radiohalos in it (VS-4), whereas four samples (10.8%) have no ^{238}U radiohalos in them (GCM-2, VS-4, GCM-38, and GCM-40). In comparison, of the 13 Ramu Schist samples three (23%) have no radiohalos in them (GCM-13, GCM-20, and ECG-9) and five samples (38.5%) have no ^{238}U radiohalos in them (GCM-13, GCM-14, GCM-20, GCM-22, and ECG-9).

The samples in table 1 are listed in geographical order for each of the two schist units, that is, the order in which the sample locations occur rafting down river. Of course, these sample locations occur also in groups because the schist units are not continuously exposed along the walls of the inner gorges, being intruded by granite plutons (fig. 1). But these groups of schist samples also occur in six metamorphic domains or lithotectonic blocks, separated by shear zones (fig. 2), with these different metamorphic domains having been subjected to different P-T conditions (fig. 3). However, comparing the data in table 1 with fig. 3, there does not appear to be any correlation between the P-T conditions in each metamorphic domain and the prevalence of radiohalos in the schists. For example, even though the six samples of Vishnu Schist in the hot Mineral Canyon block contain overall 12.31 radiohalos per slide and the eight samples from the adjacent warm Clear Creek block contain overall 27.73 radiohalos per slide, the five samples from the hot Tuna Creek block contain overall 17.81 radiohalos per slide and the four samples from the adjacent warm Topaz Canyon block only contain overall 6.50 radiohalos per slide (table 1). In contrast, in the three Vishnu Schist samples from the Middle Granite Gorge, whose P-T metamorphic conditions have not been ascertained, the radiohalos per slide numbers vary from 0.66 to 51.22. So samples from a warm metamorphic domain do not automatically contain on average more radiohalos per slide than samples from an adjacent hot metamorphic domain. This same observed pattern also seems to apply to the more limited number of Rama Schist samples. The four samples in the hot Mineral Canyon block contain overall 4.23 radiohalos per slide and the five samples from the adjacent warm Clear Creek block contain overall 8.65 radiohalos per slide, whereas the two samples in the hot Trinity Creek block only contain overall 0.57 radiohalos per slide.

Furthermore, within each metamorphic domain there is similar great variability in the abundances of radiohalos in each sample. For example, in the six Vishnu Schist samples of the hot Mineral Canyon block the radiohalos numbers per slides vary from 0.08 to 24.36 in adjacent samples (GCM-02 and VS-6 at river miles 78.3 and 78.4 side canyon respectively) and to 43.98 radiohalos per slide in a relatively nearby sample (GCM-15 at river mile 80.5 [table 1]). Similarly, in the seven samples from the hot Trinity Creek block the radiohalos numbers per slides vary from 0 to 43.78 for relatively nearby samples (VS-4 and GCM-34 at river miles 91.2 and 93.4 respectively) and in the five samples from the very hot Tuna Creek block the radiohalos numbers per slides vary from 0.58 to 30.38 in adjacent samples (GCM-38 and GCM-39 at river miles 99.4 and 100.1 respectively). In comparison, in the eight samples from the warm Clear Creek block the radiohalos numbers per slides vary from 0.06 to 67.8 for relatively nearby samples (GCM-16 and VS-1 at river miles 81.3 and 84.0 respectively) but in the four samples from the warm Topaz Canyon block the radiohalos numbers per slides only vary from 4.44 to 7.72 in adjacent samples (GCM-35 and GCM-26 at river miles 97.3 and 98.0 respectively). This same observed pattern also seems to apply to the more limited number of Rama Schist samples. In the four samples in the hot Mineral Canyon block the radiohalos numbers per slides vary from 0 to 14.54 in adjacent samples (GCM-13 and GCM-03 at river miles 79.2 and 79.4 respectively), while in the five samples from the adjacent warm Clear Creek block the radiohalos numbers per slides vary from 0 to 28.4 in adjacent samples (GCM-20 and GCM-08 respectively at river mile 84.4 on opposite sides of the river).

Two further considerations are warranted. First, the radiohalos numbers per slide for Vishnu and Rama Schist samples in the same metamorphic domains. For example, in the hot Mineral Canyon block Vishnu Schist sample VS-7 at river mile 78.4 and Ramu Schist samples GCM-12 and GCM-13 both at river mile 79.2 are only 0.8 mile apart and they have similar low radiohalos numbers per slide—VS-7 with 0.46 compared to GCM-12 with 2.32 and GCM-13 with 0, an average of 1.16 (table 1). But demonstrating how variable the abundances of radiohalos are Vishnu Schist sample VS-6 is also at river mile 78.4 near the river up a side canyon, yet it has 24.36 radiohalos per slide and Ramu Schist sample GCM-03 at river mile 79.4, only 0.2 mile from samples GCM-12 and 13 has 14.54 radiohalos per slide. On the other hand, Vishnu Schist sample GCM-15 at river mile 80.5 with 43.94 radiohalos per slide is only 0.7 mile from Ramu Schist sample GCM-14 at river mile 79.8 with only 0.04 radiohalos per slide. Similarly, in the adjacent warm Clear Creek block Vishnu Schist sample GCM-06 at river mile 84.2 contains 21.92 radiohalos per slide, whereas Ramu Schist samples GCM-07 and GCM-08 at river miles 84.3 and 84.4 respectively contain 3.34 and 28.4 radiohalos per slide respectively. Yet Ramu Schist sample GCM-20 also at river mile 84.4 contains 0 radiohalos per slide. So, there is no clear pattern, as adjacent Vishnu and Ramu Schist samples can contain similar high or low numbers of radiohalos per slide, even in the same metamorphic domain.

Second, is the abundance of radiohalos per slide related to the abundance of biotite in the schists? Fig. 9 provides a visual comparison of the abundance of biotite in nine samples, Vishnu Schist samples VS-1 to VS-7 and Ramu Schist samples ECG-8 and ECG-9. Visually, of the Vishnu Schists samples, VS-1, VS-2, and VS-3 likely have the most biotite in them (fig. 9b–d). For comparison, these samples contain 67.8, 63.44, and 25.0 radiohalos per slide (table 1). VS-1 and 2 are from the same location at river mile 84.0 and both consistently have high abundances of both biotite and radiohalos. Vishnu Schist samples VS-3 and VS-4 are also from the same location at river mile 91.2 and whereas VS-3 has more biotite and 25.0 radiohalos per slide, VS-4 has much less biotite and 0 radiohalos per slide in it. Thus, it would appear that the more biotite in a Vishnu Schist sample the greater the likelihood of more radiohalos, although samples VS-5 and VS-6 appear to contain less biotite than VS-3, yet these three samples all have about the same radiohalos numbers per slide at 21.32, 24.36 and 25.0 respectively (table 1). For comparison, Ramu Schist sample ECG-9 appears to contain more biotite than ECG-8 from the same location at river mile 118.8, though many of the dark grains in ECG-9 are hornblende (fig 9i, j), and it has 0 radiohalos per slide, whereas ECG-8 contains 12.50 radiohalos per slide (table 1). So, while the abundance of biotite is definitely a factor in the abundance of radiohalos because the radiohalos are hosted by the biotite flakes, it is also likely that the abundance of tiny zircon crystals included in the biotite flakes is essential too, because without the tiny zircon crystals there are no "point" sources of ^{238}U to decay and produce the radiohalos.

The prevalence and formation of the Po radiohalos

Next to consider are the numbers of Po radiohalos compared to the numbers of ^{238}U radiohalos and how they vary between the schist units in the different metamorphic domains or lithotectonic blocks and the samples within those domains and the schist units themselves.

Of the 37 Vishnu Schist samples, 36 (97.3%) contain Po radiohalos, and 33 (89.2%) also contain ^{238}U radiohalos (table 1). That is, one sample (VS-4) contains no radiohalos at all, whereas three samples (CGM-02, 38 and 40) only contain Po radiohalos (specifically only ^{210}Po radiohalos). For comparison, of the 13 Ramu Schist samples, ten (76.9%) contain Po radiohalos, and eight (61.5%) also contain ^{238}U radiohalos. That is, three samples (GCM-13, 20, and ECG-9) contain no radiohalos at all, whereas two samples (CGM-14 and 22) only contain Po radiohalos (specifically only ^{210}Po radiohalos). Only four of the 37 Vishnu Schist samples (10.8%) contain ^{218}Po and ^{214}Po radiohalos (table 1). Sample VS-2 contains two ^{218}Po and five ^{214}Po radiohalos while VS-3 contains two ^{218}Po and seven ^{214}Po radiohalos. Samples GCM-18 and GCM-05 each contain one ^{214}Po radiohalo.

A better measure for comparison of samples, and groups of samples in the different metamorphic domains, is the Po radiohalos per slide. Thus, the 37 Vishnu Schist samples contain an average of 9.76 Po radiohalos per slide, while the 13 Ramu Schist samples contain an average of only 3.69 Po radiohalos per slide (table 1). Furthermore, the six, seven and five Vishnu Schist samples within the hot Mineral Canyon, Trinity Creek, and Tuna Creek blocks contain 7.70, 5.48, and 12.63 Po radiohalos per slide respectively, whereas the eight and four Vishnu Schist samples within the warm Clear Creek and Topaz Canyon blocks contain 17.49 and 4.80 Po radiohalos per slide respectively. Thus, there is no clear pattern in Po radiohalos numbers per slide when hot and warm metamorphic domains are compared, except that there appear to be more Po radiohalos per slide when there are more biotite flakes in the samples within a metamorphic domain—for example, samples VS-1 and 2 in the

warm Clear Creek block as already noted above. This conclusion is likely also reflected in the variations in Po radiohalos numbers between samples within the same metamorphic domain. For example, among the six, seven and five Vishnu Schist samples within the hot Mineral Canyon, Trinity Creek, and Tuna Creek blocks the Po radiohalos numbers per slide vary from 0.08 to 22.92, 0 to 21, and 0.58 to 30.38 respectively, whereas among the eight and four Vishnu Schist samples within the warm Clear Creek and Topaz Canyon blocks the Po radiohalos numbers per slide vary from 0.06 to 45.4 (VS-1) and 46.8 (VS-2), and from 3.64 to 6.06 respectively.

Furthermore, another significant measure is the ratio of ^{210}Po radiohalos to ^{238}U radiohalos as it might reflect both the numbers of tiny zircon inclusions that are ^{238}U radiocenters in the biotite flakes and their productivity in producing ^{210}Po radiohalos via the hydrothermal fluids model for transport of Po to ^{210}Po radiocenters. So, among the six, seven and five Vishnu Schist samples within the hot Mineral Canyon, Trinity Creek, and Tuna Creek blocks the ratios of ^{210}Po radiohalos to ^{238}U radiohalos vary from 0.71:1 to 22:1, from 0.37:1 to 7:1, and from 1.86:1 to 23.5:1 respectively, and the metamorphic domains themselves average 1.67:1 (five samples), 0.84:1 (six samples), and 2.44:1 (three samples) respectively (table 1). For comparison, among the eight and four Vishnu Schist samples within the warm Clear Creek and Topaz Canyon blocks the ratios of ^{210}Po radiohalos to ^{238}U radiohalos vary from 0.54:1 to 3.24:1, and from 2.11:1 to 4.55:1 respectively, and the metamorphic domains themselves average 1.70:1 (eight samples) and 2.83:1 (four samples) respectively. Thus, generally, each ^{238}U-containing zircon radiocenter generates enough Po atoms to produce 1–2 adjacent ^{210}Po radiocenters, though in some samples more ^{210}Po radiocenters are generated while in others fewer are generated, apparently regardless of the metamorphic domain the samples are in. And sometimes the fewer the biotite flakes in a sample the more ^{210}Po radiohalos are generated per ^{238}U radiocenter—for example, VS-7 (only a few biotite flakes in fig. 9h) with a ratio of 22 ^{210}Po radiohalos for every ^{238}U radiocenter compared to VS-2 (lots of biotite flakes in fig. 9c) with a ratio of only 2.79 ^{210}Po radiohalos for every ^{238}U radiocenter. This likely reflects the numbers of tiny zircon inclusions in each biotite flake in each sample, which in turn likely reflects the compositions of the precursor sediments to the Vishnu Schist, that is, the abundance of detrital zircon grains in them.

By these measures the Ramu Schist has similar but limited statistics from only 13 samples, though there are fewer ^{210}Po radiohalos at 3.69 per slide compared with the Vishnu Schist (37 samples) at 9.76 ^{210}Po radiohalos per slide, and the average ratio of ^{210}Po radiohalos to ^{238}U radiohalos is 1.86:1 in the Ramu Schist compared to 1.64:1 in the Vishnu Schist (table 1). Similarly, within the metamorphic domains the numbers of Po radiohalos per slide for each sample vary. In the four and two samples from the hot Mineral Canyon and Trinity Creek blocks the Po radiohalos numbers per slide vary from 0 to 8.32 and from 0.10 to 0.98 respectively, averaging 2.54 and 0.54 respectively, while in the five samples from the warm Clear Creek block the Po radiohalos numbers per slide vary from 0 to 15.84, averaging 5.06. Likewise, in the eight of the 13 samples containing both radiohalo types, ^{210}Po radiohalos always outnumber the ^{238}U radiohalos, ratios varying from 1.19:1 to 16.33:1. Once again, these variations would seem to reflect the relative abundances of biotite flakes and the tiny zircon inclusions in these Ramu Schist samples, which would similarly reflects the compositions of the precursor felsic volcanics to this schist, that is, the abundance of zircon grains in them.

According to Gentry (1986, 1988) the Po radiohalos are "God's fingerprints" of fiat creation of granites, especially the ^{218}Po and ^{214}Po radiohalos because the parent ^{218}Po and ^{214}Po atoms have half-lives of only 3.1 minutes and 164 microseconds. With such fleeting existences the ^{218}Po and ^{214}Po radiohalos that each required 500 million to a billion ^{218}Po or ^{214}Po atoms to α-decay had to form virtually instantly. To Gentry that implied the host biotite flakes and thus the granites had to form virtually instantly, the expected hallmark of fiat creation by God. However, Gentry (1986, 1988) never considered or explained Po radiohalos found in metamorphic rocks. The samples in this study are all of schists in the Grand Canyon's Precambrian crystalline basement which uniformitarian geologists believe are metamorphosed shales, siltstones, and acid volcanics (rhyolites and tuffs), while creation geologists believe the same schists are created rocks which may never have been derived by metamorphism of precursor sediments and volcanics (Austin 1994; Snelling 2009, 2022b). If they are still in the form in which they were created, they should, according to Gentry's fiat creation hypothesis, contain many ^{218}Po and ^{214}Po radiohalos. But only a few Vishnu Schist samples contain a few ^{218}Po and ^{214}Po radiohalos, which implies that Gentry's hypothesis is not correct, and/or something has happened to these schists since their creation that has annealed, that is, wiped away, the postulated original ^{218}Po and ^{214}Po radiohalos.

The alternative hydrothermal fluid transport model for the formation of the Po radiohalos (Snelling and Armitage 2003; Snelling 2005) postulates that hydrothermal fluids released from the granite magmas as they crystallized and cooled

transported Po atoms from the tiny zircon crystals within biotite flakes in the granites as ^{238}U in them underwent grossly accelerated α-decay to adjacent sites within the biotite flakes where the Po atoms were chemically concentrated into radiocenters that generated the Po radiohalos. However, since Po radiohalos are also found in metamorphic rocks (Snelling 2005, 2006, 2008b, c, 2023b, this study), this implies the Po radiohalos must have formed when hydrothermal fluids were active, either in transforming the precursor sediments and volcanics into schists (Snelling 1994) or subsequently after the regional metamorphic processes were completed (Snelling 2006). While these are slower processes, Snelling (2008a) argued that host granites still had to form within 6–10 days while grossly accelerated α-decay was occurring to rapidly generate the billions of Po atoms needed to form the Po radiohalos. Similarly, Snelling (1994) argued the regional metamorphic transformation of precursor sediments and volcanics would likewise have been rapid within the Flood year, as subsequently verified by Snelling (2006) with the occurrence of orphan ^{210}Po radiohalos in metamorphic rocks in Norway that had been infiltrated by hydrothermal fluids subsequent to their initial metamorphism, and by Snelling (2008c) with the occurrence of Po radiohalos in the Cooma metamorphic complex formed during the Flood year from fossil-bearing Flood-deposited sediments. In all these instances the Po radiohalos had to also form below the 150°C annealing temperature of radiohalos (Laney and Laughlin 1981) and before the hydrothermal fluids had cooled and thus become ineffective in transporting further Po atoms. The predictions and implications of this model have subsequently been tested and have verified its validity (Snelling 2008b, c, d, 2014a, 2018; Snelling and Gates 2009).

The prediction of the hydrothermal fluid transport model for Po radiohalo formation would be that ubiquitous ^{210}Po radiohalos would form, with very few or no accompanying ^{218}Po and ^{214}Po radiohalos. Because the hydrothermal fluid process is relatively slower than fiat creation, there would not routinely be sufficient time for enough ^{218}Po and ^{214}Po atoms with half-lives of only 3.1 minutes and 164 microseconds respectively to be transported, nucleate and then α-decay to generate ^{218}Po and ^{214}Po radiohalos. On the other hand, the half-life of ^{210}Po is 138 days. Thus, more time is available for sufficient ^{210}Po atoms to be transported, nucleate and then α-decay to generate ^{210}Po radiohalos, even after the 6–10 days for the host granites to form as the released hydrothermal fluids would have continued to circulate and cool below 150°C for several more weeks. Similarly, more time would be available for ^{210}Po atoms to be transported, nucleate and then α-decay to generate ^{210}Po radiohalos as precursor sediments and volcanics were metamorphosed during the Flood into schists by hydrothermal fluids (Snelling 1994), or if the Po radiohalos in these schists were generated by hydrothermal fluids permeating them along fractures, schistosity and cleavages at a time subsequent to the regional metamorphism that formed them (Snelling 2006).

The fulfilment of this prediction of the hydrothermal fluids transport model for Po radiohalos formation can be seen in these Grand Canyon Precambrian schists. Only four of the 37 Vishnu Schist samples (10.8%) contain a few ^{218}Po and ^{214}Po radiohalos, whereas 36 (97.3%) contain ^{210}Po radiohalos and 33 (89.2%) also contain ^{238}U radiohalos (table 1). Furthermore, while three samples contain only ^{210}Po radiohalos, in most other samples there are on average 1.64 ^{210}Po radiohalos for every ^{238}U radiohalo, and it is apparent that the more biotite flakes in a sample, the more radiohalos have been generated. Thus, these statistics in the detailed elaboration above clearly support the claim that the predicted outcome of the hydrothermal fluid transport model for Po radiohalo formation is substantiated in these schist samples from Grand Canyon's Precambrian crystalline basement.

When did these Po radiohalos form?

Having established that the prevalence of ^{210}Po radiohalos in these schist samples is only consistent with the hydrothermal fluid transport model for their formation, the final question to answer is when did these Po radiohalos form? Many creation geologists would interpret these Grand Canyon schists in the continent's crystalline basement foundation rocks likely represent rocks created by fiat on Days 1 or 2 of the Creation Week before being uplifted and beveled to form the dry land on Day 3 (Austin 1994; Snelling 2009, 2022b). The reasoning for this conclusion, rather than uplifting and beveling early in the Flood as also at the Great Unconformity, has already been presented above. In Gentry's fiat creation model (1986, 1988) these schists would have been created by fiat fully-formed with the fully-developed ^{238}U, ^{218}Po, ^{214}Po, and ^{210}Po radiohalos already in them by the end of Creation Day 2 at the latest. So, why then do some samples from these two schists contain many ^{210}Po radiohalos without any accompanying ^{238}U radiohalos? The answer is that we cannot be sure these schists are still today in their original created condition, as subsequent events on Creation Day 3 and then later during the Flood probably changed them. Indeed, Jamtveit, Bucher-Nurminen, and Austrheim (1990) have demonstrated how Precambrian (pre-Flood) metamorphic rocks (granulites) in Norway were

subsequently transformed rapidly by hydrothermal fluids into another type of metamorphic rock (eclogite) during a later mountain-building episode at a time equivalent to early during the Flood, and the eclogite now has ^{210}Po radiohalos in it (Snelling 2006).

Furthermore, if God, who does not deceive us but tells us what He did, created these crystalline rocks by fiat, rather than by accelerated metamorphism of precursor sediments and volcanics that never happened, then why would He also create in them radiohalos that apparently record radioisotope decay that perhaps never happened? After all, as already discussed, we do not explain Jesus' miracle of His creation of more bread and fish from the five loaves and two fish (Matthew 14: 15–21) by suggesting the bread came from accelerated growth of wheat whose grains were crushed and then baked as bread or fish that hatched and grew at an accelerated speed. So, if God created the schists supernaturally, why would God then need to include in them radiohalos recording physical evidence of accelerated radioisotope decay? Could the radiohalos not be due instead to subsequent events, such as during the Flood? This is akin to the long-asked question of whether Adam had a navel (umbilicus)? The answer is probably not because an umbilicus is a birth scar and he did not experience birth from a human mother but was created supernaturally by God.

From his tabulated radiohalos data for numerous granites and metamorphic rocks from locations around the globe of various geological ages, both Precambrian and Phanerozoic, Snelling (2023b) clearly showed the peak occurrence of radiohalos was in Flood-related rocks when hydrothermal fluids would be prevalent during catastrophic geological processes, including for the metamorphism of Flood-deposited sediments (Snelling 1994). Yet Po radiohalos were still present, albeit in small numbers, within some Precambrian (pre-Flood) granites and metamorphics. Given that radiohalos are annealed at 150°C (Laney and Laughlin 1981), he thus proposed that any earlier pre-Flood radiohalos in those rocks may have been annealed during the tectonic upheavals of the Flood so that the radiohalos observed in them today were then generated subsequently during the Flood. Even so, any earlier radiohalos could have instead been annealed during tectonic upheaval of the Creation Day 3 uplift of the initial crustal rocks to form the dry land. Can we determine which scenario is the more likely?

Snelling (2023a) discussed the studies which have been done to determine the temperature of burial of the Cambrian Tapeats Sandstone in Grand Canyon. Because that sandstone layer sits on top of the Great Unconformity and in many places rests directly on the Precambrian schists sampled in this study, the temperature of burial of the Tapeats would be a guide to the temperature these schists were potentially subjected to during the Flood. Snelling (2023a) detailed the various burial temperature estimation methods used on a tuff bed found within the Tapeats and on the Proterozoic basement rocks, which included zircon and apatite fission-track ages (Dumitru, Duddy, and Green 1994; Kelley, Chapin, and Karlstrom 2001; Kelley and Karlstrom 2012; Naeser et al. 1989, 2001), apatite (U-Th)/He and ^{4}He/^{3}He thermochronology (Flowers et al. 2007, 2009; Flowers, Wernicke, and Farley 2008; Flowers and Farley 2012), and smectite/illite ratios (Essene and Peacor 1995; Hillier et al. 1995; Hower 1981; Huang, Longo, and Pevear 1993; Pollastro 1993; Pytte and Reynolds 1989; Renac and Meunier 1995; Smart and Clayton 1985; Velde and Espitalié 1989; Velde and Lanson 1993). He found that the consensus from all these estimation methods to be that the Tapeats Sandstone prior to the Laramide deformation responsible for uplifting the Colorado Plateau was subjected to a burial temperature of 110–130°C, which is below the 150°C annealing temperature of radiohalos (Laney and Laughlin 1981).

However, Peak et al. (2021) and Thurston et al. (2022) used zircon (U-Th)/He thermochronology data obtained from the Precambrian crystalline basement rocks themselves in eastern Grand Canyon to constrain their thermal history. They found that their data and models were highly sensitive to late-stage reheating due to burial beneath ~3–4 km of Phanerozoic strata prior to ca. 60 Ma. Their models that best matched observed date-equivalent uranium trends showed maximum burial temperatures of 140–160°C, which agree with the available apatite (U-Th)/He and apatite fission-track data. While this temperature range straddles the 150°C annealing temperature of radiohalos, it is an estimate of the maximum burial temperature. Thus, coupled with the 110–130°C burial temperature for the overlying Tapeats Sandstone which was also based on some samples from the underlying Proterozoic crystalline basement, the lower temperature of 140°C should be considered the probable maximum burial temperature during the Flood for these Grand Canyon schists. So, any pre-Flood radiohalos in them may not have been annealed during the Flood.

On the other hand, it is possible that the tectonic upheaval on Creation Day 3 responsible for the uplifting of these continental rocks in the original crust created on Creation Days 1–2 would have generated sufficient heat to anneal any radiohalos present in these schists. There was also subsequent burial under the Grand Canyon Supergroup. Thurston et al. (2024) using combined zircon (U-Th)/He and K-feldspar ^{40}Ar/^{39}Ar thermochronometers concluded from their modeling that the Precambrian crystalline

basement rocks were at 150–200°C (at 5–8 km depth) until their rapid exhumation to the surface when the Great Unconformity was generated. This burial temperature is above the radiohalos annealing temperature, so any radiohalos in the crystalline basement rocks would have been annealed. However, we cannot be certain, because the events of Creation Day 3 also involved fiat supernatural activity that did not necessarily follow today's thermodynamic rules, just as when Jesus the Creator (John 1:1–3, Colossians 1:15–17) turned water into wine (John 2:1–11). In any case, the relatively few ^{218}Po and ^{214}Po radiohalos and the abundance of ^{210}Po radiohalos sometimes without accompanying ^{238}U radiohalos in these Grand Canyon Precambrian schists would seem to rule out Gentry's fiat creation model for the formation of the Po radiohalos observed today in these rocks.

Instead, we need to examine more closely the applicability of the hydrothermal fluid model for the generation of these Po radiohalos. Two processes are crucial to the model, namely, grossly accelerated radioactive decay, and generation and circulation of hydrothermal fluids. The grossly accelerated radioactive decay of ^{238}U in zircon inclusions in biotite flakes was needed to generate rapidly the sufficient quantities of the Po isotopes (^{218}Po, ^{214}Po, and ^{210}Po), and the hydrothermal fluids were needed to transport rapidly these Po isotopes to adjacent nucleation sites within biotite flakes which became Po radiocenters that then formed the Po radiohalos around them.

However, the evidence (helium diffusion, radiohalos, fission tracks, discordant isochrons ages by different radioisotope dating methods on the same rock units, and radiocarbon in fossil materials) only points with certainty to accelerated radioactive decay having occurred during the Flood (Vardiman, Snelling, and Chaffin 2005), which could have begun deep in the crust or mantle weeks or months prior to the breaking up of the "fountains of the great deep" (Genesis 7:11). Indeed, as discussed above, it can be argued that it is not necessary to postulate grossly accelerated radioactive decay during Creation Days 1–3 because that was a time frame in which the Creator's fiat supernatural activity occurred, before today's post-Creation-Week operational and thermodynamics rules were instigated to sustain the created order. It would seem somewhat presumptuous to suggest that God needed to use accelerated radioisotope decay to accompany His process of fiat creation of these rocks.

And as for the needed hydrothermal fluids to rapidly transport the Po isotopes, those were generated by being expelled from the crystallizing and cooling granite magmas only within plutons that formed during the Flood (Snelling and Woodmorappe 1998; Snelling 2008a), and by hydrothermal fluids produced by water buried with the sediments during the Flood having metamorphosed those sediments (Snelling 1994). However, if these Grand Canyon Precambrian schists, and the granites accompanying them, were supernaturally created by fiat as fully-formed on Creation Days 1–2, as already discussed and established above, then they did not need to be metamorphosed and cool from precursor sediments and volcanic rocks and thus neither the schists nor their accompanying granites thereby generated any hydrothermal fluids. Furthermore, there would have been no metamorphism of sediment and volcanic layers to form schists during the geologically quiet and tectonically stable pre-Flood period. Therefore, the hydrothermal fluids needed to transport the Po isotopes to form the Po radiohalos we now observe in these schists had to be generated by other means during the Flood, at the same time as the grossly accelerated radioactive decay was occurring that rapidly produced the needed quantities of Po isotopes.

Two ingredients were readily available during the Flood to produce and circulate hydrothermal fluids, namely, the water that was buried within the sedimentary layers as they were rapidly deposited, and heat generated by their deep burial and by the grossly accelerated radioactive decay. Lest the objection be raised that the heat from the grossly accelerated radioactive decay would have been too excessive, the survival of the radiohalos negates that objection as the temperature could not have reached 150°C. Once generated those hydrothermal fluids would then have circulated down from the sedimentary layers into the underlying Grand Canyon Precambrian crystalline basement, as discussed below. There the hydrothermal fluids could have penetrated into the schists through fractures, along the schistosity planes, around grain boundaries, and then along the cleavage planes within the biotite flakes, where they dissolved the Po isotopes being produced and ejected rapidly from zircon inclusions and rapidly transported them to generate adjacent Po radiohalos. That hydrothermal fluids have penetrated along fractures and along cleavage planes in minerals such as fluorite and biotite has been repeatedly documented since first noted by Schilling (1926), Henderson (1939), and Henderson and Sparks (1939), and is evidenced by the hydrothermal alteration of the biotite adjacent to the fractures and along cleavages.

Ideally, to test this model further, schist samples would need to be collected systematically below the Great Unconformity to see if there are more radiohalos in samples closer to the Great Unconformity and along fractures in the schists and then fewer radiohalos further at depth and in the unfractured schists.

The depths below the Great Unconformity were not measured for the present set of samples, although some depths can be estimated for some of them. However, that may not provide sufficient data to test this model. A better approach would be to select two or three profiles of schists to progressively sample from the Great Unconformity downwards and along and away from fractures. However, that involves two logistical difficulties, namely, the physical effort to scale down massive cliffs safely, and obtaining the necessary research and sampling permit from the Grand Canyon National Park's Research Office.

It is admitted that it may seem difficult to envisage water from the overlying sediments permeating down into the crystalline basement rocks which were under hydrostatic pressure. However, water trapped in marine sediments being subducted with an underlying oceanic plate in a subduction zone is believed to be expelled at depth into the overlying mantle wedge, which is equally under considerable hydrostatic pressure, but there the water causes brittle fracturing and partial melting to occur. Thus water must find its way around grains, and along cleavages and fractures, however tight they may be, as in the following examples. Such infiltration of metamorphic rocks by hydrothermal fluids has been recognized in brittle granulites that were at the time at a depth of up to 50 km in Norway. Early during the Flood, earthquakes helped to propel the hydrothermal fluids up to several kilometers along shear zones up to tens of meters thick in hydraulic fracture systems within the granulites during mountain-building (Camacho et al. 2005; Jamtveit, Austrheim, and Malthe-Sorenssen 2000; Jamtveit, Bucher-Nurminen, and Austrheim 1990; Kelley 2005). There in the shear zones the hydrothermal fluids generated ^{210}Po radiohalos in the resultant eclogite (Snelling 2006). Similarly, economic uranium deposits in Canada and Australia are found in Precambrian schists beneath unconformities overlain by sandstones at the bases of thick sediment piles. Those uranium deposits have likely been formed by connate waters in the sandstones becoming hydrothermal fluids with dissolved U in them that permeated downwards across the unconformities and penetrated hundreds of meters into the underlying schists along faults, fractures, and their schistosity where they deposited the U in zones that were conducive chemically (often associated with graphitic schists) and structurally (due to fractures and the schistosity) (Marmont 1987). Therefore, if uniformitarians concede descending connate waters can penetrate crystalline rocks, especially when aided by earthquakes, then it would have been clearly achievable during the Flood when geological processes were operating at cataclysmic rates associated with catastrophic plate tectonics (Austin et al. 1994).

This would not have been as effective of a process for generating and driving hydrothermal fluid circulation as the expulsion of hydrothermal fluids from crystallizing and cooling granite magmas in plutons or from metamorphism of Flood-deposited sediments, nor would similar large volumes of hydrothermal fluids have been generated. It would also have been a relatively slower process. That conclusion is consistent with the argument here that the schists were rocks supernaturally created during the early Creation Week, rather than during the earliest Flood as proposed by some creation geologists. It is also consistent with just the few ^{218}Po and ^{214}Po radiohalos, because the fleeting existence of the ^{218}Po and ^{214}Po atoms (half-lives of 3.1 minutes and 164 microseconds respectively) would have decayed before being carried to nucleating ^{218}Po and ^{214}Po radiocenters. It is also consistent with the occurrence of some ^{210}Po radiohalos without adjacent ^{238}U radiohalos. This required the hydrothermal fluids to travel further from the sources of the Po isotopes to the distant nucleating ^{210}Po radiocenters, aided by the longer existence of the ^{210}Po atoms due to their 138 day half-life. Indeed, the process of generating these ^{210}Po radiohalos could have continued for several months during the Flood year, until the hydrothermal fluids started cooling and their circulation ceased, particularly in the waning months of the Flood. This process would also have been inefficient, because of the smaller volumes of hydrothermal fluids. Consistent with this is the fewer ^{210}Po radiohalos in the Grand Canyon Precambrian granite plutons compared with granite plutons formed during the Flood (Snelling 2023b, 2025) which have abundant Po radiohalos generated from hydrothermal fluids expelled by crystallizing and cooling granite magmas generated during the Flood. The lower numbers of Po radiohalos in these Grand Canyon Precambrian schists and other Precambrian (pre-Flood) metamorphic rocks (Snelling 2023b) are also consistent with the similar low numbers of Po radiohalos generated by metamorphism of latest Precambrian-Paleozoic sediment layers during the Flood (Snelling 1994, 2006, 2008b, c). And it is also consistent with the wide variations in the numbers of ^{210}Po radiohalos between the different schist samples in and between each Grand Canyon lithotectonic block or metamorphic domain. Ultimately, the numbers of Po radiohalos generated in these schists depended on the abundances of biotite flakes and tiny zircon inclusions in them to generate the needed Po atoms, and then the volume and flow of the transporting hydrothermal fluids.

Summary and Conclusions

The schists within Grand Canyon's Precambrian crystalline basement exposed in the Canyon's inner

gorges were possibly created supernaturally on Creation Days 1–2 as the foundation rocks for the continental crust. It is suggested that they were then uplifted and beveled as part of the upheaval on Creation Day 3 when God made the dry land. Furthermore, it is suggested that at the onset of the Flood they were beveled further and exposed before the fossil-bearing Flood sediment layers were deposited unconformably over them. Today we observe ^{238}U and ^{210}Po radiohalos in most of these schists. These are a physical record of radioactive decay that resulted in damage to the host biotite flakes by α-particles produced in the ^{238}U decay chain within tiny zircon inclusions. The ^{210}Po radiohalos are enigmatic due to the very short half-life of the parent ^{210}Po atoms and the need for billions of ^{210}Po atoms separated from their ^{238}U decay source. Two models have been proposed previously to resolve that enigma—creation by fiat of the host rocks (granites and also schists) with the Po radiohalos in them during Creation Days 1–2, or rapid transport of the Po atoms by hydrothermal fluids while grossly accelerated radioactive decay was occurring during the Flood.

Fifty samples were collected from two biotite-bearing schist units, and the radiohalos in them identified and statistically counted in prepared microscope slides. Of the 37 Vishnu Schist samples, 36 (97.3%) contain Po radiohalos, while 33 (89.2%) also contain ^{238}U radiohalos. Of the 13 Ramu Schist samples, ten (76.9%) contain ^{210}Po radiohalos, while eight (61.5%) also contain ^{238}U radiohalos. However, only four of the 37 Vishnu Schist samples (10.8%) contain ^{218}Po and ^{214}Po radiohalos. The radiohalos numbers vary between the schist samples within each lithotectonic block or metamorphic domain and between the blocks or domains, so the different apparent metamorphic conditions were irrelevant. The two factors that control radiohalos numbers are the abundance of biotite flakes available to host radiohalos and the abundance of tiny zircon inclusions in them for generating ^{238}U radiohalos and providing the Po atoms for generating adjacent Po radiohalos. Furthermore, there are similar low numbers of radiohalos in these schists compared to metamorphic rocks that formed during the Flood, which along with the relative lack of ^{218}Po and ^{214}Po radiohalos in these schists compared to metamorphic rocks that formed during the Flood is consistent with the hydrothermal fluid model for the formation of these Po radiohalos.

If any radiohalos were created in these supernaturally created schists, which would seem unlikely, they were subsequently annealed during the Creation Day 3 upheaval and the onset of the Flood. Thus, these data are consistent only with the hydrothermal fluid transport model for the formation of the Po radiohalos during the Flood. Water trapped in the Flood-deposited sediment layers was likely heated by the burial temperatures and by the residual heat generated by grossly accelerated radioactive decay. These hydrothermal fluids circulated down and infiltrated into the underlying basement schists via fractures, schistosity and cleavages where they rapidly transported Po atoms produced by grossly accelerated decay of the ^{238}U contained in tiny zircon crystals in biotite flakes in the schists and deposited them in nucleating radiocenters that thus generated the Po radiohalos, some without adjacent ^{238}U radiohalos. This was a slower and less effective process that likely lasted months. The ^{210}Po atoms were longer-lived and thus transported further by hydrothermal fluids of similar volume and circulation generated from heating of Flood-deposited sediment layers as those expelled by regional metamorphism of Flood-deposited sediments during the Flood.

Acknowledgements

The several research and collecting permits issued by the Grand Canyon National Park that made this study possible are acknowledged and its Research Office staff are thanked. The field support of Tom Vail of Canyon Ministries and of the various crews of Arizona River Runners was essential and much appreciated. Mark Armitage assisted with the preparation of the fifty slides for each sample and the counting of the radiohalos, which assistance was crucial. The use of the Cedarville University Geology Department's research petrographic microscope is acknowledged. This research was funded initially by the Institute for Creation Research and then subsequently by Answers in Genesis, and by their generous donors who gave specifically for research. The helpful and useful feedback from the reviewers is acknowledged and was appreciated, but I am responsible for the final content.

References

Anderson, C.A., and Leon T. Silver. 1976. "Yavapai Series—A Greenstone Belt." In *Tectonic Digest*. Edited by J.C. Wilt, and J.P. Jenny. *Arizona Geological Society Digest* 10: 13–26.

Armitage, Mark H., and Andrew A. Snelling. 2008. "Radiohalos and Diamonds: Are Diamonds Really For Ever?" In *Proceedings of the Sixth International Conference on Creationism*. Edited by Andrew A. Snelling, 323–334. Pittsburgh, Pennsylvania: Creation Science Fellowship; and Dallas, Texas: Institute for Creation Research.

Austin, Steven A. 1994. *Grand Canyon: Monument to Catastrophe*. Santee, California: Institute for Creation Research.

Austin, Steven A., and Kurt P. Wise. 1994. "The Pre-Flood/Flood Boundary: As Defined in Grand Canyon and Eastern

Mojave Desert, California." In *Proceedings of the Third International Conference on Creationism*. Edited by Robert E. Walsh, 37–47. Pittsburgh, Pennsylvania: Creation Science Fellowship.

Austin, Steven A., John R. Baumgardner, D. Russell Humphreys, Andrew A. Snelling, Larry Vardiman, and Kurt P. Wise. 1994. "Catastrophic Plate Tectonics: A Global Flood Model of Earth History." In *Proceedings of the Third International Conference on Creationism*. Edited by Robert E. Walsh, 609–621. Pittsburgh, Pennsylvania: Creation Science Fellowship.

Babcock, R.S. 1990. "Precambrian Crystalline Core." In *Grand Canyon Geology*. 1st ed. Edited by Stanley S. Beus, and Michael Morales, 11–28. New York, New York: Oxford University Press.

Babcock, R.S., E.H. Brown, M.D. Clark, and D.E. Livingston. 1979. "Geology of the Older Precambrian Rocks of the Grand Canyon. Part II. The Zoroaster Plutonic Complex and Related Rocks." *Precambrian Research* 8: 243–275.

Bagnall, K.W. 1957. *Chemistry of the Rare Radioelements: Polonium-Actinium*. London, United Kingdom: Butterworths.

Bateman, Paul C., and Bryan W. Chappell. 1979. "Crystallization, Fractionation, and Solidification of the Tuolumne Intrusive Series, Yosemite National Park, California." *Geological Society of America Bulletin* 90, no.5 (May 1): 465–482.

Baumgardner, John R. 2000. "Distribution of Radioactive Isotopes in the Earth. In *Radioisotopes and the Age of the Earth: A Young-Earth Creationist Research Initiative*. Edited by Larry Vardiman, Andrew A. Snelling, and Eugene F. Chaffin, 49–94. El Cajon, California: Institute for Creation Research; and St Joseph, Missouri: Creation Research Society.

Bower, William R., Richard A.D. Pattrick, Carolyn I. Pearce, Giles T.R. Droop, and Sarah J. Haigh. 2016a. "Radiation Damage Haloes in Biotite Investigated Using High-Resolution Transmission Electron Microscopy." *American Mineralogist* 101, no.1 (January 1): 105–110.

Bower, William R., Carolyn I. Pearce, Andrew D. Smith, Simon M. Plimblott, J. Frederick W. Mosselmans, Sarah J. Haigh, James P. McKinley, and Richard A.D. Pattrick. 2016b. "Radiation Damage in Biotite Mica by Accelerated α-Particles: A Synchrotron Microfocus X-Ray Diffraction and X-Ray Absorption Spectroscopy Study." *American Mineralogist* 101, no.4 (April 1): 928–942.

Bowring, Samuel A., and Karl E. Karlstrom. 1990. "Growth, Stabilization, and Reactivation of Proterozoic Lithosphere in the Southwestern United States." *Geology* 18, no.12 (December 1): 1203–1206.

Brown, E.H., R.S. Babcock, M.D. Clark, and D.E. Livingston. 1979. "Geology of the Older Precambrian Rocks of the Grand Canyon. Part I. Petrology and Structure of the Vishnu Complex." *Precambrian Research* 8, nos.3–4 (April): 219–241.

Camacho, Alfredo, James K.W. Lee, Bastiaan J. Hensen, and Jean Braun, 2005. "Short-Lived Orogenic Cycles and the Eclogitization of Cold Crust by Spasmodic Hot Fluids." *Nature* 435, no.7046 (30 June): 1191–1196.

Campbell, I., and J.H. Maxson. 1938. "Geological Studies of the Archean Rocks at the Grand Canyon." *Carnegie Institution of Washington Year Book* 37: 359–364.

Clarey, Timothy L. 2020. *Carved in Stone: Geological Evidence of the Worldwide Flood*. Dallas, Texas: Institute for Creation Research.

Clarey, Timothy L., and Davis J. Werner. 2023. "A Progressive Global Flood Model Confirmed by Rock Data Across Five Continents." In *Proceedings of the Ninth International Conference on Creationism*. Edited by John H. Whitmore, 412–445. Cedarville, Ohio: Cedarville University International Conference on Creationism.

Clark, M.D. 1976. "The Geology and Petrochemistry of the Precambrian Metamorphic Rocks of the Grand Canyon, Arizona." Ph.D. Thesis (unpublished). Leicester, England: University of Leicester.

Clark, M.D. 1979. "Geology of the Older Precambrian Rocks of the Grand Canyon: Part III. Petrology of the Mafic Schists and Amphibolites." *Precambrian Research* 8, nos. 3–4 (April): 277–302.

Condie, Kent C. 1986. "Geochemistry and Tectonic Setting of Early Proterozoic Supracrustal Rocks in the Southwestern United States." *Journal of Geology* 94, no.6 (November): 845–864.

Craig, J., U. Biffi, R.F. Galimberti, K.A.R. Ghori, J.D. Gorter, N. Hakhoo, D.P. Le Heron, J. Thurowe, and M. Vecoli. 2013. "The Palaeobiology and Geochemistry of Precambrian Hydrocarbon Source Rocks." *Marine and Petroleum Geology* 40 (February): 1–47.

Crick, Ian H., C.J. Boreham, A.C. Cook, and T.G. Powell. 1988. "Petroleum Geology and Geochemistry of Middle Proterozoic McArthur Basin, Northern Australia II: Assessment of Source Rock Potential." *American Association of Petroleum Geologists Bulletin* 72, no.12 (December 1): 1495–1514.

Dickin, Alan P. 2005. *Radiogenic Isotope Geology*. 2nd ed. Cambridge, England: Cambridge University Press.

Dumitru, Trevor A., Ian R. Duddy, and Paul F. Green. 1994. "Mesozoic–Cenozoic Burial, Uplift, and Erosion History of the West-Central Colorado Plateau." *Geology* 22, no.6 (June 1): 499–502.

Dumond, Gregory, Kevin H. Mahan, Michael L. Williams, and Karl E. Karlstrom. 2007. "Crustal Segmentation, Composite Looping Pressure-Temperature Paths, and Magma-Enhanced Metamorphic Field Gradients: Upper Granite Gorge, Grand Canyon, USA." *Geological Society of America Bulletin* 119, nos.1–2 (January/February): 202–220.

Dutkiewicz, A., H. Volk, J. Ridley, and S.C. George. 2007. "Precambrian Inclusion Oils in the Roper Group: A Review." In *Proceedings of the Central Australian Basins Symposium*. Edited by T.J. Munson, and G.J. Ambrose, 326–348. Darwin, Australia: Northern Territory Geological Survey, *Special Publication 2*.

Essene, E.J., and P.R. Peacor. 1995. "Clay Mineral Thermometry—A Critical Perspective." *Clays and Clay Minerals* 43, no.5 (October): 540–553.

Flowers, Rebecca M., and Ken A. Farley. 2012. "Apatite $^{4}He/^{3}He$ and (U-Th)/He Evidence for an Ancient Grand Canyon." *Science* 338, no.6114 (December 21): 1616–1619.

Flowers, Rebecca M., D.L. Shuster, B.P. Wernicke, and Ken A. Farley. 2007. "Radiation Damage Control on Apatite (U-Th)/He Dates from the Grand Canyon Region, Colorado Plateau." *Geology* 35, no.5 (May 1): 447–450.

Flowers, Rebecca M., B.P. Wernicke, and Ken A. Farley. 2008. "Unroofing, Incision and Uplift History of the

Southwestern Colorado Plateau from Apatite (U-Th)/He Thermochronometry." *Geological Society of America Bulletin* 120, nos. 5–6 (May 1): 571–587.

Flowers, Rebecca M., Richard A. Ketcham, David L. Shuster, and Kenneth A. Farley. 2009. "Apatite (U–Th)/He Thermochronometry Using a Radiation Damage Accumulation and Annealing Model." *Geochimica et Cosmochimica Acta* 73, no. 8 (15 April): 2347–2365.

Fremlin, J.H. 1975. "Spectacle Haloes." *Nature* 258, no. 5532 (20 November): 269.

Gentry, Robert V. 1967. "Extinct Radioactivity and the Discovery of a New Pleochroic Halo." *Nature* 213, no. 5075 (4 February): 487–489.

Gentry, Robert V. 1968. "Fossil Alpha-Recoil Analysis of Certain Variant Radioactive Halos." *Science* 160, no. 3833 (14 June): 1228–1230.

Gentry, Robert V. 1970. "Giant Radioactive Halos: Indicators of Unknown Radioactivity." *Science* 169, no. 3946 (August 14): 670–673.

Gentry, Robert V. 1971. "Radiohalos: Some Unique Lead Isotopic Ratios and Unknown Alpha Radioactivity." *Science* 173, no. 3998 (20 August): 727–731.

Gentry, Robert V. 1973. "Radioactive Halos." *Annual Review of Nuclear Science* 23 (December): 347–362.

Gentry, Robert V. 1974. "Radiohalos in a Radiochronological and Cosmological Perspective." *Science* 184, no. 4132 (April 5): 62–66.

Gentry, Robert V. 1975. "Spectacle Haloes." *Nature* 258 no. 5532 (20 November): 269–270.

Gentry, Robert V. 1979. "Time: Measured Responses." *EOS, Transactions of the American Geophysical Union* 60, no. 22 (29 May): 474.

Gentry, Robert V. 1980. "Polonium Halos". *EOS, Transactions of the American Geophysical Union* 61, no. 27 (1 July): 514.

Gentry, Robert V. 1982. "Creationism Again". *Physics Today* 35, no. 10 (1 October): 13.

Gentry, Robert V. 1983. "Creationism Still Again." *Physics Today* 36, no. 4 (April): 13–15.

Gentry, Robert V. 1984. "Radioactive Halos in a Radiochronological and Cosmological Perspective." In *Proceedings of the 63rd Annual Meeting, Pacific Division, American Association for the Advancement of Science* 1, no. 3 (April 30): 38–65.

Gentry, Robert V. 1986. "Radioactive Halos: Implications for Creation." In *Proceedings of the First International Conference on Creationism*. Vol. 2. Edited by Robert E. Walsh, Christopher L. Brooks, and R.S. Crowell, 89–100. Pittsburgh, Pennsylvania: Creation Science Fellowship.

Gentry, Robert V. 1988. *Creation's Tiny Mystery*. Knoxville, Tennessee: Earth Science Associates.

Gentry, Robert V. 1989. "Response to Wise." *Creation Research Society Quarterly* 25, no. 4 (March): 176–180.

Gentry, Robert V. 1998. "Radiohalos in Diamonds." *Creation Ex Nihilo Technical Journal* 12, no. 3 (December): 287–290.

Gentry, Robert V., T.A. Cahill, N.R. Fletcher, H.C. Kaufmann, L.R. Medsker, J.W. Nelson, and R.G. Flocchini. 1976. "Evidence for Primordial Superheavy Elements." *Physical Review Letters* 37, no. 1 (5 July): 11–15.

Gentry, Robert V., S.S. Christy, J.F. McLaughlin, and J.A. McHugh. 1973. "Ion Microprobe Confirmation of Pb Isotope Ratios and Search for Isomer Precursors in Polonium Radiohalos." *Nature* 244 no. 5414 (3 August): 282–283.

Gentry, Robert V., W.H. Christie, D.H. Smith, J.W. Boyle, S.S. Christy, and J.F. McLaughlin. 1978. "Implications on Unknown Radioactivity of Giant and Dwarf Haloes in Scandinavian Rocks." *Nature* 274, no. 5670 (3 August): 457–459.

Glazner, Allen F., and Breck R. Johnson. 2013. "Late Crystallization of K-Feldspar and the Paradox of Megacrystic Granites." *Contributions to Mineralogy and Petrology* 166 (5 July): 777–779.

Glazner, Allen F., Victor R. Baker, John M. Bartley, Kevin M. Bohacs, and Drew S. Coleman. 2022. "The Rocks Don't Lie, But They can be Misunderstood." *Geology Today* 32, no. 10 (October): 4–10.

Harada, Koh, William C. Burnett, Paul A. LaRock, and James B. Cowart. 1989. "Polonium in Florida Groundwater and its Possible Relationship to the Sulfur Cycle and Bacteria." *Geochimica et Cosmochimica Acta* 53, no. 1 (January): 143–150.

Hawkins, David P., Samuel A. Bowring, Bradley R. Ilg, Karl E. Karlstrom, and Michael L. Williams. 1996. "U-Pb Geochronologic Constraints on the Paleoproterozoic Crustal Evolution of the Upper Granite Gorge, Grand Canyon, Arizona." *Geological Society of America Bulletin* 108, no. 9 (September 1): 1167–1181.

Henderson, George Hugh. 1939. "A Quantitative Study of Pleochroic Haloes—V. The Genesis of Haloes." *Proceedings of the Royal Society of London, Series A* 173, no. 953 (28 November): 250–264.

Henderson, George Hugh, and S. Bateson. 1934. "A Quantitative Study of Pleochroic Haloes—I." *Proceedings of the Royal Society of London, Series A* 145, no. 855 (2 July): 563–581.

Henderson, George Hugh, and F.W. Sparks. 1939. "A Quantitative Study of Pleochroic Haloes—IV. New Types of Haloes." *Proceedings of the Royal Society of London, Series A* 173, no. 953 (28 November): 238–249.

Henderson, George Hugh, and L.G. Turnbull. 1934. "A Quantitative Study of Pleochroic Haloes—II." *Proceedings of the Royal Society of London, Series A* 145, no. 855 (2 July): 582–598.

Henderson, George Hugh, C.M. Mushkat, and D.P. Crawford. 1934. "A Quantitative Study of Pleochroic Haloes—III Thorium." *Proceedings of the Royal Society of London, Series A* 158, no. 893 (1 January): 199–211.

Hillier, S., J. Mátyás, A. Matter, and G. Vasseur. 1995. "Illite/Smectite Diagenesis and its Variable Correlation with Vitrinite Reflectance in the Pannonian Basin." *Clays and Clay Minerals* 43: 174–183.

Holmes, Arthur. 1931. "Radioactivity and Geological Time." In *Physics of the Earth—IV. The Age of the Earth. Bulletin of the National Research Council* 80: 124–460.

Hower, J. 1981. "Shale Diagenesis." In *Clays and the Resource Geologist*. Edited by F.J. Longstaffe, 60–80. Quebec City, Canada: Mineralogical Association of Canada, *Short Course Handbook 7*.

Huang, Wuu-Liang, John M. Longo, and David R. Pevear. 1993. "An Experimentally Derived Kinetic Model for Smectite-to-Illite Conversion and its Use as a Geothermometer." *Clays and Clay Minerals* 41 (1 April): 162–177.

Humphreys, D. Russell. 2000. "Accelerated Nuclear Decay: A Viable Hypothesis?" In *Radioisotopes and the Age of the Earth: A Young-Earth Creationist Research Initiative*.

Edited by Larry Vardiman, Andrew A. Snelling, and Eugene F. Chaffin, 333–379. El Cajon, California: Institute for Creation Research; and St Joseph, Missouri: Creation Research Society.

Humphreys, D. Russell. 2005. "Young Helium Diffusion Age of Zircons Supports Accelerated Nuclear Decay." In *Radioisotopes and the Age of the Earth: Results of a Young-Earth Creationist Research Initiative*. Edited by Larry Vardiman, Andrew A. Snelling and Eugene F. Chaffin, 25–100. El Cajon, California: Institute for Creation Research, and Chino Valley, Arizona: Creation Research Society.

Hussain, N., T.M. Church, G.W. Luther III, and W.S. Moore. 1995. "^{210}Po and ^{210}Pb Disequilibrium in the Hydrothermal Vent Fluids in Chimney Deposits from Juan de Fuca Ridge." *Geophysical Research Letters* 22, no. 23 (1 December): 3175–3178.

Iimori, S., and J. Yoshimura. 1926. "Pleochroic Halos in Biotite: Probable Existence of the Independent Origin of the Actinium Series." *Scientific Papers of the Institute of Physical and Chemical Research* 5, no. 66: 11–24.

Ilg, Bradley R., Karl E. Karlstrom, David P. Hawkins, and Michael L. Williams. 1996. "Tectonic Evolution of Paleoproterozoic Rocks in the Grand Canyon: Insights into Middle-Crustal Processes." *Geological Society of America Bulletin* 108, no. 9 (September 1): 1149–1166.

Jackson, M.J., T.G. Powell, R.E. Summons, and I.P. Sweet. 1986. "Hydrocarbon Shows and Petroleum Source Rocks in Sediments as Old as 1.7×10^9 Years." *Nature* 322, no. 6081 (21 August): 727–729.

Jamtveit, Bjørn, Kurt Bucher-Nurminen, and Håkon Austrheim. 1990. "Fluid Controlled Eclogitization of Granulites in Deep Crustal Shear Zones, Bergen Arcs, Western Norway." *Contributions to Mineralogy and Petrology* 104 (February): 184–193.

Jamtveit, Bjørn, Håkon Austrheim, and Anders Malthe-Sorenssen. 2000. "Accelerated Hydration of the Earth's Deep Crust Induced by Stress Perturbations." *Nature* 408, no. 6808 (2 November): 75–78.

Joly, J. 1907. "Pleochroic Halos." *Philosophical Magazine* 13: 381–383.

Joly, J. 1917a. "Radio-Active Halos." *Philosophical Transactions of the Royal Society of London, Series A* 217: 51–79.

Joly, J. 1917b. "Radio-Active Halos." *Nature* 99: 456–458, 476–478.

Joly, J. 1923. "Pleochroic Haloes of Various Geological Ages." *Proceedings of the Royal Society of London, Series A* 102, no. 719 (March 1): 682–705.

Joly, J. 1924. "The Radioactivity of the Rocks." *Nature* 114, no. 2857 (2 August): 160–164.

Karlstrom, Karl E., and Samuel A. Bowring. 1993. "Proterozoic Orogenic History in Arizona, Transcontinental Proterozoic Provinces." In *Precambrian of the Conterminous U.S.*, vol. C-2 of *Geology of North America*. Edited by W.R. Van Schmus, and M.E. Bickford, 188–211. Boulder, Colorado: Geological Society of America.

Karlstrom, Karl E., and J. Michael Timmons. 2012. "Many Unconformities Make One 'Great Unconformity'." In *Grand Canyon Geology: Two Billion Years of Earth's History*. Edited by J. Michael Timmons, and Karl E. Karlstrom, 73–79. Boulder, Colorado: Geological Society of America, *Special Paper 489*.

Karlstrom Karl E., B.R. Ilg, M.L. Williams, D.P. Hawkins, Samuel A. Bowring, and S.J. Seaman. 2003. "Paleoproterozoic Rocks of the Granite Gorges." In *Grand Canyon Geology*. 2nd ed. Edited by Stanley S. Beus, and Michael Morales, 9–38. New York, New York: Oxford University Press.

Karlstrom Karl E., Bradley R. Ilg, David P. Hawkins, Michael L. Williams, Gregory Dumond, Kevin Mahan, and Samuel A. Bowring. 2012. "Vishnu Basement Rocks of the Upper Granite Gorge: Continent Formation 1.84 to 1.66 Billion Years Ago." In *Grand Canyon Geology: Two Billion Years of Earth's History*. Edited by J. Michael Timmons, and Karl E. Karlstrom, 7–24. Boulder, Colorado: Geological Society of America, *Special Paper 489*.

Kelley, Shari A., Charles E. Chapin, and Karl E. Karlstrom. 2001. "Laramide Cooling Histories of Grand Canyon, Arizona, and the Front Range, Colorado, Determined from Apatite Fission-Track Thermochronology." In *Colorado River: Origin and Evolution*. Edited by Richard A. Young, and Earle E. Spamer, 37–42. Grand Canyon, Arizona: Grand Canyon Association, *Monograph 12*.

Kelley, Shari A., and Karl E. Karlstrom. 2012. "The Laramide and Post-Laramide Uplift and Erosional History of the Eastern Grand Canyon: Evidence from Apatite Fission-Track Thermochronology." In *Grand Canyon Geology: Two Billion Years of Earth's History*. Edited by J. Michael Timmons, and Karl E. Karlstrom, 109–117. Boulder, Colorado: Geological Society of America, *Special Paper 489*.

Kelley, Simon. 2005. "Hot Fluids and Cold Crust." *Nature* 435, no. 7046 (30 June): 1171.

Kerr-Lawson, D.E. 1927. "Pleochroic Haloes in Biotite from near Murray Bay." *University of Toronto Studies in Geology Series* 24: 54–71.

Kerr-Lawson, D.E. 1928. "Pleochroic Haloes in Biotite." *University of Toronto Studies in Geology Series* 27: 15–27.

Laney, Randy, and A. William Laughlin. 1981. "Natural Annealing of Pleochroic Haloes in Biotite Samples from Deep Drill Holes, Fenton Hill, New Mexico." *Geophysical Research Letters* 8, no. 5 (May): 501–504.

LaRock, P.A., J.-H. Hyun, S. Boutelle, W.C. Burnett, and C.D. Hull. 1996. "Bacterial Mobilization of Polonium." *Geochimica et Cosmochimica Acta* 60, no. 22 (November): 4321–4328.

LeCloarec, M.F., M. Pennisi, E. Corazza, and G. Lambert. 1994. "Origin of Fumarolic Fluids Emitted from a Nonerupting Volcano: Radionuclide Constraints at Vulcano (Aeolian Islands, Italy)." *Geochimica et Cosmochimica Acta* 58, no. 20 (October): 4401–4410.

Lingen, J.S. van der. 1926. "Ueber Pleochroitische Höfe." *Zentralel. Mineralogie und Geologie, Abteilung A*. 177–183.

Marmont, Soussan. 1987. "Ore Deposit Models #13. Unconformity-Type Uranium Deposits." *Geoscience Canada* 14, no. 4 (December): 219–229.

Mügge, O. 1907. "Radioaktivität als Ursuche der Pleochroitischen Höfe des Cordierite." *Zentralel. Mineralogie und Geologie* 1907: 397–399.

Naeser, Chris W., Ian R. Duddy, Donald P. Elston, Terry A. Dumitru and Paul F. Green. 1989. "Fission-Track Dating: Ages for Cambrian Strata and Laramide and Post-Middle Eocene Cooling Events from the Grand Canyon, Arizona." In *Geology of Grand Canyon, Northern Arizona (with Colorado River Guides)*. Edited by Donald P. Elston,

George H. Billingsley, and Richard A. Young, 139–144. Washington, DC: American Geophysical Union.

Naeser, Chris W., Ian R. Duddy, Donald P. Elston, Terry A. Dumitru and Paul F. Green. 2001. "Fission-Track Analysis of Apatite and Zircon from Grand Canyon, Arizona." In *Colorado River: Origin and Evolution*. Edited by Richard A. Young, and Earle E. Spamer, 31–36. Grand Canyon, Arizona: Grand Canyon Association, *Monograph 12*.

Noble, Levi F., and J. Fred Hunter. 1916. "A Reconnaissance of the Archean Complex of the Granite Gorge, Grand Canyon, Arizona." *US Geological Survey Professional Paper* 98-I: 95–113.

Peak, B.A., Rebecca M. Flowers, F.A. Macdonald, and J.M. Cottle. 2021. "Zircon (U-Th)/He Thermochronology Reveals Pre-Great Unconformity Paleotopography in the Grand Canyon Region, USA." *Geology* 49, no. 12 (August 12): 1462–146.

Peters, Shanan E., and Robert R. Gaines. 2012. "Formation of the 'Great Unconformity' as a Trigger for the Cambrian Explosion." *Nature* 484, no. 7394 (18 April): 363–366.

Pollastro, Richard M. 1993. "Considerations and Applications of the Illite/Smectite Geothermometer in Hydrocarbon-Bearing Rocks of Miocene to Mississippian Age." *Clays and Clay Minerals* 41, no. 2 (April): 119–133.

Powell, John Wesley. 1876. *Exploration of the Colorado River of the West*. Washington, D.C.: Smithsonian Institution.

Pytte, A.M., and R.C. Reynolds. 1989. "The Thermal Transformation of Smectite to Illite." In *Thermal History of Sedimentary Basins*. Edited by N.D. Naeser, and T.H. McCulloh, 133–140. Berlin, Germany: Springer-Verlag.

Ramdohr, Paul. 1933. "Ueber die Blaue Kuppe bei Eschwege und benach-barte Basaltvorkommen." *Neues Jahrbuch für Mineralogie Beilageband Abteilung A* 67: 53–65.

Ramdohr, Paul. 1957. "Neue Beobachtungen über Radioaktive Höfe und über Radioaktive Sprengungen." *Abhandlungen der Deutschen Akademie der Wissenschaften zu Berlin, Klasse für Chemie, Geologie und Biologie* 2: 1–17.

Ramdohr, Paul. 1960. "Neue Beobachtungen an Radioacktiven Höfen in Verschiedenen Mineralien mit Kritischen Bemerkungen zur Auswertung der Höfe zur Altersbestimmung." *Geologische Rundschau* 49: 253–263.

Renac, C., and A. Meunier. 1995. "Reconstruction of Palaeothermal Conditions in the Passive Margin Using Illite-Smectite Mixed-Layer Series (BA1 Scientific Deep Drill-Hole, Ardeche, France)." *Clay Minerals* 30, no. 2 (June): 107–118.

Rubin, Kenna Harmony. 1997. "Degassing of Metals and Metalloids from Erupting Seamount and Mid-Ocean Ridge Volcanoes: Observations and Predictions." *Geochimica et Cosmochimica Acta* 61, no. 17 (September): 3525–3542.

Schilling, A. 1926. "Die Radioacktiven Höfe im Flusspat von Wölsendorf." *Neues Jahrbuch für Mineralogie, Geologie und Palaeontology, Abteilung A* 53: 241–265.

Schulze, Daniel J., and Lutz Nasdala. 2016. "Unusual Paired Pattern of Radiohaloes on a Diamond Crystal from Guaniamo (Venezuela)." *Lithos* 265 (15 November): 177–181.

Shufledt, Owen P., Karl E. Karlstrom, George E. Gehrels, and Katherine E. Howard. 2010. "Archean Detrital Zircons in the Proterozoic Vishnu Schist of the Grand Canyon, Arizona: Implications for Crustal Architecture and Nuna Supercontinent Reconstructions." *Geology* 38, no. 12 (December 1): 1099–1102.

Smart, G., and T. Clayton. 1985. "The Progressive Illitization of Interstratified Illite-Smectite from Carboniferous Sediments of Northern England and its Relationship to Organic Maturity Indicators." *Clay Minerals* 30, no. 4 (December): 455–466.

Snelling, Andrew A. 1994. "Towards a Creationist Explanation of Regional Metamorphism." *Creation Ex Nihilo Technical Journal* 8, no. 1 (May): 51–77.

Snelling, Andrew A. 2000. Radiohalos. In *Radioisotopes and the Age of the Earth: A Young-Earth Creationist Research Initiative*. Edited by Larry Vardiman, Andrew A. Snelling, and Eugene F. Chaffin, 381–468. El Cajon, California: Institute for Creation Research, and St. Joseph, Missouri: Creation Research Society.

Snelling, Andrew A. 2005. "Radiohalos in Granites: Evidence for Accelerated Nuclear Decay." In *Radioisotopes and the Age of the Earth: Results of a Young-Earth Creationist Research Initiative*. Edited by Larry Vardiman, Andrew A. Snelling, and Eugene F. Chaffin, 101–207. El Cajon, CA: Institute for Creation Research, and Chino Valley, Arizona: Creation Research Society.

Snelling, Andrew A. 2006. "Confirmation of Rapid Metamorphism of Rocks." *Acts & Facts* 35, no. 2 (February 1): Impact Article #392. El Cajon, California: Institute for Creation Research.

Snelling, Andrew A. 2008a "Catastrophic Granite Formation: Rapid Melting of Source Rocks, and Rapid Magma Intrusion and Cooling." *Answers Research Journal* 1 (February 6): 11–25. https://answersresearchjournal.org/catastrophic-granite-formation/.

Snelling, Andrew A. 2008b. "Testing the Hydrothermal Fluid Transport Model for Polonium Radiohalo Formation: The Thunderhead Sandstone, Great Smoky Mountains, Tennessee–North Carolina." *Answers Research Journal* 1 (March 26): 53–64. https://answersresearchjournal.org/polonium-radiohalo-testing/.

Snelling, Andrew A. 2008c. "Radiohalos in the Cooma Metamorphic Complex, New South Wales, Australia: The Mode and Rate of Regional Metamorphism." In *Proceedings of the Sixth International Conference on Creationism* Edited by Andrew A. Snelling, 371–387. Pittsburgh, Pennsylvania: Creation Science Fellowship, and Dallas, Texas: Institute for Creation Research.

Snelling, Andrew A. 2008d. "Radiohalos in the Shap Granite, Lake District, England: Evidence that Removes Objections to Flood Geology." In *Proceedings of the Sixth International Conference on Creationism*. Edited by Andrew A. Snelling, 389–405. Pittsburgh, Pennsylvania: Creation Science Fellowship, and Dallas, Texas: Institute for Creation Research.

Snelling, Andrew A. 2008e. "Significance of Highly Discordant Radioisotope Dates for Precambrian Amphibolites in Grand Canyon, USA." In *Proceedings of the Sixth International Conference on Creationism*. Edited by Andrew A. Snelling, 407–424. Pittsburgh, Pennsylvania: Creation Science Fellowship, and Dallas, Texas: Institute for Creation Research.

Snelling, Andrew A. 2009. *Earth's Catastrophic Past: Geology, Creation and the Flood*. Dallas, Texas: Institute for Creation Research.Snelling, Andrew A. 2014a. "Radiohalos in Multiple, Sequentially Intruded Phases of the Bathurst Batholith, NSW, Australia: Evidence for Rapid Granite

Formation during the Flood." *Answers Research Journal* 7 (March 5): 49–81. https://answersresearchjournal.org/radiohalos-bathurst-batholith-australia/.

Snelling, Andrew A. 2014b. "Radioisotope Dating of Meteorites: I. The Allende CV3 Carbonaceous Chondrite." *Answers Research Journal* 7 (April 16): 103–145. https://answersresearchjournal.org/radioisotope-dating-meteorites-1/.

Snelling, Andrew A. 2014c. "Radioisotope Dating of Meteorites II: The Ordinary and Enstatite Chondrites." *Answers Research Journal* 7 (August 20): 239–296. https://answersresearchjournal.org/radioisotope-dating-chondrites-2/.

Snelling, Andrew A. 2014d. "Radioisotope Dating of Meteorites: III. The Eucrites (Basaltic Achondrites)." *Answers Research Journal* 7 (December 31): 533–583. https://answersresearchjournal.org/radioisotope-dating-meteorites-3/.

Snelling, Andrew A. 2015a. "Radioisotope Dating of Meteorites: IV. The Primitive and other Achondrites." *Answers Research Journal* 8 (May 6): 209–251. https://answersresearchjournal.org/radioisotope-dating-meteorites-4/.

Snelling, Andrew A. 2015b. "Radioisotope Dating of Meteorites: V. Isochron Ages of Groups of Meteorites." *Answers Research Journal* 8 (December 16): 449–478. https://answersresearchjournal.org/radioisotope-dating-meteorites-5/.

Snelling, Andrew A. 2018. "Radiohalos as an Exploration Pathfinder for Granite-Related Hydrothermal Ore Veins: A Case Study in the New England Batholith, Eastern Australia." In *Proceedings of the Eighth International Conference on Creationism*. Edited by John H. Whitmore, 567–580. Pittsburgh, Pennsylvania: Creation Science Fellowship.

Snelling, Andrew A. 2021a. "The Petrology of the Tapeats Sandstone, Tonto Group, Grand Canyon, Arizona." *Answers Research Journal* 14 (June 23): 159–254. https://answersresearchjournal.org/petrology-tapeats-sandstone-tonto-group/.

Snelling, Andrew A. 2021b. "The Petrology of the Bright Angel Formation, Tonto Group, Grand Canyon, Arizona." *Answers Research Journal* 14 (September 8): 303–415. https://answersresearchjournal.org/petrology-bright-angel-tonto-group/.

Snelling, Andrew A. 2022a. "The Petrology of the Muav Formation, Tonto Group, Grand Canyon, Arizona." *Answers Research Journal* 15 (August 10): 139–262. https://answersresearchjournal.org/geology/petrology-muav-formation-tonto-group/.

Snelling, Andrew A. 2022b. *The Genesis Flood Revisited*. Green Forest, Arkansas: Master Books; and Hebron, Kentucky: Answers in Genesis.

Snelling, Andrew A. 2023a. "The Carbon Canyon Fold, Eastern Grand Canyon, Arizona." *Answers Research Journal* 16 (February 22): 1–124. https://answersresearchjournal.org/geology/carbon-canyon-fold-arizona/.

Snelling, Andrew A. 2023b. "Radiohalos Through Earth History—What Clues Can They Provide Us?" In *Proceedings of the Ninth International Conference on Creationism*. Edited by John H. Whitmore, 540–560. Cedarville, Ohio: Cedarville University International Conference on Creationism.

Snelling, Andrew A. 2025. "Radiohalos in the Precambrian Crystalline Basement Rocks of Grand Canyon. Part 1. The Granites." *Answers Research Journal* 18 (May 21): 197–229. https://answersresearchjournal.org/geology/radiohalos-precambrian-grand-canyon-part-1/.

Snelling, Andrew A., and John Woodmorappe. 1998. "The Cooling of Thick Igneous Bodies on a Young Earth." In *Proceedings of the Fourth International Conference on Creationism*. Edited by Robert E. Walsh, 527–545. Pittsburgh, Pennsylvania: Creation Science Fellowship.

Snelling, Andrew A., and Mark H. Armitage. 2003. "Radiohalos: A Tale of Three Granitic Plutons." In *Proceedings of the Fifth International Conference on Creationism*. Edited by Robert L. Ivey, 243–267. Pittsburgh, Pennsylvania: Creation Science Fellowship.

Snelling, Andrew A., John R. Baumgardner, and Larry Vardiman. 2003. "Abundant Po Radiohalos in Phanerozoic Granites and Timescale Implications for their Formation." *EOS, Transactions of the American Geophysical Union* 84, no. 46, Fall Meeting Supplement, Abstract V32C-1046.

Snelling, Andrew A., and Dallel Gates. 2009. "Implications of Polonium Radiohalos in Nested Plutons of the Tuolumne Intrusive Suite, Yosemite, California." *Answers Research Journal* 2 (April 8): 53–77. https://answersresearchjournal.org/polonium-radiohalos-yosemite/.

Stark M. 1936. "Pleochroitische (Radioaktive) Höfe ihre Verbreitung in den Gesteinen und Veränderlichheit." *Chemie der Erde* 10: 566–630.

Sun, S.-S. 1980. "Lead Isotopic Study of Young Volcanic Rocks from Mid-Ocean Ridges, Ocean Islands and Island Arcs." *Philosophical Transactions of the Royal Society A* 297, no. 1431 (24 July): 409–440.

Thurston, Olivia G., William R. Guenthner, Karl E. Karlstrom, Jason W. Ricketts, Matthew T. Heizler, and J. Michael Timmons. 2022. "Zircon (U-Th)/He Thermochronology of Grand Canyon Resolves 1250 Ma Unroofing at the Great Unconformity and <20 Ma Canyon Carving." *Geology* 50, no. 2 (November 2): 222–226.

Thurston, Olivia G., William R. Guenthner, Karl E. Karlstrom, Matthew T. Heizler, Jason W. Ricketts, and K.T. McDannell. 2024. "Deep-Time Thermal History of the Great Unconformity in the Grand Canyon, USA: Combined Zircon (U-Th)/He and K-Feldspar $^{40}Ar/^{39}Ar$ Thermochronometers." *Geological Society of America Bulletin* 136, nos. 11–12 (May 6): 4815–4835.

Timmons, J. Michael, Karl E. Karlstrom, Matthew T. Heizler, Samuel A. Bowring, George E. Gehrels, and Laura J. Crossey. 2005. "Tectonic Inferences from the ca. 1254–1100 Ma Unkar Group and Nankoweap Formation, Grand Canyon: Intracratonic Deformation and Basin Formation during Protracted Grenville Orogenesis." *Geological Society of America Bulletin* 117, no. 11 (November): 1573–1595.

Timmons, J. Michael, John Bloch, Kathryn Fletcher, Karl E. Karlstrom, Matthew T. Heizler, and Laura J. Crossey. 2012. "The Grand Canyon Unkar Group: Mesoproterozoic Basin Formation in the Continental Interior during Supercontinent Assembly." In *Grand Canyon Geology: Two Billion Years of Earth's History*. Edited by J. Michael Timmons, and Karl E. Karlstrom, 25–47. Boulder, Colorado: Geological Society of America, *Special Paper 489*.

Vallance, Thomas G. 1967. "Mafic Rock Alteration and Isochemical Development of Some Cordierite-Anthophyllite Rocks." *Journal of Petrology* 8, no. 1 (1 February): 84–96.

Vardiman, Larry, Andrew A. Snelling, and Eugene F. Chaffin. eds. 2005. *Radioisotopes and the Age of the Earth: Results of a Young-Earth Creationist Research Initiative*. El Cajon, California: Institute for Creation Research, and Chino Valley, Arizona: Creation Research Society.

Velde, B., and J. Espitalié. 1989. "Comparison of Kerogen Maturation and Illite/Smectite Composition in Diagenesis." *Journal of Petroleum Geology* 12, no. 1 (January): 103–110, 1989.

Velde, B., and B. Lanson. 1993. "Comparison of I/S Transformation and Maturity of Organic Matter at Elevated Temperatures." *Clays and Clay Minerals* 41, no. 2 (April): 178–183.

Walcott, C.D. 1889. "A Study of a Line of Displacement in the Grand Canyon of the Colorado in Northern Arizona." *Geological Society of America Bulletin* 1: 49–64.

Walcott, C.D. 1894. "Precambrian Igneous Rocks of the Unkar Terrane, Grand Canyon on the Colorado." *US Geological Survey 14th Annual Report for 1892/3*, part 2: 497–519.

Whitmore, John H., Raymond Strom, Stephen Cheung, and Paul A. Garner. 2014. "The Petrology of the Coconino Sandstone (Permian), Arizona, USA." *Answers Research Journal* 7 (December 10): 499–532. https://answersresearchjournal.org/petrology-of-the-coconino-sandstone/.

Whitmore, John H., and Paul A. Garner. 2018. "The Coconino Sandstone (Permian, Arizona, USA): Implications for the Origin of Ancient Cross-bedded Sandstones." In *Proceedings of the Eighth International Conference on Creationism*, Edited by John H. Whitmore, 581–627. Pittsburgh, Pennsylvania: Creation Science Fellowship.

Wiman, E. 1930. "Studies of Some Archaean Rocks in the Neighbourhood of Uppsala, Sweden, and their Geological Position." *Bulletin of the Geological Institute, University of Uppsala* 23: 1–170.

Wise, Kurt P. 1989. "Radioactive Halos: Geological Concerns." *Creation Research Society Quarterly* 25, no. 4 (March): 171–176.

Wise, Kurt P., and Andrew A. Snelling. 2005. "A Note on the Pre-Flood/Flood Boundary in the Grand Canyon." *Origins* 58 (June 1): 7–29.